

ABSTRACT

BHAUMIK, JAYEETA. Synthetic Porphyrinic Macrocycles for Photodynamic Therapy and Other Biological Applications. (Under the Direction of Professor Jonathan S. Lindsey).

Synthetic porphyrinic macrocycles are invaluable for use in a wide variety of biological applications. Such applications include photodynamic therapy (PDT) for treatment of cancer, age-related macular degeneration (AMD), and microbial infections. Several metal chelates of protoporphyrin IX molecules [Zn(II), Pd(II), In(III), and Ga(III)] were prepared from the corresponding free base porphyrin. The metalloporphyrins were tested for anti-microbial PDT. Metalloporphyrins bearing cationic substituents showed better killing of gram-negative bacteria, whereas the free base porphyrin showed strong activity against gram-positive bacteria.

Porphyrins bearing imidazolium substituents are valuable owing to the positive charge of the imidazolium group, which can impart water solubility to the porphyrin construct. To facilitate synthesis and handling of imidazole-substituted porphyrins, heteronuclear (^{11}B , ^{15}N) NMR spectroscopy was employed to fully characterize the various imidazole-substituted precursors to the porphyrins, including the dialkylboron complexes thereof. Metal chelates of imidazolium-porphyrins [Zn(II), Pd(II), and In(III)] were prepared starting from non-polar *trans*-AB porphyrins. Imidazolium-porphyrins bearing cationic or anionic substituents were examined for the efficiency of killing cancer cells (e.g., HeLa and CT26 carcinoma cells). The effectiveness of cell killing was observed in the following order: Pd(II) > cationic In(III) > cationic Zn(II) > anionic Zn(II) imidazolium-porphyrin.

Hydroxymethyl-porphyrins and hydroxymethyl-chlorins were synthesized for studies of self-assembly in analogy with the structure and function of the natural pigment

bacteriochlorophyll *c*. Various acyclic precursors containing a hydroxymethyl moiety (e.g., Mukaiyama reagents, 1-acyldipyrromethane) were prepared so that the hydroxymethyl group could be incorporated prior to the formation of the tetrapyrrole macrocycle.

Formyl-chlorins were prepared for studies of the effect of the formyl group on the absorption spectral properties. Both hydroxymethyl-chlorins and formyl-chlorins were synthesized by the palladium-mediated coupling of the corresponding bromo-chlorin. Two routes were employed: (1) synthesis of a hydroxymethyl-chlorin via Stille coupling, followed by PCC-mediated oxidation to access the formyl-chlorin, and (2) palladium-catalyzed reductive carbonylation of a bromo-chlorin to access the formyl-chlorin.

The ability to incorporate imidazole (and imidazolium), hydroxymethyl, and formyl groups at designated sites in porphyrins and chlorins affords valuable methodology for constructing molecular architectures of use in a variety of biological and materials chemistry applications.

**Synthetic Porphyrinic Macrocycles for Photodynamic Therapy
and Other Biological Applications**

by

Jayeeta Bhaumik

A Dissertation Submitted to the Graduate Faculty of

North Carolina State University

in partial fulfillment of the requirements for the Degree of

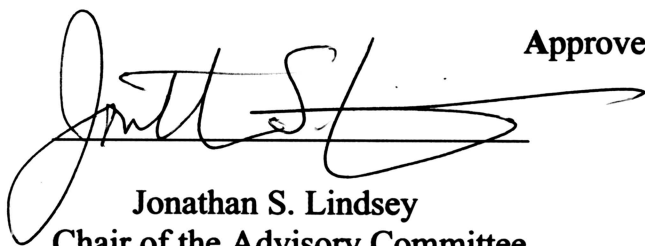
Doctor of Philosophy

Chemistry

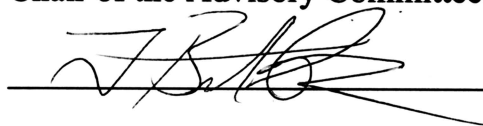
Raleigh, North Carolina, USA

Spring 2007

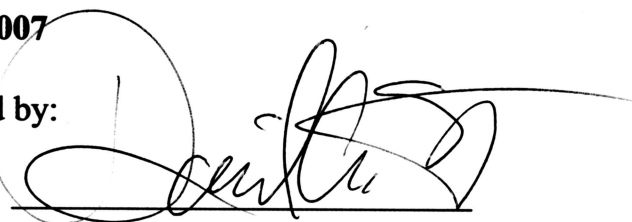
Approved by:



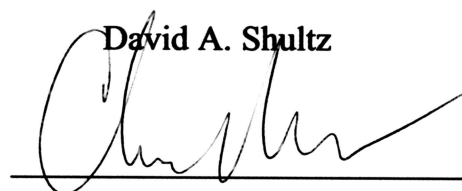
Jonathan S. Lindsey
Chair of the Advisory Committee



T. Brent Gunnoe



David A. Shultz



Christian Melander

DEDICATION

This doctoral research work is dedicated to my parents and my teachers

BIOGRAPHY

Jayeeta Bhaumik, from Kolkata, West Bengal, India, joined North Carolina State University in Fall 2002 for pursuing her Ph.D. in Organic Chemistry. She started her doctoral research under the supervision of Jonathan S. Lindsey at the Department of Chemistry. After completing a Master's degree at NCSU in early 2006 she continued research towards finishing the Ph.D. degree. During her ~5 years stay at NCSU she considers that she has found that plenty of changes took place in her life. She broadened her knowledge of chemistry through research, and realized how to carry out independent research, learned how to collaborate with research group members. After her doctoral work she would like to continue post-doctoral research on chemistry with potential medicinal and/or biological applications. Further on she will contribute her so far acquired knowledge in chemistry for serving the society by teaching and/or research.

'Jayeeta' in her mother language Bengali means 'The woman who wins'. Jayeeta wants to prove the meaning to be true for her throughout life by her curiosity for knowledge of science, and a good heart and a pure mind to help society.

ACKNOWLEDGEMENTS

I would like to express gratitude to my advisor, Prof. Jonathan. S. Lindsey, for several reasons few of them being an excellent mentor, an enduring supervisor, admirable and an outstanding teacher. All guidance on research and scientific writing from him will be helpful in order to succeed in achieving my career goal in future pathway.

I am also thankful to my advisory committee members, Dr. David A. Shultz, Dr. T. Brent Gunnoe, and Dr. Christian Melander for serving as my committee members. I also thank my previous committee member, Prof. Daniel L. Comins. I want to express regards towards Dr. S. Sankar for giving me good quality training in NMR spectroscopy. I would like to show appreciation to Prof. Lindsey's group members from Fall 2002 until now (Spring 2007) for all their help and suggestions from time to time.

I am grateful to my parents whose inspiration and support was always with me to continue higher studies. Encouragement from all my teachers from elementary school up to university level helped me to be enthusiastic about science. I could not succeed in achieving a doctoral degree without any of their presence in some part of my academic career.

I acknowledge my husband (Dr. Joydev K. Laha) for being patient during my Ph.D. studies and help me with mental support. I would like to thank my cousin (Dr. Manasi G. Saha) and her family at Raleigh, NC for supporting me throughout my doctoral studies. All of my relatives (brother, sister, cousins, uncles, aunts) and my friends (near and far) who care for me and be happy any of my achievements, I share my happiness with all of them.

I wish my grandma ("Beu") would be alive to see me completing my doctoral degree. I will remember her forever due to her inspirations in obtaining higher education.

TABLE OF CONTENTS

	Page
List of Charts.....	ix
List of Equations.....	xi
List of Figures.....	xii
List of Schemes.....	xiv
List of Tables.....	xvi
Chapter I: Porphyrinic Molecules in Photodynamic Therapy and Other Applications	
1. Porphyrinic Molecules.....	1
2. Photodynamic Therapy	3
3. Imidazolium-Porphyrins.....	7
4. Protoporphyrin IX Molecules.....	9
5. Overview.....	12
References.....	13
Chapter II: Synthesis, Photophysical Properties and Photodynamic Therapeutic Applications of Metallo–Protoporphyrin IX Molecules	
Abstract.....	16
Introduction.....	17
Results and Discussion.....	20
Conclusion.....	32
Experimental Section.....	33

References.....	37
-----------------	----

**Chapter III: Imidazole-Substituted Porphyrins with Central Metal Substituents
as Photosensitizers for Photodynamic Therapy**

Abstract.....	41
Introduction.....	42
Results and Discussion.....	44
Conclusion.....	55
Experimental Section.....	57
References.....	60

**Chapter IV: ^{11}B NMR and ^{15}N NMR Spectroscopic Studies of Imidazolyl–Pyrrolic
Compounds**

Introduction.....	64
Results and Discussion.....	67
Outlook.....	75
Experimental Section.....	75
References.....	77

**Chapter V: Dialkylboron Complexation as a Means of Masking Both Nitrogens
Present in Tetrahydrodipyrins**

Introduction.....	79
Results and Discussion.....	83

Experimental Section.....84

References.....87

Chapter VI: Synthesis of *Meso*-Hydroxymethyl Porphyrins for Studies in

Self-Assembly

Introduction.....89

Results and Discussion.....92

Conclusion.....97

Experimental Section.....98

References.....105

Chapter VII: Studies in Chlorin Chemistry

Introduction.....106

Results and Discussion.....111

Conclusion.....115

Experimental Section.....116

References.....124

Chapter VIII: Synthesis of Formyl-Substituted Chlorins as Tools for

Tuning Absorption Spectroscopic Properties

Introduction.....127

Results and Discussion.....129

Outlook.....	146
Experimental Section.....	146
References.....	152

LIST OF CHARTS

Chapter I

Chart 1. Structure of porphyrinic molecules.....	1
Chart 2. Naturally occurring porphyrinic molecules.....	2
Chart 3. Cationic imidazolium-porphyrins, which interact with DNA or act as a SOD mimic.....	3
Chart 4. Structures of manganese(III) porphyrins analyzed as SOD mimics.....	8

Chapter III

Chart 1. Structure of metallo-imidazolium porphyrins.....	45
--	----

Chapter IV

Chart 1. ^{15}N NMR chemical shift assignments of imidazolyl -pyrrolic compounds.....	68
Chart 2. ^{11}B NMR chemical shift assignments of imidazolyl -pyrrolic compounds.....	74

Chapter V

Chart 1. Structure of various hydroporphyrins.....	79
Chart 2. Structure of various hydrodipyrins.....	79
Chart 3. Different types of acyldipyrromethanes.....	80
Chart 4. Dialkylboron complexes of acyldipyrromethanes.....	81
Chart 5. Boron-dipyrin complexes.....	82

Chapter VI

Chart 1. Natural pigments (chlorophyll <i>a</i> , bacteriochlorophyll <i>c</i>) and numbering system of chlorin.....	89
Chart 2. Self-assembling architecture of a hydroxymethyl porphyrin.....	91
Chart 3. Retrosynthetic approach towards hydroxymethyl porphyrins	93

Chapter VII

Chart 1. Naturally occurring and synthetic porphyrinic molecules.	107
Chart 2. Synthesis of chlorins via the condensation of an eastern and a western half	108
Chart 3. Self-assembling natural pigment bacteriochlorophyll <i>c</i>	110

Chapter VIII

Chart 1. Various proposed routes to formyl-substituted chlorins... ..	132
Chart 2. Palladium catalyzed reductive carbonylation.....	143

LIST OF EQUATIONS

Chapter V

Equation 1. Synthesis of a chlorin.....	80
Equation 2. Synthesis of a bacteriochlorin.....	80
Equation 3. Synthesis of a dialkylboron complex of a tetrahydrodipyrin.....	83

Chapter VIII

Equation 1. Tributyltin magnesium chloride synthesis.....	130
Equation 2. Diethoxymethyltributyltin synthesis.....	130
Equation 3. 2-Tributylstannyl-1,3-dioxane synthesis.....	130
Equation 4. Hydroxymethyl tributyltin synthesis.....	130
Equation 5. Carbon monoxide mediated formylation of an aryl halide.....	131
Equation 6. Formylation of an aryl halide via Stille coupling.....	131
Equation 7. Formylation of an aryl halide using $\text{Mo}(\text{CO})_6$	131

LIST OF FIGURES

Chapter I

Figure 1. Jablonski diagram of a typical photosensitizer.....4

Figure 2. Mechanism of photodynamic therapy for killing cancer cells.....5

Chapter II

Figure 1. Heme receptor structure of gram-positive bacteria.....18

Figure 2. Survival fractions of *S. aureus* grown either in BHI or in BHI containing dipyrindyl, and incubated with **H₂PPIX**.....24

Figure 3. Survival fractions of *S. aureus* grown either in BHI or in BHI containing dipyrindyl, and incubated with **ClInPPIX**.....26

Figure 4. Survival fractions of *E. coli* grown either in BHI or in BHI containing dipyrindyl, and incubated with **H₂PPIX**.....27

Figure 5. Survival fractions of *E. coli* grown either in BHI or in BHI containing dipyrindyl, and incubated with **ClInPPIX**.....29

Chapter III

Figure 1. Killing of HeLa cervical cancer and murine CT26 colon cancer cells with imidazole-substituted porphyrins.....48

Figure 2. Graphs of photosensitizer concentration-dependent dark toxicity (A and C) and phototoxicity (B and D) after white light delivered to HeLa cells (A and B) and CT26 cells (C and D).....50

Figure 3. Effect of varying the incubation time on PDT killing of HeLa cells mediated by **MH2** or **MH4** and white light.....52

Figure 4. Cell uptake of **MH2** and **MH3** by HeLa and CT26 cells after 24 h incubation time determined by fluorescence spectrophotometry of cell extracts.....54

Chapter IV

Figure 1. ¹H NMR spectra for a free-base dipyrin and a zinc chelate of a dipyrin.....65

Figure 2. Demonstration of different types of nitrogen and boron atoms in the imidazolyl-pyrrolic compounds.....68

Figure 3. 2D ¹⁵N NMR (gHSQC) data for **9-BBN-3**. Due to the presence of only one free pyrrolic N-H, a single peak was observed at -226.4 ppm.....71

Figure 4. 2D ¹⁵N NMR (gHMBC) data for **9-BBN-3**.....72

Chapter VIII

Figure 1. Absorption spectrum of 13-hydroxymethyl chlorin (**16**).....144

Figure 2. Absorption spectrum of 13-hydroxymethyl chlorin (**20**).....145

Figure 3: Absorption spectrum of 5-formyl chlorin (**6**).....145

Figure 4. Absorption spectrum of 13-formyl chlorin (**18**).....145

LIST OF SCHEMES

Chapter II

Scheme 1. Synthesis of various metal chelates of protoporphyrin IX.....21

Chapter III

Scheme 1. Synthesis of indium(III) chelate of an imidazolium-porphyrin.....46

Chapter VI

Scheme 1. Synthesis of a silyl-protected glycolic acid and a *S*-pyridyl thioester.....94

Scheme 2. Synthesis of a hydroxymethyl-containing 1-acyldipyrromethane.....95

Scheme 3. Synthesis of silyl-protected hydroxymethyl porphyrins.....96

Chapter VII

Scheme 1. Synthesis of a pivaloyl-protected glycolic acid and a *S*-pyridyl thioester.....111

Scheme 2. Synthesis of a pivaloyl-protected hydroxymethyl-containing
1-acyldipyrromethane.....112

Scheme 3. Synthesis of hydromethyl-containing chlorins.....114

Chapter VIII

Scheme 1. Synthesis of a 5-formyl chlorin.....134

Scheme 2. Attempts to synthesize a chlorin bearing an acetal moiety.....135

Scheme 3. Attempts to synthesize a chlorin bearing a cyclic acetal moiety.....136

Scheme 4. Attempts to synthesize a 15-formyl chlorin.....138

Scheme 5. Preparation of a 13-formyl-substituted chlorin via Stille coupling.....	140
Scheme 6. Synthesis of a 13-hydroxymethyl-substituted chlorin.....	141
Scheme 7. Preparation of a 13-formyl-substituted chlorin via reductive carbonylation..	143

LIST OF TABLES

Chapter II

Table 1. Characterization data for various protoporphyrin IX compounds.....23

Chapter IV

Table 1. ^{15}N NMR spectroscopic data for imidazolyl-containing compounds.....69

Table 2. ^{11}B NMR spectroscopic data for boron-complexes of dipyrromethanes.....73

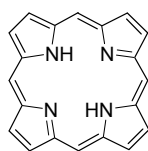
Chapter I: Porphyrinic Molecules in Photodynamic Therapy and Other Applications

Introduction

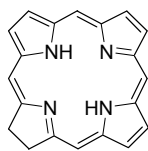
1. Porphyrinic Molecules

The porphyrinic family of molecules encompasses one of the most important sets of biologically relevant molecules, including heme, the chlorophylls, and vitamin B₁₂. Synthetic porphyrinic macrocycles have been widely used in applications ranging across the biomedical sciences and materials sciences. Examples of the former include photodynamic therapy, whereas examples of the latter include information storage and molecular-based solar cells. The placement of various functional groups at the periphery of porphyrins is essential for controlling the desired molecular function. For example, porphyrins bearing charges often exhibit water-solubility, which is desirable for a number of biological applications.

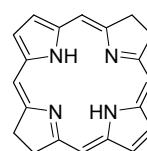
Porphyrinic molecules (e.g., porphyrins, chlorins and bacteriochlorins) are tetrapyrrolic macrocycles (Chart 1). Porphyrins, chlorins and bacteriochlorins are aromatic compounds and each absorbs visible light.



Porphyrin



Chlorin



Bacteriochlorin

Chart 1

Porphyrinic macrocycles are present in important naturally occurring pigments such as heme, chlorophylls and bacteriochlorophylls (Chart 2). A number of porphyrin-based photosensitizers have been found to be very useful for killing cancer cells.

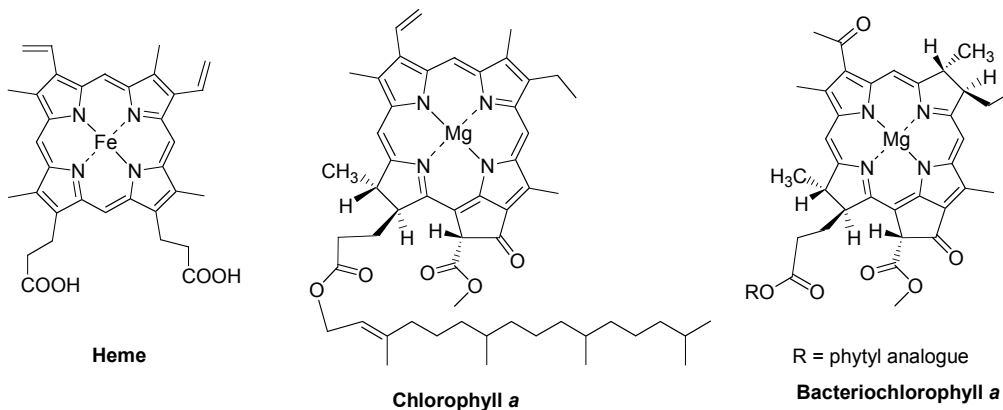


Chart 2

In order for porphyrinic macrocycles to be applicable for PDT and other biological studies, a certain level of water-solubility is desired. Among various ways to achieve water solubility, the inclusion of highly polar groups such as amine, hydroxyl, and carboxylic acid moieties can be considered. Alternatively, incorporation of positive or negatively charged substituents in the macrocycles helps to impart water-solubility. Porphyrinic molecules that bear anionic groups versus cationic groups often exhibit substantial differences in activity in PDT studies. Most commonly, cationic porphyrins are more powerful than the corresponding anionic species towards killing microbial cells as photosensitizers via PDT. A key thrust of this thesis has been to develop more effective synthetic approaches for preparing porphyrinic molecules of use in a number of biomedical applications, including PDT.

2. Photodynamic Therapy

Photodynamic therapy makes use of non-toxic photosensitizers, visible or near-infrared light along with molecular oxygen to generate singlet oxygen, which kills malignant cells. In contrast to surgery, radiotherapy or chemotherapy, PDT often affords a more focused effect, because the phototoxicity is present only where the light is provided.¹

The activity of a typical photosensitizer is illustrated through a standard Jablonski diagram (Figure 1).² On absorption of energy ($h\nu$) in the form of light, a photosensitizer is excited from the ground state to the singlet excited state (path A). Some energy may be emitted via a radiative pathway, and thus some photosensitizer molecules may relax back to the ground state (fluorescence, path B). Other molecules can undergo internal conversion (path C), whereas the remaining molecules undergo intersystem crossing and reach the excited triplet state (path D). The emission of light upon radiative relaxation by the molecules traveling from excited triplet state to the ground state is called phosphorescence (path E). The triplet state energy can also be absorbed by triplet oxygen ($^3\text{O}_2$) whereupon highly active singlet oxygen ($^1\text{O}_2$) is often generated (path F). Singlet oxygen is a powerful active species that plays an essential role in killing of cancer cells.

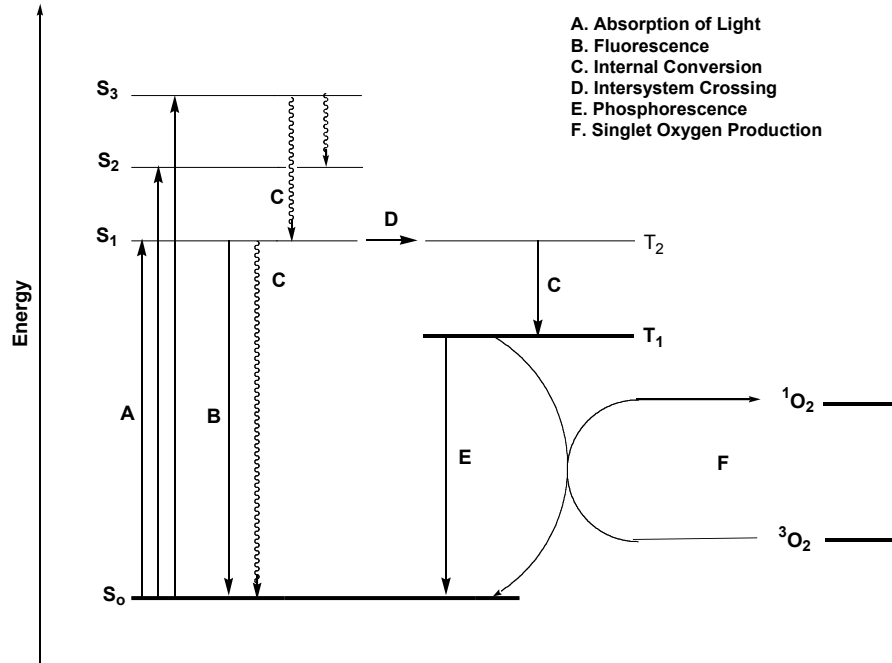


Figure 1: Modified Jablonki diagram for a typical photosensitizer.

PDT is not only used for cancer treatment but also to treat age-related macular degeneration (AMD), which is a disease that slowly decreases sharp, central vision. In addition, PDT is used for inactivation of microbial infections.

PDT typically entails generation of singlet oxygen. There are two mechanisms through which singlet oxygen can destroy cancer cells. In PDT-mediated cancer treatment, the drug (photosensitizer) initially localizes near the outer carcinoma cell membrane. Later, microvascular cells are destroyed by singlet oxygen. In an alternative route, the photosensitizer dye can penetrate cell membranes and destroy mitochondria thereby causing cell death or apoptosis. The former mechanism is more common and consistent for AMD and cancer.³ Members of the porphyrin family (porphyrins, chlorins, bacteriochlorins) are

potential candidates for PDT due to their strong light absorption, high triplet quantum yield, and long excited triplet state lifetime.⁴

An essential requirement for a molecule to act as a photosensitizer is that it must strongly absorb in the visible (if not the near-infrared) region. With an increase in the absorption intensity in the red region the capacity of tissue penetration increases. Key steps of photodynamic therapy include the following: (1) injection of a photosensitizer into the diseased organism, (2) accumulation of the photosensitizer near the diseased tissue, (3) activation of photosensitizer by light irradiation, and (4) destruction of unwanted or diseased cells by the photosensitizer without affecting healthy cells at other sites in the organism.

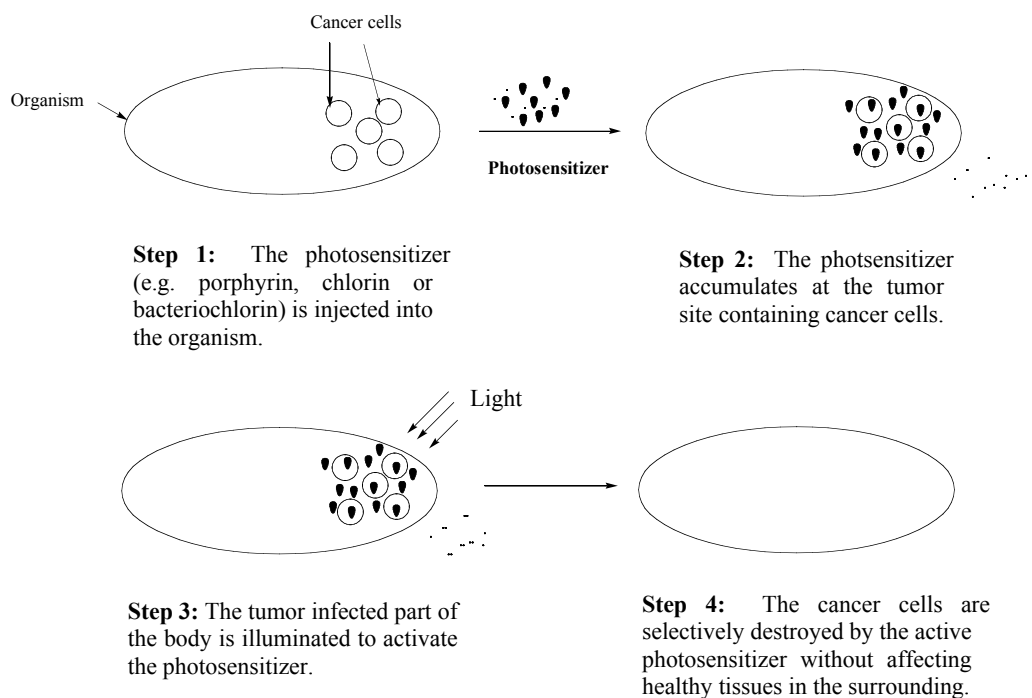


Figure 2: Mechanism of photodynamic therapy for killing cancer cells.

There are numerous potential PDT agents under investigation, including Vertoporphin (a benzoporphyrin derivative) for treating age-related macular degeneration (AMD),⁵ and Photofrin[®] (Porfimer sodium), for treating Barrett's lymphoma (esophageal cancer).⁶ Photofrin II is a complex mixture of monomer, dimer and higher oligomers obtained by partial purification of haematoporphyrin derivative (HpD). There are certain limitations for using Photofrin, such as a weak molecular absorption coefficient in the red region (i.e., at the clinically useful 630 nm wavelength).

PDT with use of lasers and photosensitizers to treat tumors in the human body was first applied in 1980's by Dr. T. J. Dougherty of the Roswell Park Cancer Institute in New York. He treated lung cancer by the intravenous delivery of HpD (5.0 mg/kg body weight) 72 hrs prior to shining the laser. This is the first known example where PDT was used to treat a patient with lung cancer. The patient remained disease-free for up to five-years.⁷

Another valuable porphyrinic photosensitizer is protoporphyrin IX. Protoporphyrin IX (PPIX) is the ligand for heme, and can be obtained by the removal of Fe(II) ion from heme. PPIX molecules (free base and metal chelates) are efficient photosensitizers. One attractive delivery strategy is to administer δ -aminolevulinic acid (ALA), the biosynthetic precursor to PPIX and heme. In this approach, the cells of the body respond by biosynthesizing PPIX, and the lack of sufficient iron (or iron-insertion enzymes at the location of biosynthesis) leads to production of PPIX. PPIX, like most free base porphyrins, is a potent photosensitizer, whereas the iron chelate is not.

Recent work by Kobuke's group showed the efficiency of water-soluble imidazolyl-porphyrins as PDT agents.⁸ The phototoxicity of the bis(imidazolyl)-porphyrins was tested on HeLa cells. The water-soluble imidazolyl-porphyrins showed cell killing capacity

comparable to hematoporphyrin (Hp) derivatives. A key part of this thesis has been to learn how to better synthesize, characterize, and manipulate imidazole-porphyrins, which has required the development of new synthetic methodology.

3. Imidazolium-Porphyrins

Photodynamic antimicrobial chemotherapy (PACT) or antimicrobial PDT has recently been used as a means of oxidative damage of microbial pathogens.⁹ Photosensitizers with different structural features show variable efficacy toward killing bacteria. Recent studies revealed better activity of porphyrins bearing cationic groups than those bearing anionic groups towards both Gram positive and Gram negative bacteria.

One of the most studied cationic porphyrins is *meso*-tetrakis(*N*-methylpyridinium-4-yl)porphyrin (TMPyP). Three binding modes have been described for the interaction of TMPyP with DNA: (i) intercalation, (ii), outside groove binding, (iii) outside binding with porphyrin self-stacking. Studies on the interaction of porphyrins with DNA showed that cationic porphyrins can easily bind to the negatively charged backbone of DNA.¹⁰ It was also found that the β -substituted cationic porphyrins exhibit a different binding mode with stronger interaction with DNA versus the corresponding *meso*-substituted porphyrins. Stronger interaction in this case can be attributed to the larger steric and electronic effects on β -substituted porphyrins over the *meso*-substituted porphyrins. Cationic porphyrins are able to undergo palladium-catalyzed cross-coupling reactions in both aqueous and organic medium;^{11,12} therefore, further derivatization of the cationic porphyrins is possible.

Imidazoles are known to possess a range of medicinal uses.^{13,14} Imidazoles are known to act as antibacterial agents, antifungal agents, and anti-inflammatory agents.¹³

Depending on the groups present at the 2- or 4/5- position of the imidazole unit, the reactivity and the biological activities of imidazoles vary drastically.

Cationic porphyrins are potential candidates for PDT (and also DNA-cleavage agents). Dicationic bis(imidazoliumyl)-substituted metalloporphyrins interact with DNA¹⁵ and tetracationic tetrakis(imidazoliumyl)-substituted metalloporphyrins function as potent SOD (superoxide dismutase) mimics (Chart 3).¹⁶ SOD activity was examined for both alkylimidazole- and alkylpyridyl-substituted porphyrins. The SOD activity of manganese(III) porphyrins is governed by their metal-centered redox potential, and a number of structural variations, including *meso* and β -substitution (Chart 4).¹⁷ While SOD activity is not relevant to our work described herein, the pursuit of SOD activity has led to the synthesis of a variety of imidazolium-porphyrins. Conversely, the synthetic methodology described herein may be useful in such SOD studies.

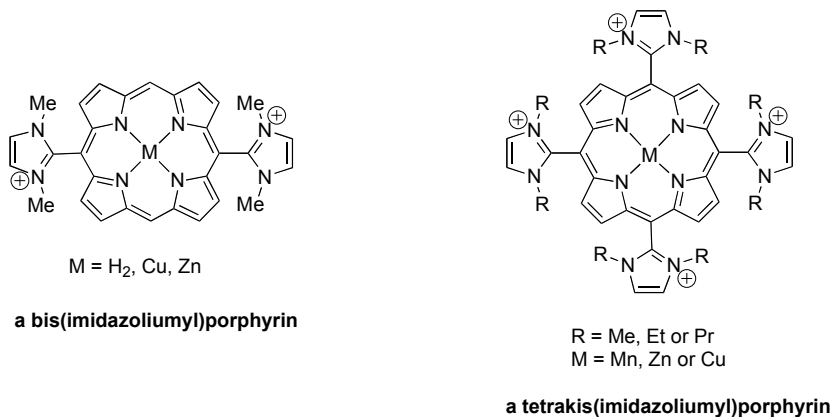


Chart 3

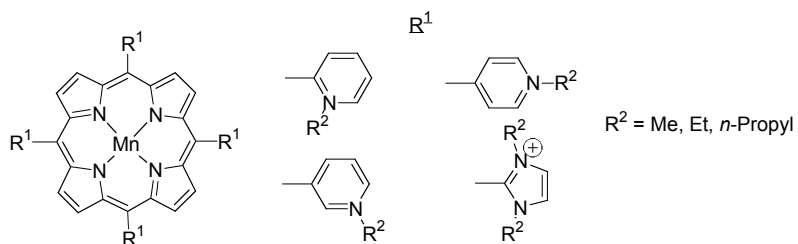


Chart 4

4. Protoporphyrin IX Molecules

Iron-containing [Fe(II)] protoporphyrin IX (PPIX) is called heme.¹⁸ Heme is an essential constituent of cells. Heme serves as the prosthetic group for enzymes such as cytochromes and peroxidases. Heme is also responsible for the oxygen-carrying capacity of hemoglobin. Apart from its role as an essential constituent of a variety of proteins, heme is known to induce cellular differentiation.

Protoporphyrin IX and its metal derivatives have been used as photosensitizers in photodynamic therapy (PDT) for the treatment of cancer. PPIX after penetration into human red blood cells can release oxygen thereby changing the morphology of the cells. Also, from the spectrophotometric studies it was observed that PPIX can interact with hemoglobin and myoglobin and can form a complex.¹⁹ Hepatocellular carcinoma can be cured by the application of PPIX molecules. *In vitro* and *in vivo* studies show that protoporphyrins accumulate into hepatocytes after the administration of δ -aminolevulinic acid and kill those cells and tissues upon irradiation of laser light.²⁰ Differential binding of Fe(II) and Zn(II) PPIX to synthetic four-helix bundles has been observed.²¹ PPIX dimethyl esters were converted to the corresponding chlorin derivative which demonstrated strong absorption at nearly 670 nm. The chlorin prepared herein showed remarkable anti-tumor activity as a photosensitizer.²² Cobalt protoporphyrin IX (CoPPIX), which is a synthetic analog of heme, can enhance tremendous and prolonged decreases in appetite and body weight in various animals.²³

A discussion of heme would be incomplete without mentioning malaria. Malaria is one of the major public health hazards, infecting 300–500 million people and killing about 1 million people, mostly children, each year [World Health Organization (WHO) 2001]. The

situation deteriorated due to the spread of both drug-resistant *Plasmodium* strains and insecticide-resistant vectors. It is known that the malaria parasite can obtain heme by the degradation of hemoglobin. Afterwards, hemozoin (malaria pigment) is formed. Hemozoin can destroy heme by reacting with hydrogen peroxide or glutathione. Polymerization of β -hematin [ferriprotoporphyrin IX, Fe(III)PPIX] prevents heme toxicity and is the primary target of the quinoline type antimalarial drugs. The metalloporphyrins are potent inhibitors of heme polymerization due to a π - π interaction between heme and the central metal ion. Hence the in vitro antimalarial activity against *Plasmodium falciparum* and heme polymerization were evaluated for more than ten metalloprotoporphyrins [e. g. Ga(III), Ag(II), Pd(II), Co(II), Mn(II), Sn(II), Cr(III)].²⁴ The Ag(II), Pd(II), Co(II) and Mn(II) chelates of protoporphyrin IX strongly inhibited growth, whereas the PPIX chelates that incorporate Sn and Cr showed weak antimalarial activity.

Apart from the importance of PPIX and its metal derivatives described above, PPIX compounds are also considered to be promising candidates for anti-cancer chemotherapeutics,^{25,26} anti-viral agents²⁷ and anti-bacterial agents²⁸. Light-activated antimicrobial materials with potential applications in civilian settings have been prepared by grafting PPIX and ZnPPIX macromolecules to nylon fibers.²⁹ Naturally occurring ZnPPIX present in erythrocytes was found to inhibit FePPIX crystallization in *Plasmodium* through binding with FePPIX crystals.³⁰ Additionally, nature uses PPIX to generate *chlorophyllide a*, which is a precursor to chlorophyll pigments.³¹ The phototoxicity of protoporphyrin IX as a photosensitizer has been studied on peptidyl derivatives such as diarginine diprotoporphyrinate (PP(Arg)₂) and *N,N*-diphenylalanyl protoporphyrin (PP(Phe)₂).³² However, both (PP(Arg)₂) and (PP(Phe)₂) showed weaker phototoxicity than PPIX. Weaker

phototoxicity of (PP(Arg)₂) compared to PPIX can be explained in terms of the greater solubility of the title compound compared to PPIX. Weaker phototoxicity of (PP(Phe)₂) is presumably due to the steric hindrance by the phenylalanyl substituents on the pyrrole ring.

Protoporphyrin IX exhibits amphiphilic properties because of the presence of two peripheral adjacent propionate groups and a large hydrophobic surface.³³ In alkaline aqueous solutions PPIX molecules are expected to form stable face-to-face dimers with head-to-tail disposition of the charged carboxylate groups. Due to the formation of a hydrogen-bonded network between the partially neutralized carboxylic acid side chains at intermediate pH values, an extended supramolecular structure can form. In the presence of water or pyridine, heamin chloride [the trivalent Fe(III)Cl species] forms the corresponding coordination complex.³⁴

In this thesis, we also have prepared a series of metal chelates of protoporphyrin IX and examined the activity of such metal chelates in PDT. It was to our surprise that the synthetic manipulations for preparing metal chelates of protoporphyrin IX are not thoroughly described in the literature, and not without difficulties. The chief limitation stems from the presence of the two vinyl groups on one side of the macrocycle and two propionic acid substituents on the other side, thereby affording an amphipathic molecule with inherent solubility limitations.

The solubility limitations of protoporphyrin IX have caused difficulties in characterization. In order to develop a method for forensic characterization of the use of blood agar in the preparation of Bacillus spores, a group of scientists (Fenselau and coworkers) from the University of Maryland and the FBI have found that aqueous ammonium hydroxide to be the best solvent for PPIX.³⁵ Fenselau and coworkers have also

found that sinapic acid is the best matrix for MALDI-TOF analysis of PPIX due to the minimal presence of an interfering matrix and the production of good signal intensity when compared to the other matrices such as 4-hydroxy- α -cyanocinnamic acid (HCCA) and 2,5-dihydroxybenzoic acid (DHB). Characterization of the cobalt(III)protoporphyrin IX chelate was performed by MALDI-TOF-MS analysis to prove the efficiency of the above-mentioned matrix.

5. Overview

The following sections delineate our work in preparing novel porphyrin-containing molecules for studies in PDT. As part of methodology development for preparing imidazole-porphyrins, we have carried out extensive heteronuclear (^{11}B , ^{15}N) NMR spectroscopy of imidazole-substituted dipyrromethane intermediates. Dialkylboron complexation has been used to facilitate handling of such intermediates. Finally, a study aimed at gaining access to hydroxymethyl-porphyrins was carried out, followed by an exploratory investigation of routes to formyl-chlorins. Taken together, this work advances the available methodology for preparing a variety of porphyrinic molecules, including those of interest for PDT and other biological applications.

References

- (1) Castano, A. P.; Mroz, P.; Hamblin, M. R. *Nature Rev. Cancer* **2006**, *6*, 535–545.
- (2) Sternberg, E. D.; Dolphin, D.; Brückner, C. *Tetrahedron* **1998**, *54*, 4151–4202.
- (3) <http://www.coherent.com/Applications> (Web accession date 3/20/2007)
- (4) Yu, J. H.; Weng, Y. X.; Wang, X. S.; Zhang, L.; Zhang, B. W.; Cao, Y.; J. *Photochem. Photobiol. C. Chem.* **2003**, *156*, 139–144.
- (5) Gibbs, S. L.; Chen, B.; Ohara, J. A.; Hoopes, P. J.; Hasan, T.; Pogue, B. W. *Proc. SPIE* **2006**, *6139* (Optical Methods for Tumor Treatment and Detection: Mechanisms and Techniques in Photodynamic Therapy XV), 613906/1–613906/10.
- (6) Schaffer, M.; Schaffer, P. M.; Hofstetter, A.; Dühmke, E.; Jori, G. *Photochem. Photobiol. Sci.* **2002**, *1*, 438–439.
- (7) Kato, H.; Konaka, C.; Kawate, N.; Shinohara, H.; Kinoshita, K.; Noguchi, M.; Ootomo, S.; Hayata, Y. *Chest* **1986**, *90*, 768–770.
- (8) Ogawa, K.; Hasegawa, H.; Inaba, Y.; Kobuke, Y.; Inouye, H.; Kanemitsu, Y.; Kohno, E.; Hirano, T.; Ogura, S.-I.; Okura, I. *J. Med. Chem.* **2006**, *49*, 2276–2283.
- (9) Banfi, S.; Caruso, E.; Buccafurni, L.; battini, V.; Zazzaron, S.; Barbieri, P.; Orlandi, V.; *J. Photochem. Photobiol. B: Biology* **2006**, *85*, 28–38.
- (10) Chen, B.; Wu, S.; Li, A.; Liang, F.; Zhou, X.; Cao, X.; He, Z. *Tetrahedron* **2006**, *62*, 5487–5497.
- (11) (a) Tremblay-Morin, J.-P.; Ali, H.; van Lier, J. E. *Tetrahedron Lett.* **2005**, *46*, 6999–7002. (b) Tremblay-Morin, J.-P.; Ali, H.; van Lier, J. E. *Tetrahedron Lett.* **2006**, *47*, 3043–3046.

- (12) Simons, R.; Garrison, J. C.; Kofron, W. G.; Tessier, C. A.; Youngs, W. J. *Tetrahedron Lett.* **2002**, *43*, 3423–3425.
- (13) De Luca, L. *Curr. Med. Chem.* **2006**, *13*, 1–23.
- (14) Boiani, M.; González, M. *Mini-Reviews Med. Chem.* **2005**, *5*, 409–424.
- (15) Yamamoto, T.; Tjahjono, D. H.; Yoshioka, N.; Inoue, H. *Bull. Chem. Soc. Jpn.* **2003**, *76*, 1947–1955.
- (16) Kachadourian, R.; Johnson, C. A.; Min, E.; Spasojevic, I.; Day, B. J. *Biochem. Pharmacol.* **2004**, *67*, 77–85.
- (17) Kachadourian, R.; Menzeleev, R.; Agha, B.; Bocckino, S. B.; Day, B. J. *J. Chromatogr. B* **2002**, *767*, 61–67.
- (18) Palma, J. F.; Gao, X.; Lin, C.-H.; Wu, S.; Solomon, W. B. *Blood* **1994**, *84*, 1288–1297.
- (19) Sil, S.; Bose, T.; Roy, D.; Chakraborti, S. *J. Biosci.* **2004**, *29*, 281–291.
- (20) Egger, N. G.; Schoenecker Jr., J. A.; Gourley, W. K.; Motamedi, M.; Anderson, K. E.; Weinman, S. A. *J. Hepatol.* **1997**, *26*, 913–920.
- (21) Sharp, R. E.; Diers, J. R.; Bocian, D. F.; Dutton, P. L. *J. Am. Chem. Soc.* **1998**, *120*, 7103–7104.
- (22) Nakae, Y.; Fukusaki, E.; Kajiyama, S.; Kobayashi, A.; Nakajima, S.; Sakata, I. *J. Photochem. Photobiol. A. Chem.* **2005**, *174*, 187–193.
- (23) Galbraith, R. A.; Furukawa, M.; Li, M. *Brain Res.* **2006**, *1101*, 85–91.
- (24) Begum, K.; Kim, H.-S.; Kumar, V.; Stojiljkovic, I.; Wataya, Y. *Parasitol. Res.* **2003**, *90*, 221–224.
- (25) Ding, L.; Etemad-Moghadam G.; Meunier, B. *Biochemistry* **1990**, *29*, 7868–7875.

- (26) Ding, L.; Etemad-Moghadam G.; Cros, S.; Auclair, C.; Meunier, B. *J. Med. Chem.* **1991**, *34*, 900–906.
- (27) Ding, L.; Baljarini, J.; Schols, D.; Meunier, B.; De Clercq, E. *Biochem. Pharmacol.* **1992**, *44*, 1675–1679.
- (28) Stojilkovic, I.; Kumar, V.; Srinivasan, N. *Mol. Microbiol.* **1999**, *31*, 429–442.
- (29) Bozka, J.; Sherrill, J.; Michielsen, S.; Stojilkovic, I. *J. Polymer Sci.* **2003**, *41*, 2297–2303.
- (30) Iyer, J. K.; Shi, L.; Shankar, A. H.; Sullivan Jr., D. J. *Mol. Medicine* **2003**, *9*, 175–182.
- (31) Willows, R. D. *Nat. Prod. Rep.* **2003**, *20*, 327–341.
- (32) Bugaj, A.; Morlière, P.; Santus, R.; Haigle, J.; Dyderski, S. *Photochem. Photobiol.* **2004**, *80*, 486–491.
- (33) Scolaro, L. M.; Castriciano, M.; Romeo, A.; Patanè, S.; Cefali, E.; Allegrini, M. *J. Phys. Chem. B* **2002**, *106*, 2453–2459.
- (34) Mazumder, S.; Dugad, L. B.; Medhi, A. K.; Mitra, S. *J. Chem. Soc. Dalton. Trans.* **1988**, 2797–2801.
- (35) Whiteaker, J. R.; Fenselau, C. C.; Fetterolf, D.; Steele, D.; Wilson, D. *Anal. Chem.* **2004**, *76*, 2836–2841.

Chapter II: Synthesis, Photophysical Properties and Photodynamic Therapeutic Applications of Metallo–Protoporphyrin IX Molecules

Abstract

It has been known for many years that many microbes (particularly virulent bacteria) express specific receptors for heme and various metalloporphyrins. Nevertheless, there are no published reports that take advantage of this potential targeting opportunity to deliver photoactive tetrapyrroles to microbes. Several metal chelates of protoporphyrin IX [Ga(III), Pd(II), In (III)] were synthesized by metalation of the free base porphyrin. We have compared free base and indium-substituted protoporphyrins; these compounds should mimic the shape of the heme molecule (Fe(II)-protoporphyrin). We also examined the effect of the iron-chelator dipyridyl, which is known to induce heme receptor expression of bacteria *in vitro* by iron deprivation. Significant bacterial killing has been obtained using these porphyrin derivatives. Markedly increased killing was observed both in Gram-positive and Gram-negative bacteria after up-regulating heme receptors by iron deprivation.

The work described in this chapter stems from a collaboration with Prof. Michael Hamblin and coworkers at Harvard Medical School.

Introduction

Iron (Fe) is an essential element for most organisms, which must be obtained from the local environment. In the case of pathogenic bacteria, this fundamental element must be acquired from the fluids and tissues of the infected host. A variety of systems have evolved in bacteria for efficient acquisition of host-bound iron. Iron overload is toxic for bacterial cells, and assimilation of iron is strictly regulated.¹⁻³ Most of the bacterial genes involved in iron assimilation are expressed only under conditions of iron deficiency.^{4,5} When the intracellular iron concentration rises, these genes are repressed. While the iron-containing proteins transferrin, lactoferrin and ferritin are minor sources of microbial iron, the prevalence of heme-bound iron (80% of total body iron) means that heme [Fe(II)protoporphyrin] is the preferred source. Heme can be taken up directly or can be taken up by recognition of heme bound to proteins (hemoglobin, hemopexin, albumin, haptoglobin etc). Systems identified in *Yersinia*,⁶ *Vibrio cholerae*,⁷ *Serratia marcescens*,⁸ *Neisseriae*,⁹ *Hemophilus ducreyi*,¹⁰ *Hemophilus influenzae*,¹¹ *Shigella dysenteriae* and *E. coli*¹² are very well characterized. The heme uptake system of *Y. enterocolitica* is the most studied (Figure 1); the outer membrane receptor HemR transports heme into the periplasm by an energy-dependent process. HemR mutants are unable to grow on heme as a source of iron and/or porphyrin. *Y. enterocolitica* proteins HemT, HemU and HemV are involved in the transport of heme through the cytoplasmic membrane.¹³ Accordingly, HemT, HemU or HemV mutants accumulate heme in the periplasm, and HemU and HemV mutants are impaired in their use of heme as an iron source.

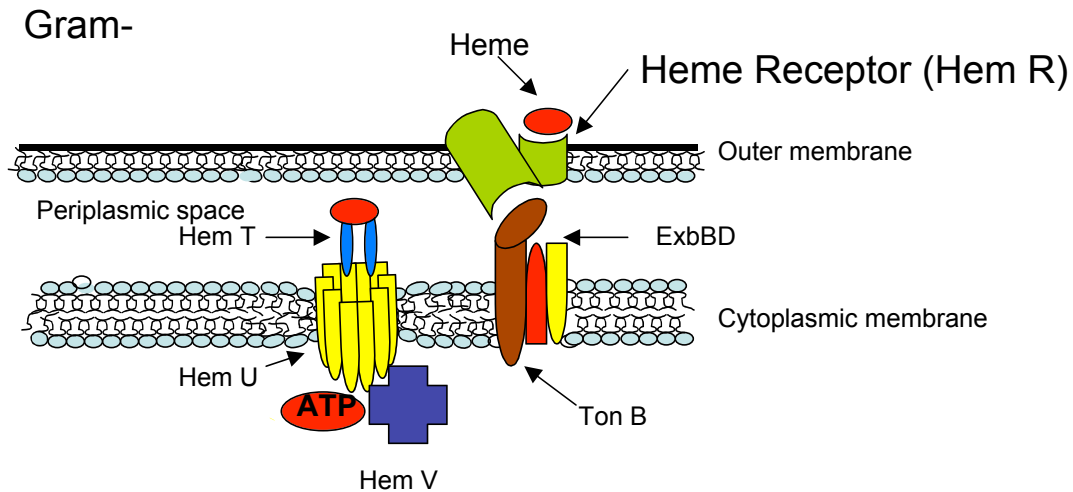


Figure 1. Heme receptor structure of Gram-negative *Yersinia enterocolitica* showing the HemR-TonB and HemT, U, V systems.

Heme uptake systems are also widespread among Gram-positive bacteria: *S. aureus*,¹⁴ *Streptococcus pneumoniae*,¹⁵ and *S. pyogenes*¹⁶ are all proficient in heme utilization. The heme uptake systems are induced to maximal expression in the iron-limiting conditions of human host fluids and tissues.¹⁷ Some bacterial species need to utilize the protoporphyrin in heme in addition to the iron because they lack one or more necessary enzymes in the heme biosynthesis pathway. This requirement applies to *Porphyromonas gingivalis*¹⁸ and *H. influenzae*.¹⁹

There has been surprisingly little research reported in the literature concerning the substrate specificity of heme uptake systems with regard to recognizing porphyrins with different metal substituents (non-Fe) and also recognizing porphyrins with different ring substituents (non-PPIX structures). Stojiljkovic et al. studied the antibacterial effect of many metal-substituted protoporphyrin derivatives and found that Ga-PPIX and In-PPIX in

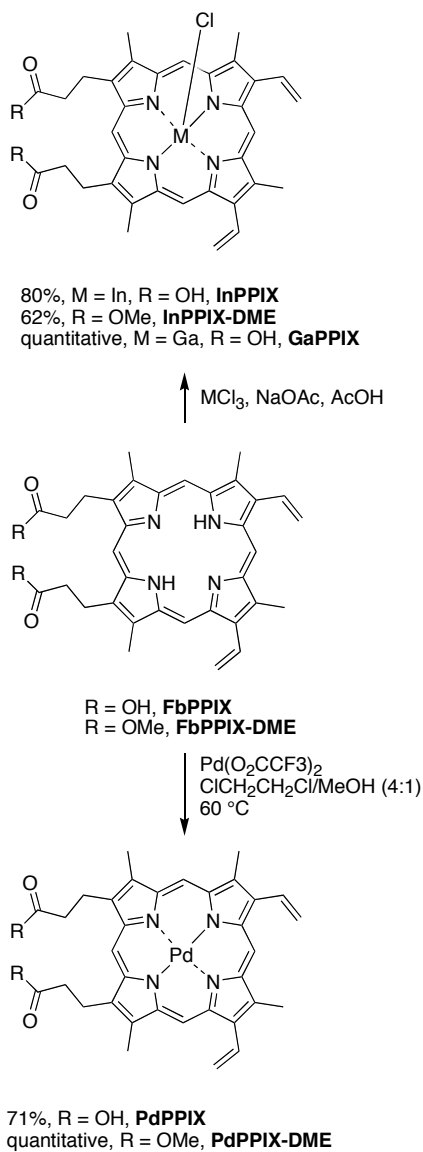
particular were bactericidal (in the dark) compared to most other metals.²⁰ It so happens that both Ga-PPIX and In-PPIX are highly effective photosensitizer due to the heavy atom effect, which increases the lifetime of the triplet state. In a set of experiments involving *E. coli* and *Y. enterocolitica* mutants of heme uptake pathway as well as by altering the level of available iron and heme in the medium, Stojiljkovic et al. demonstrated that these metalloporphyrins were recognized by heme receptors on the cell surface. It should be noted that the uptake of these porphyrins into the cells was not examined by Stojiljkovic et al. Only the growth inhibition was explained by inhibition of some vital function by these metal ions. Therefore it is uncertain whether other metalated porphyrins (e.g., Zn(II) or Pd(II)] that were not found to be highly effective, were or were not recognized by heme receptors, because these metalloporphyrins may not have had any toxicity. A study looked at some variations in the structure of heme and porphyrin analogues and their recognition by heme receptors in *P. gingivalis*.²¹ In so doing, the central metal and vinyl groups were found to have small effects on recognition, but the propionic acid side chains were very important.

Here we report the metalation of free-base protoporphyrin IX and its dimethyl ester derivative using palladium, indium or gallium salts. The solubility of the starting porphyrins as well as the resulting metal species has been examined in various solvents. All metalloprotoporphyrin derivatives were characterized by absorption spectroscopy, mass spectrometry and HPLC analysis. Taken together, the availability of different metal chelates of PPIX molecules opens access to comprehensively explore their photophysical properties and medicinal applications.

Results and Discussion

A. Synthesis of Metal Chelates of Protoporphyrin IX Molecules.

1. Metalation of Free-Base Protoporphyrin IX. Demetalation of iron from the inner core of the naturally occurring heme (an iron containing PPIX) affords free-base PPIX. PPIX thus obtained was used for further metalation.²³ Protoporphyrin IX has been metalated with a variety of metals, including Zn(II), Ga (III), Ag(II), Pd(II), Co(II), Mn(II), Sn(II), Cr(III) and In(III). However, the syntheses typically are not clearly reported or the metalloporphyrins are not thoroughly characterized. We employed commercially available free-base protoporphyrin IX (**H₂PPIX**) and protoporphyrin IX dimethyl ester (**H₂PPIX-DME**) for metalation with the corresponding metal salts such as Pd(O₂CCF₃)₂, InCl₃ and GaCl₃. The corresponding palladium, indium and gallium metal chelates of the porphyrins were obtained (Scheme 1).



Scheme 1

(a) Palladium Insertion. Following a general procedure for palladium insertion into porphyrins,²⁴ a suspension of porphyrin **H₂PPIX** in 1,2-dichloroethane/MeOH was treated with Pd(O₂CCF₃)₂. The reaction mixture was then heated at 60 °C for 22 h, affording the desired porphyrin **PdPPIX** in 71% yield (Scheme 1). Porphyrin **H₂PPIX-DME** on treatment with similar reaction conditions afforded **PdPPIX-DME** in quantitative yield. Due to possible aggregation of the palladium protoporphyrin IX molecules satisfactory ¹H NMR

data could not be obtained. However, porphyrins **PdPPIX** and **PdPPIX-DME** were characterized by absorption spectroscopy and by LDMS or MALDI-MS analysis. The purity of these compounds was established by HPLC analysis.

(b) Indium Insertion. Following a general procedure for indium insertion,²⁵ porphyrin **FbPPIX** was treated with InCl_3 , NaOAc and glacial acetic acid. The reaction mixture was heated to reflux for 22 h to afford porphyrin **ClInPPIX** in 80% yield (Scheme 1). Following a similar procedure, porphyrin **H₂PPIX-DME** was metalated to give **ClInPPIX-DME** in 62% yield.

(c) Gallium Insertion. Non-iron metalloporphyrins possess antibacterial activity against Hb/haem-utilizing bacteria.²⁰ Gallium protoporphyrin IX is known to have very strong antibacterial activity against gram-positive bacteria, gram-negative bacteria and mycobacteria. Keeping these beneficial applications in mind, we decided to insert Ga(III) into the PPIX macrocycle. Following a procedure for gallium metalation,²⁶ a sample of porphyrin **H₂PPIX** was treated with GaCl_3 and the mixture was heated to reflux in $\text{CH}_2\text{Cl}_2/\text{EtOH}$ for 12 h, affording **ClGaPPIX** in quantitative yield. In an alternative route, PPIX was metalated using GaCl_3 , acetic acid and NaOAc.²⁷

2. Solubility of Protoporphyrin IX Compounds. We have observed that the solubility of this class of compounds varies drastically depending upon the functional group (e.g. COOH vs COOMe group) and the metal atoms [e.g. Pd(II), In(III) or Ga(III)]. The observations of solubility studies are listed below:

- The free-base protoporphyrin IX (**H₂PPIX**) was found to be insoluble in CH_2Cl_2 , sparingly soluble in THF, and soluble in DMF. In comparison, **H₂PPIX-DME** was quite non-polar and was highly soluble in CH_2Cl_2 .

- Both the palladium chelates of the protoporphyrin IX (**PdPPIX** and **PdPPIX-DME**) were soluble in THF.
- In contrast, the indium chelate of the dimethyl ester species (**ClInPPIX-DME**) was partially soluble in THF whereas the corresponding carboxylic acid derivative **ClInPPIX** was completely insoluble in THF. The indium chelate of the free-base protoporphyrin IX (**ClInPPIX**) was even sparingly soluble in DMF. **ClInPPIX** was found to be soluble in water only in the presence of an inorganic base such as Na₂CO₃ or NH₄OH.
- Zinc protoporphyrin IX (**ZnPPIX**) was found to be highly soluble in THF with no aggregation.
- **ClGaPPIX** was found to be partially soluble in MeOH, was insoluble in neutral water, but dissolved well in water at pH ~8 (achieved by the addition of a few drops of NH₄OH into water).

3. Characterization of the Protoporphyrin IX Compounds. Due to the presence of extensive aggregation, satisfactory NMR spectroscopic data (¹H NMR, variable temperature NMR) could not be obtained for the metal chelates of PPIX molecules. Even though we were unable to obtain NMR spectroscopic data, we have been able to confirm the molecular formula by mass spectrometric analysis (LDMS or MALDI). We also performed HPLC analysis [size-exclusion chromatography (SEC) or reverse-phase (RP)] to establish the purity and integrity of the porphyrinic species. In all cases of metalloprotoporphyrin IX molecules either a sharp single peak or a broad peak (due to extensive aggregation) was observed indicating the presence of only one major product with no formation of polymeric

byproducts. The characterization data for all protoporphyrin IX species examined herein are summarized in Table 1.

Table 1: Characterization Data for Various Protoporphyrin IX Compounds.

Entry	UV-vis (nm)	Fluorescence (nm)	LDMS	MALDI	ESI-MS	HPLC (min)
H₂PPIX	406, 505, 540, 575, 630 (DMF)	640, 705	562.1	---	---	12.05 (SEC, THF)
H₂PPIX-DME	406, 505, 541, 576, 631 (CH ₂ Cl ₂)	640, 705	---	---	---	12.14 (SEC, THF)
ZnPPIX	418, 546, 583 (THF)	---	625.1	---	---	11.99 (SEC, THF)
PdPPIX	397, 515, 548 (THF)	---	669–812	669.6–785.7 (HCCA)	---	11.98 (SEC, THF)
PdPPIX-DME	400, 517, 549, 562 (CH ₂ Cl ₂)	---	697–820	---	---	12.02 (SEC, THF)
CuPPIX	425, 549, 582 (DMF)	---	---	671.9 (HCCA)	630.2 [(-), M ⁺ – COOH]	22.14 (RP, MeOH/H ₂ O)
CuPPIX-DME	425, 550, 583 (CH ₂ Cl ₂)	---	706.5	---	---	11.26 (SEC, THF)
ClGaPPIX	400, 535, 571 (MeOH)	525, 630	665.4	665.4 (HCCA)		19.17 (SEC, THF)

B. Results of Photodynamic Inactivation (PDI).

When *S. aureus* was grown in BHI and then PDI was carried out with 10 μM of H₂PPIX and delivery of white light at an intensity of up to 40 J/cm², phototoxicity of up to 4

logs was obtained. However, when bacteria were grown in the presence of 100 μM dipyriddy (to chelate all the available iron), the killing was increased dramatically (4-5 logs increased killing, Figure 2).

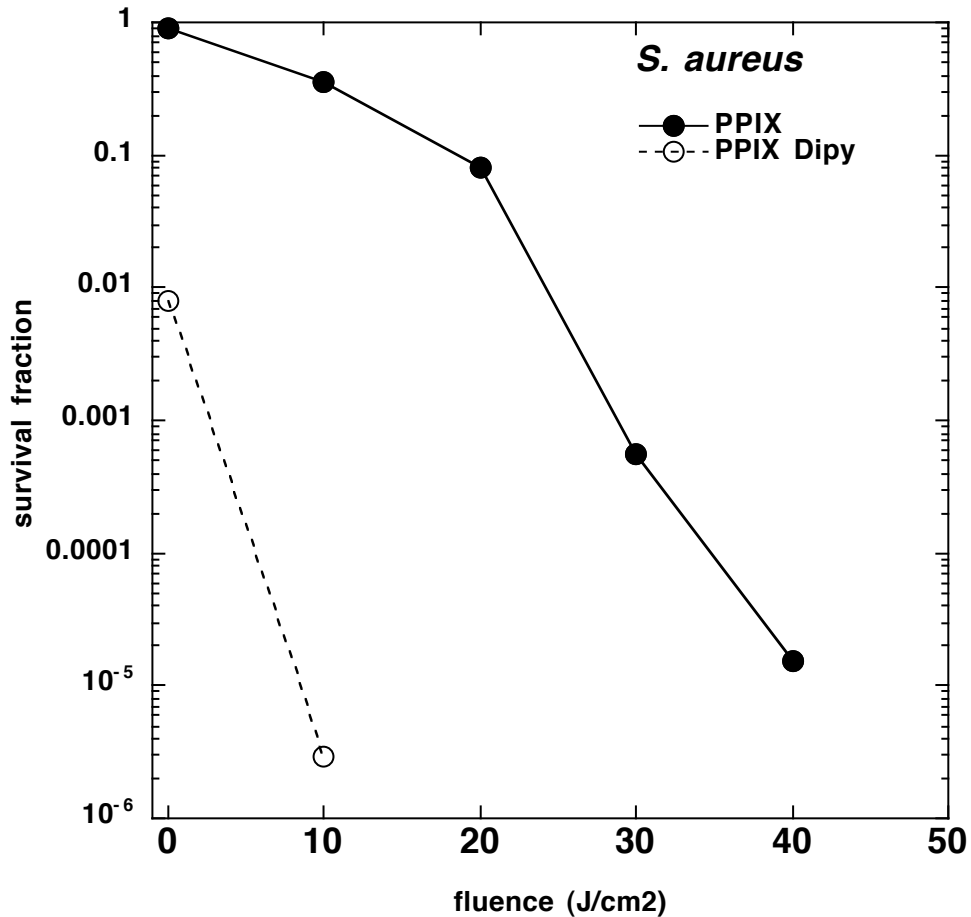


Figure 2. Survival fractions of *S. aureus* (10^8 cells/mL) grown either in BHI or in BHI containing 100 μM dipyriddy, and incubated with 10 μM H_2PPIX for 30 minutes followed by a wash and illumination with white light (400-700 nm) delivered at 100 mW/cm^2 . Aliquots were withdrawn at intervals for CFU determination.

When **ClInPPIX** was used as the photosensitizer at 10 μM , application of 40 J/cm^2 of white light gave up to 2 logs of killing in regular BHI, and up to 4 logs of killing when 100 μM dipyrindyl was added (Figure 3). Thus, **ClInPPIX** affords a higher degree of potentiation.

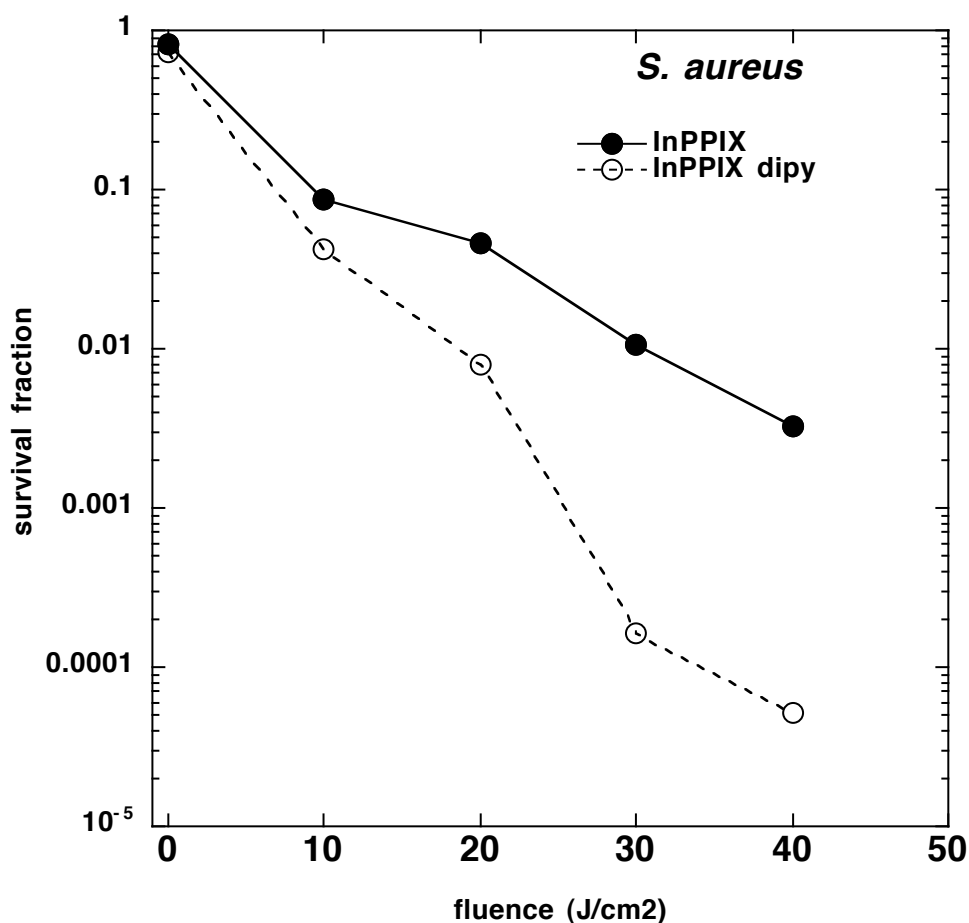


Figure 3. Survival fractions of *S. aureus* (10^8 cells/mL) grown either in BHI or in BHI containing 100 μM dipyrindyl, and incubated with 10 μM **ClInPPIX** for 30 minutes followed by a wash and illumination with white light (400-700 nm) delivered at 100 mW/cm^2 . Aliquots were withdrawn at intervals for CFU determination.

When *E. coli* grown in regular BHI was incubated with 100 μM **H₂PPIX** (a higher concentration was necessary for Gram-negative cells) followed by white light, up to 4 logs killing was obtained. Growth under iron-restricted conditions increased this amount of photokilling to 5-6 logs at the lowest light dose (Figure 4).

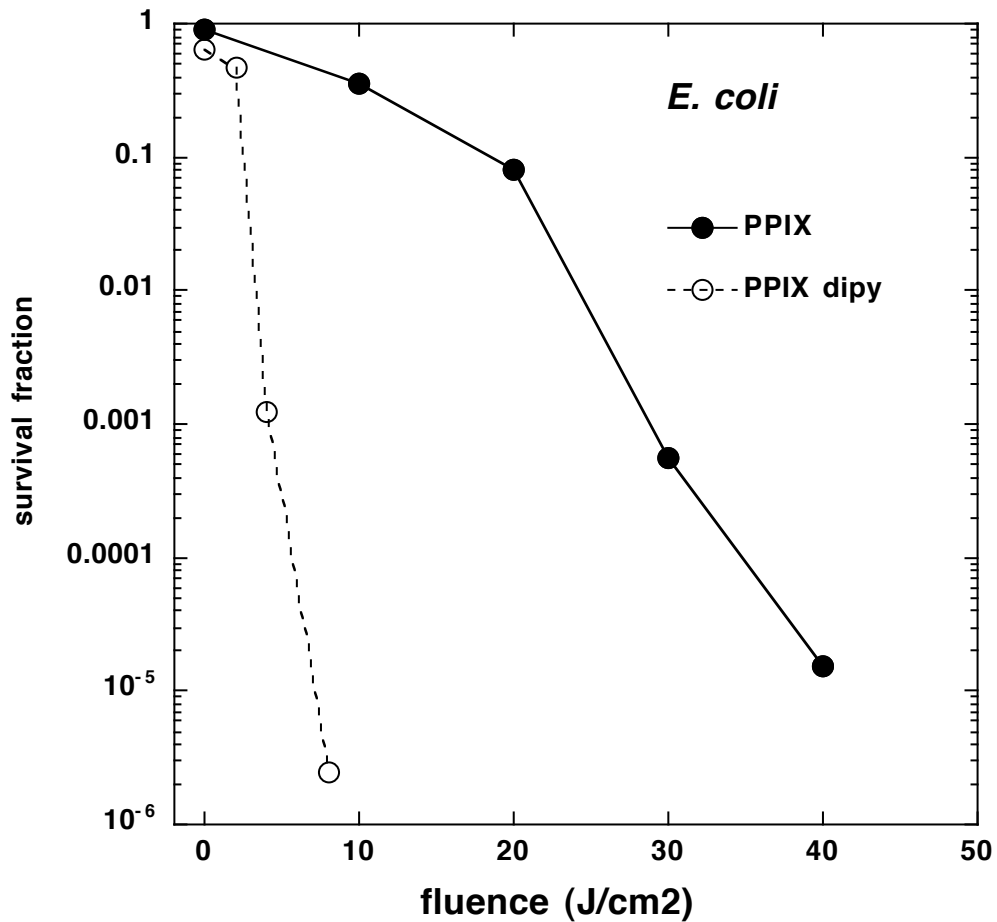


Figure 4. Survival fractions of *E. coli* (10^8 cells/mL) grown either in BHI or in BHI containing 100 μM dipyrindyl, and incubated with 100 μM **H₂PPIX** for 30 minutes followed by a wash and illumination with white light (400-700 nm)

delivered at 100 mW/cm². Aliquots were withdrawn at intervals for CFU determination.

When 100 uM **ClInPPIX** was used there was almost no killing observed in cells grown in BHI containing normal iron concentrations. However, when the cells were grown in the presence of dipyrityl there was a tremendous increase in the PDI killing observed with almost 6 logs at a low fluence of white light (8 J/cm²) (Figure 5).

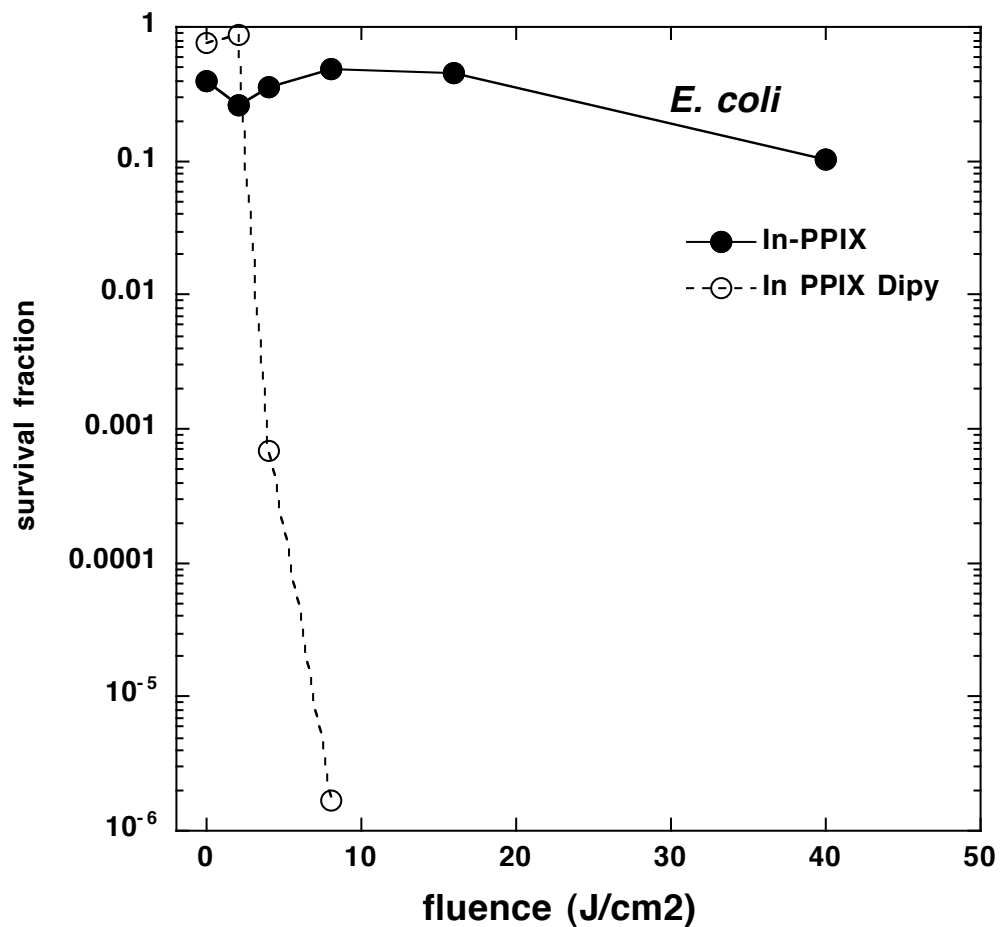


Figure 5. Survival fractions of *E. coli* (10^8 cells/mL) grown either in BHI or in BHI containing $100 \mu\text{M}$ dipyriddy, and incubated with $100 \mu\text{M}$ **ClInPPIX** for 30 minutes followed by a wash and illumination with white light (400-700 nm) delivered at $100 \text{ mW}/\text{cm}^2$. Aliquots were withdrawn at intervals for CFU determination.

C. Discussion

The prospect that heme uptake pathways could be exploited for delivery of PDT agents holds the promise for new therapeutic treatments. The data obtained herein suggest that heme receptors can be upregulated in the absence of iron and that they can recognize both **H₂PPIX** and the **ClInPPIX** derivative. Although both porphyrins demonstrated an increase of PDI killing when heme receptors were upregulated by iron deprivation, the degree of increase was different between species and porphyrins. The degree of increased killing was greatest for **H₂PPIX** in the case of the Gram-positive *S. aureus*, while for the Gram-negative *E. coli* the reverse was the case, with a greater increase of killing found when **ClInPPIX** was used. This reverse of the order of potentiation of killing may be due to differential recognition of the two porphyrins by the heme receptors of the two bacterial species. As described earlier, there are many types of heme transport systems and heme recognition units present in different microbial species; moreover, there may well be different recognition motifs operating in *S. aureus* and *E. coli* that could explain these observations. This recognition of porphyrins by heme receptors has to be combined with the fact that non-cationic species such as PPIX are known to be effective photosensitizers against Gram-positive bacteria. Such photosensitizers could effectively penetrate and photoinactivate the cells without recognition or transport by heme receptors. It appears that the heme receptors of *S. aureus* may therefore recognize the free base PPIX more than the indium chelate, while the heme receptors of *E. coli* preferentially recognize the indium derivative.

Since many authors have demonstrated that the ability to utilize heme efficiently as a

source of iron and/or porphyrin is a hallmark of virulence and pathogenicity, this finding suggests a possible route to specifically target disease-causing bacteria for photokilling thereby increasing selectivity for target pathogens.

Conclusion

We have successfully inserted Pd(II), In(III), and Ga(III) metals into the free base protoporphyrin IX and to the corresponding ester derivative. We have been able to characterize all newly synthesized metalloporphyrins using mass spectrometry and absorption spectroscopy. We have also investigated the solubility of the metalloporphyrins in various polar and nonpolar solvents. Synthesis of three different varieties of PPIX molecules opened access to determine their photophysical properties as well as medicinal properties. Thereafter a comparative study on structure versus properties relationship can be performed. The free base and indium chelate of protoporphyrin IX derivative were utilized for photodynamic inactivation studies (PDI) performed on Gram-positive and Gram-negative bacteria. Free base protoporphyrin IX (**H₂PPIX**) showed an increased degree of killing towards Gram-positive bacteria whereas indium chelate of protoporphyrin IX (**ClInPPIX**) revealed an increased rate of killing of Gram-negative bacteria. The different extent of killing of bacteria by different protoporphyrin IX species can possibly be explained in terms of differential recognition of the two porphyrins by the heme receptors of the two bacterial species.

Experimental Section

General. H₂PPIX and ZnPPIX were purchased from Sigma-Aldrich Company, and H₂PPIX-DME was purchased from Frontier-Scientific.

Microbial strains and culture conditions. *Staphylococcus aureus* (ATCC #35556) and *Escherichia coli* (ATCC #25922) were cultured in brain-heart infusion (BHI) broth (Difco, BD Diagnostic Systems, Sparks, MD) at 37 °C in aerobic conditions in a shaker at 150 rpm. Exponential cultures obtained by reculturing stationary overnight precultures were used for all experiments. *E. coli* and *S. aureus* were grown in fresh medium for approximately 1 h to a density of 10⁸ cells/mL; the OD values at 650 nm were 0.6 and 0.8, respectively. Cells were used for experiments in mid-log growth phase.

Light source. A non-coherent lamp (LumaCare LC122, MBG Technologies, Inc. Newport Beach, CA) fitted with a broad-band white light band-pass filter (400-700 nm) was employed. The lamp was adjusted to give a uniform spot of 4 cm diameter with an irradiance of 200 mW/cm² as measured with a power meter (model DMM 199 with 201 Standard head, Coherent, Santa Clara, CA)

Photodynamic inactivation (PDI) studies. The porphyrins were dissolved in DMSO to give 5-mM solutions, which were stored in the dark at room temperature. The bacterial suspension was centrifuged (4000 g for 10 min) after incubation with porphyrins, and resuspended in fresh PBS before illumination; this procedure is referred to as a wash. *E. coli* and *S. aureus* were used at concentrations of 10⁸ cells per mL. Illumination was carried out from above with cell suspensions in wells of a 24-well plate, and aliquots were removed at times corresponding to the delivery of calculated fluences of light. These aliquots were serially diluted in PBS and streaked on square BHI or YM agar plates according to the

method of Jett et al.²² Survival fractions were calculated with reference to cells incubated in PBS alone. Values on killing curves at 0 J/cm² represent the dark toxicity of the porphyrins. Cells treated with light and no photosensitizer showed any loss of viability.

Palladium(II) protoporphyrin IX (PdPPIX). Following a general procedure for palladium metalation,²⁴ a sample of **H₂PPIX** (68 mg, 0.12 mmol) in 1,2-dichloroethane/MeOH (4:1, 2.4 mL) was treated with Pd(O₂CCF₃)₂ (80 mg, 0.24 mmol). The resulting suspension was stirred and heated to 60 °C for 22 h. The mixture was concentrated and the solid residue was purified by column chromatography [alumina, toluene/THF (HPLC grade) (1:1)] to afford a red purple solid (57 mg, 71%): LDMS obsd 669.6, calcd 666.2 (C₃₄H₃₂N₄O₄Pd); HPLC (SEC, THF) 11.98 min; λ_{abs} (THF) 397, 515, 548 nm.

Palladium(II) protoporphyrin IX dimethyl ester (PdPPIX-DME). Following a general procedure for palladium insertion,²⁴ a mixture of **H₂PPIX-DME** (12 mg, 0.020 mmol) in 1,2-dichloroethane/MeOH (4:1, 0.40 mL) was treated with Pd(O₂CCF₃)₂ (13 mg, 0.040 mmol). The entire reaction mixture was stirred and heated to 60 °C for 24 h. The resulting mixture was concentrated, and the remaining solid residue was chromatographed [alumina, toluene/THF (HPLC grade) (1:1)] affording a red purple solid (14 mg, quantitative): LDMS obsd 697.4 calcd 694.2 (C₃₆H₃₆N₄O₄Pd); HPLC (SEC, THF) 12.02 min; λ_{abs} (CH₂Cl₂) 400, 517, 549, 562 nm.

Indium(III) protoporphyrin IX (ClInPPIX).²⁵ A mixture of **H₂PPIX** (68 mg, 0.12 mmol), InCl₃ (0.66 g, 3.0 mmol), NaOAc (59 mg, 0.72 mmol) and glacial acetic acid (60 mL) was stirred vigorously and refluxed for 22 h under argon. The reaction mixture was cooled to room temperature and concentrated. The resulting residue was repeatedly washed

with water to remove the excessive salt and trace amount of **H₂PPIX**. The solid residue was then dried under vacuum to afford a dark purple solid (70 mg, 80%, assuming a chloride counter ion): MALDI (HCCA) obsd 671.9, calcd 675.2 (C₃₄H₃₂N₄O₄In); ESI-MS (-) 630.2; HPLC (Reverse-phase, water/MeOH) 22.14 min; λ_{abs} (DMF) 425, 549, 582 nm.

Indium(III) protoporphyrin IX dimethyl ester (ClInPPIX-DME). Following a procedure for indium metalation of porphyrins,²⁵ A mixture of **H₂PPIX-DME** (12 mg, 0.02 mmol), InCl₃ (0.11 g, 0.50 mmol), NaOAc (10 mg, 0.12 mmol) and glacial acetic acid (10 mL) was stirred vigorously and refluxed for 24 h under argon. The reaction mixture was cooled to room temperature and concentrated. The resulting residue was taken in a separatory funnel containing a mixture of CH₂Cl₂ and water. The organic layer was separated. The aqueous layer was extracted with CH₂Cl₂ and ethyl acetate. The organic extracts were combined, washed (saturated aqueous NaHCO₃ solution), separated, dried (Na₂SO₄) and concentrated to afford a dark purple solid (9.0 mg, 62%, assuming a chloride counter ion): LDMS obsd 706.5, calcd 703.2 (C₃₆H₃₆N₄O₄In); HPLC (SEC, THF) 11.26 min; λ_{abs} (CH₂Cl₂) 425, 550, 583 nm.

Gallium(III) protoporphyrin IX (ClGaPPIX). Following a procedure for gallium metalation,²⁶ porphyrin **H₂PPIX** was dissolved in a mixture of CH₂Cl₂/EtOH (2:1) and then GaCl₃ was added. The resulting mixture was then heated to reflux for 12 h. The reaction mixture was then cooled to room temperature and concentrated. The resulting residue was taken in large volume of a mixture of ethyl acetate and water. The organic layer was separated. The aqueous layer was extracted once with ethyl acetate. The organic layers were combined and washed with water, dried (Na₂SO₄) and concentrated. The solid residue thus obtained upon treatment with ether, sonicated and centrifuged. The supernatant was

decanted and the remaining solid residue was dried to afford an orange-red solid (33 mg, quantitative): LDMS obsd 665.4, calcd 664.1 ($C_{34}H_{32}N_4O_4GaCl$); HPLC (SEC, THF) 19.17 min; λ_{abs} (MeOH) 400, 535, 571 nm; λ_{em} (MeOH) 525, 630 nm.

References

- (1) "Bacterial solutions to the iron-supply problem. Trends," Braun, V.; Killmann, H. *Biochem. Sci.* **1999**, *24*, 104–109.
- (2) "Iron acquisition by Gram-positive bacterial pathogens," Brown, J. S.; Holden, D. W. *Microbes Infect.* **2002**, *4*, 1149–1156.
- (3) "Bacterial iron sources: from siderophores to hemophores," Wandersman, C.; Delepelaire, P. *Annu. Rev. Microbiol.* **2004**, *58*, 611–647.
- (4) "Emerging strategies in microbial haem capture," Genco, C. A.; Dixon, D. W. *Mol. Microbiol.* **2001**, *39*, 1–11.
- (5) "Quelling the red menace: haem capture by bacteria," Lee, B. C. *Mol. Microbiol.* **1995**, *18*, 383–390.
- (6) "Hemin uptake system of *Yersinia enterocolitica*: similarities with other TonB-dependent systems in gram-negative bacteria," Stojiljkovic, I.; Hantke, K. *Embo. J.* **1992**, *11*, 4359–4367.
- (7) "Cloning and characterization of the *Vibrio cholerae* genes encoding the utilization of iron from haemin and haemoglobin," Henderson, D. P.; Payne, S. M. *Mol. Microbiol.* **1993**, *7*, 461–469.
- (8) "A new type of hemophore-dependent heme acquisition system of *Serratia marcescens* reconstituted in *Escherichia coli*," Ghigo, J. M.; Letoffe, S.; Wandersman, C. *J. Bacteriol.* **1997**, *179*, 3572–3579.
- (9) "The *Neisseria meningitidis* haemoglobin receptor: its role in iron utilization and virulence," Stojiljkovic, I.; Hwa, V.; de Saint Martin, L.; O'Gaora, P.; Nassif, X.; Heffron, F.; So, M. *Mol. Microbiol.* **1995**, *15*, 531–541.

- (10) "Role of the *Haemophilus ducreyi* Ton system in internalization of heme from hemoglobin," Elkins, C.; Totten, P. A.; Olsen, B.; Thomas, C. E. *Infect. Immun.* **1998**, *66*, 151–160.
- (11) "A gene cluster involved in the utilization of both free heme and heme:hempoxin by *Haemophilus influenzae* type b." Cope, L. D.; Yogev, R.; Muller-Eberhard, U.; Hansen, E. J. *J. Bacteriol.* **1995**, *177*, 2644–2653.
- (12) "Genetics and regulation of heme iron transport in *Shigella dysenteriae* and detection of an analogous system in *Escherichia coli* O157:H7," Mills, M.; Payne, S. M. *J. Bacteriol.* **1995**, *177*, 3004–3009.
- (13) "Transport of haemin across the cytoplasmic membrane through a haemin-specific periplasmic binding-protein-dependent transport system in *Yersinia enterocolitica*," Stojiljkovic, I.; Hantke, K. *Mol. Microbiol.* **1994**, *13*, 719–732.
- (14) "Iron-source preference of *Staphylococcus aureus* infections," Skaar, E. P.; Humayun, M.; Bae, T.; DeBord, K. L.; Schneewind, O. *Science* **2004**, *305*, 1626–1628.
- (15) "Hemin utilization is related to virulence of *Streptococcus pneumoniae*," Tai, S. S.; Lee, C. J.; Winter, R. E. *Infect. Immun.* **1993**, *61*, 5401–5405.
- (16) "Acquisition of iron from host proteins by the group A streptococcus," Eichenbaum, Z.; Muller, E.; Morse, S. A.; Scott, J. R. *Infect. Immun.* **1996**, *64*, 5428–5429.
- (17) "Transcription of genes encoding iron and heme acquisition proteins of *Haemophilus influenzae* during acute otitis media," Whitby, P. W.; Sim, K. E.; Morton, D. J.; Patel, J. A.; Stull, T. L. *Infect. Immun.* **1997**, *65*, 4696–4700.

- (18) "Effect of protoporphyrin IX limitation on porphyromonas gingivalis," Schifferle, R. E.; Shostad, S. A.; Bayers-Thering, M. T.; Dyer, D. W.; Neiders, M. E. *J. Endod.* **1996**, *22*, 352–355.
- (19) "Porphyrin ring source can alter the outer membrane protein profile of non-typable Haemophilus influenzae," MacIver, I.; O'Reilly, T.; Brown, M. R. *J. Med. Microbiol.* **1990**, *31*, 163–168.
- (20) "Non-iron metalloporphyrins: potent antibacterial compounds that exploit haem/Hb uptake systems of pathogenic bacteria," Stojiljkovic, I.; Kumar, V.; Srinivasan, N. *Mol. Microbiol.* **1999**, *31*, 429–442.
- (21) "Porphyrin-mediated cell surface heme capture from hemoglobin by Porphyromonas gingivalis," Paramaesvaran, M.; Nguyen, K. A.; Caldon, E.; McDonald, J. A.; Najdi, S.; Gonzaga, G.; Langley, D. B.; DeCarlo, A.; Crossley, M. J.; Hunter, N.; Collyer, C. A. *J. Bacteriol.* **2003**, *185*, 2528–2537.
- (22) "Simplified agar plate method for quantifying viable bacteria," Jett, B. D.; Hatter, K. L.; Huycke, M. M.; Gilmore, M. S. *Biotechniques* **1997**, *23*, 648–650.
- (23) "Porphyrin metalation catalyzed by a small RNA molecule," Conn, M. M.; Prudent, J. R.; Schultz, P. G. *J. Am. Chem. Soc.* **1996**, *118*, 7012–7013.
- (24) "Direct Synthesis of Palladium Porphyrins from Acyldipyrrromethanes," Sharada, D. S.; Muresan, A. Z.; Muthukumaran, K.; Lindsey, J. S. *J. Org. Chem.* **2005**, *70*, 3500–3510.
- (25) "Motional freedom of the central metal atom in apohemoglobin reconstituted with ¹¹¹In: protoporphyrin IX. Time-differential perturbed gamma-ray angular

- correlations,” Marshall, A. G.; Lee, K. M.; Martin, P. W. *J. Chem. Phys.* **1983**, *78*, 1528–1532.
- (26) “Staircase-form assembly with 5,15-bis(imidazol-4-yl)porphyrinitogallium steps,” Nagata, N.; Kugimiya, S.-I.; Fujiwara, E.-I.; Kobuke, Y. *New J. Chem.* **2003**, *27*, 1389–1390.
- (27) “Syntheses et caractéristiques physicochimiques de gallioporphyrynes à liaison σ métal-carbone,” Coutsolelous, A.; Guillard, R. *J. Organomet. Chem.* **1983**, *253*, 273–282.

Chapter III: Imidazole-Substituted Porphyrins with Central Metal Substituents as Photosensitizers for Photodynamic Therapy

Abstract

Imidazole-substituted metalloporphyrins are a novel class of potential photosensitizers for photodynamic therapy (PDT) of various diseases including cancer. Four compounds bearing charged substituents were tested in in vitro PDT studies using a human (HeLa) and a mouse (CT26) cancer cell line: an anionic Zn(II) imidazolium–porphyrin and a homologous series of three quaternized cationic imidazolium–metalloporphyrins containing Zn(II), Pd(II) and In(III)-Cl as central ligands. There was a dramatic difference between the relative phototoxicity of these compounds: Pd(II) cationic > In(III)-Cl cationic > Zn(II) cationic > Zn(II) anionic. The phototoxicity was dependent on delivered dose of white light, and on the duration of the incubation time. HeLa cells were more susceptible than CT26 cells. Induction of apoptosis was demonstrated using a fluorescent caspase assay. Fluorescent microscopy of the Zn chelate of the imidazolium–porphyrin showed localization in lysosomes; generation of intracellular ROS was demonstrated by fluorescence microscopy using dichlorodihydrofluorescein. The Pd-containing cationic porphyrin in particular has potential as a photosensitizer for PDT and its structure may also give pointers to optimum molecular features for further improved synthetic designs.

The work described in this chapter stems from a collaboration with Prof. Michael Hamblin and coworkers at Harvard Medical School.

Introduction

Photodynamic therapy (PDT) is an emerging therapy for many diseases including cancer, neovascular and hyperproliferative disorders and infections. The therapy relies on the triple interaction between a non-toxic photosensitizer or dye molecule, harmless visible light of an appropriate wavelength to be absorbed by the photosensitizer, and molecular oxygen. On absorbing a photon the photosensitizer enters the excited singlet state that then undergoes intersystem crossing to a long-lived triplet state. The triplet excited-state energy is then transferred to the ground state of oxygen (triplet state) to form the reactive excited singlet oxygen, which can damage biomolecules and kill cells.¹ Many of the traditional photosensitizers that have been used clinically are based on the porphyrin or tetrapyrrole nucleus found in such preparations as hematoporphyrin derivative.² There is a considerable amount of interest in designing and synthesizing new porphyrinoid structures with improved characteristics for investigation as possible new PDT drugs.³ These desired improved properties include: being pure characterizable compounds, having large absorption peaks in the red and near-infrared regions on the electromagnetic spectrum, and having high uptake in cancer or other pathogenic cells.⁴ For photosensitizers designed to kill cancer or other mammalian cells, it has been found that the intracellular localization of the photosensitizer is another important parameter, with photosensitizers that localize in mitochondria tending to be more powerful in killing cells than those that are found in other locations such as lysosomes.⁵

Cationic porphyrins have attracted considerable attention as effective photodynamic sensitizers.⁶ These porphyrins bind nucleic acids and have been used to selectively photocleave DNA, inhibit telomerases, and serve as carriers for oligonucleotide delivery to

tumors. The interactions of cationic porphyrins bearing five-membered rings at the *meso*-positions [e.g. *meso*-tetrakis(1,2-dimethylpyrazolium-4-yl)porphyrin [**MPzP**, M = H₂; Cu(II); Zn(II)] with synthetic polynucleotides such as poly(dG-dC)₂ and poly(dA-dT)₂ have been characterized.⁷ The process of binding the porphyrin to the polynucleotides is exothermic (and enthalpically driven) for **H₂PzP**, whereas it is endothermic (and entropically driven) for **CuPzP** and **ZnPzP**. These results have revealed that the kind of central metal ion of the metalloporphyrins influences the characteristic of the binding of the porphyrins to the DNA molecule.

Imidazolium–porphyrins are macrocycles of interest due to their biomedically relevant properties, including interaction with DNA⁸ and activity as SOD mimics.⁹ Such porphyrins with biological activities are known to contain more than one (two to four) imidazolium unit. We are interested in the photophysical properties and photosensitizing activity of metalloporphyrins that bear only one imidazolium group. Our goal is to characterize the structure-activity relationships with respect to the central metal in the imidazolium–porphyrins and the photodynamic activity.

Much experimental work has been carried out with imidazolium porphyrins owing to their activity as SOD mimics, particularly for possible treatments for oxidative stress. Oxidative stress and chronic inflammation are important features in the pathogenesis of chronic obstructive pulmonary disease (COPD).¹⁰ In this regard, it was observed that Mn(III)-*meso*-tetrakis(*N,N'*-diethyl-1,3-imidazolium-2-yl)porphyrin could act as a catalytic antioxidant for reducing tobacco smoke-induced inflammation.¹¹ Both Mn(III) *meso*-tetrakis(methoxyethoxyethylimidazolium-2-yl)porphyrin and Mn(III)-*meso*-tetrakis(methoxyethoxyethylpyridinium-2-yl)porphyrin exhibited higher SOD-like activity

than any *meso*-substituted Mn(III) porphyrin-based SOD mimic.¹² Non-cationic porphyrins such as *meso*-(4- α -bromoacetamidophenyl)triphenylporphyrin and its Zn(II), Cu(II), Ni(II) and Co(II) chelates were prepared, which were found to have activity against DNA replication inhibition in mouse melanoma B16 cells. The intercalation of Cu(II)porphyrin with plasmid DNA was detected.¹³ Photodynamic therapy (PDT) was applied for *Staphylococcus aureus* infected burn wounds in mice by using *meso*-phenyl-tris(*N*-methyl-4-pyridyl)porphyrin (PTMPP).¹⁴

Here we report the synthesis of a series of metal chelates [Zn(II), Pd(II) and In(III)] of dialkyl imidazolium–porphyrins. Photophysical and PDT studies were performed with the synthetic metalloimidazolium–porphyrins. A series of four recently prepared¹⁵ compounds were tested as photosensitizers for in vitro PDT using a human (HeLa cervical squamous carcinoma) and a mouse (CT26 colon adenocarcinoma) cancer cell line. These compounds were as follows: an anionic Zn imidazolium–porphyrin and a homologous series of three quaternized cationic imidazolium–metalloporphyrins containing Zn, Pd and In-Cl as central ligands.

Results and Discussion

A. Synthesis of Imidazole-Substituted Porphyrins.

Zn(II) and Pd(II) chelates of a cationic imidazolium–porphyrin and Zn(II) chelate of an anionic imidazolium–porphyrin (termed **MH2**, **MH4**, and **MH3** respectively) were prepared following the procedures described in the literature (Chart 1).¹⁵

Porphyrin **Zn-1-SEM** was deprotected by treating with conc. HCl in refluxing EtOH,¹⁶ affording the corresponding free-base porphyrin **1** (Scheme 1). Refluxing a mixture

of porphyrin **1** and InCl_3 in DMF for 40 h afforded indium-chelated porphyrin **CIIn-1**. Porphyrin **CIIn-1** was heated with EtI in DMF at 65 °C for 3 days affording dialkyl imidazolium–porphyrin **MH10** as a green solid. Quaternization of the porphyrin **CIIn-1** was achieved by alkylation at the pyrrolic and imino nitrogen atoms of the imidazole unit of porphyrin. Starting from the porphyrin **Zn-1-SEM** to the resulting indium imidazolium–porphyrin (**MH10**), the overall yield in three steps was 33% (assuming an iodide counterion).

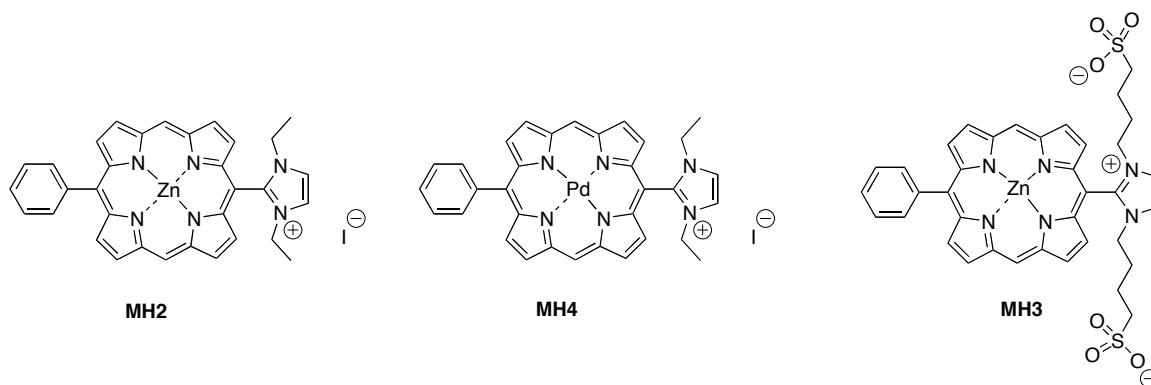
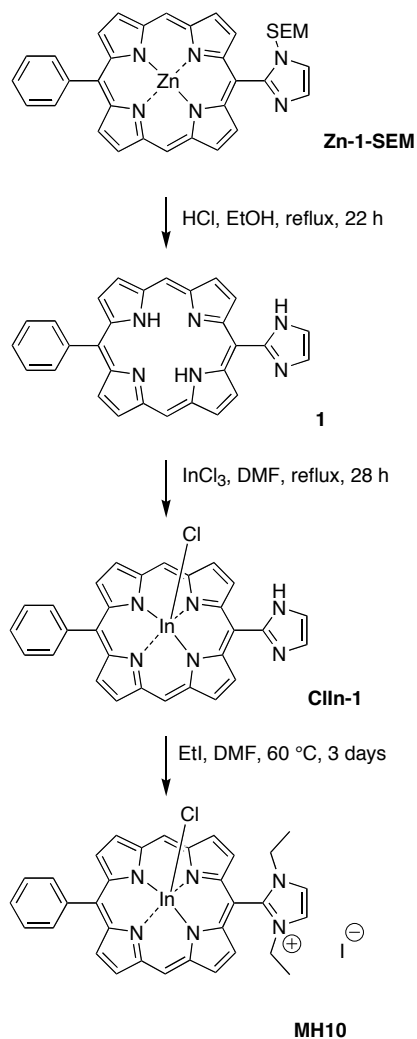


Chart 1



Scheme 1

B. Results of PDT Experiments.

We initially used a concentration of 5 μM of the compounds **MH3** and **MH2** incubated with cells for 24 h and illuminated with broad-band white light. Figure 1A depicts the light-dose dependent loss of mitochondrial activity in the two cell lines for **MH3** and Figure 1B shows the phototoxic dose response with **MH2**. In both lines **MH2** (Figure 1B) was highly effective at killing the cancer cells, while **MH3** had no effect (Figure 1A). In the case of the human HeLa cells (Figure 1B) 5 μM of **MH2** and 20 J/cm^2 killed 95% of the cells

almost reaching the level of detection of the assay, while HeLa cells were completely unharmed after 5 μM of **MH3** and 20 J/cm^2 . The mouse colon carcinoma line CT26 was less sensitive to **MH2**-mediated PDT than HeLa cells. When we tested **MH4** at 5 μM against both these cell lines, we observed large amounts of dark toxicity. Accordingly, it was difficult to measure further phototoxicity, and in addition, it appeared that the phototoxic effect was complete at the lowest fluence delivered. Therefore, we progressively reduced the concentration of **MH4** in the incubation until the value of 0.5 μM was reached. Figure 1C demonstrates a good light-dose dependent killing relationship with both cell lines, and that HeLa cells are significantly more sensitive than are CT26.

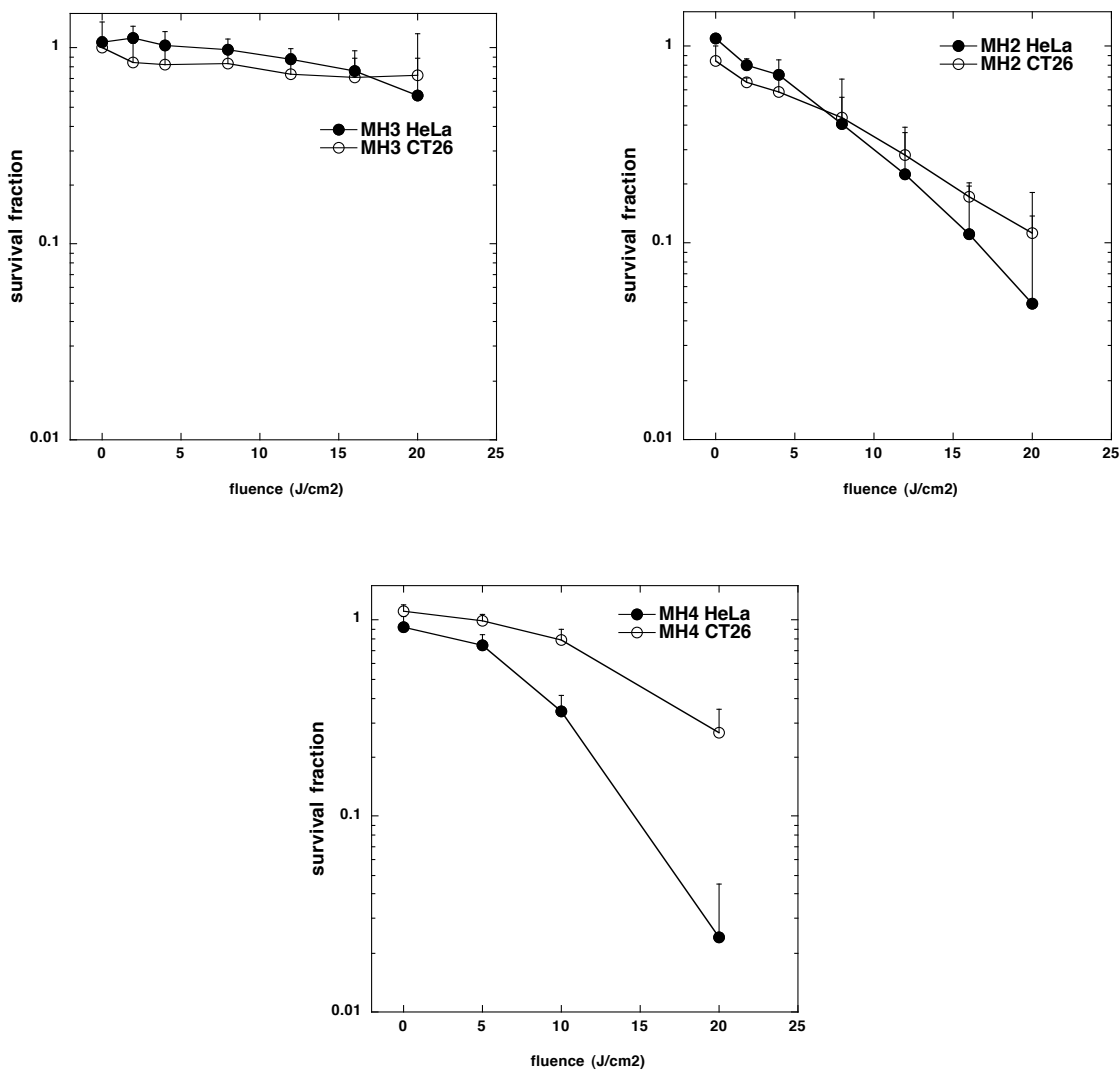
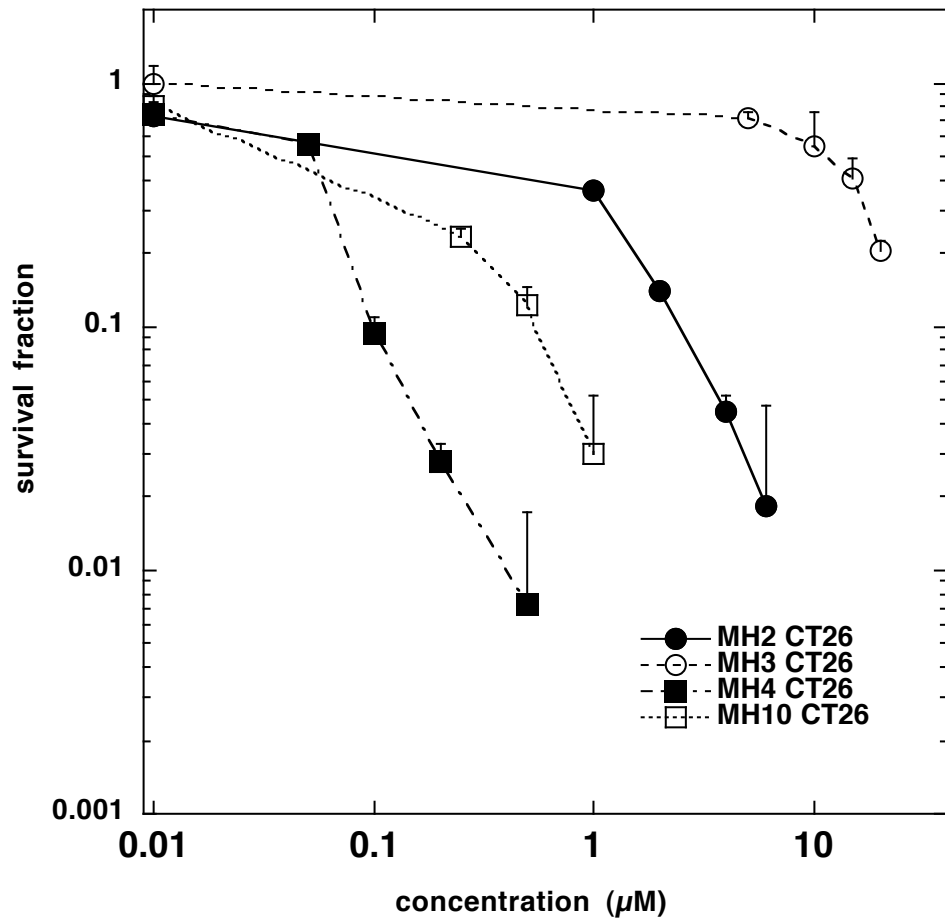


Figure 1. Broad-band white light-dose dependent killing of HeLa cervical cancer and murine CT26 colon cancer cells in culture after incubation for 24 h with imidazole porphyrins. (A) **MH3** at 5 μ M; (B) **MH2** at 5 μ M; (C) **MH4** at 0.5 μ M. Data points are means of 8 wells and bars are SD. Statistically significant differences; 1 symbol $P < 0.05$, 2 symbols $P < 0.01$, 3 symbols $P < 0.01$.

Because we did not obtain any PDT-mediated killing of any cell line using **MH3** as a photosensitizer at 5 μM , and we had to reduce the concentration of **MH4** to one tenth (0.5 μM) in order to detect light-dose dependence phototoxicity, we decided to use an increasing range of concentrations of all the photosensitizer and deliver only one constant fluence of white light (10 J/cm^2) in order to be able to derive meaningful comparisons of the effectiveness of the different compounds as photosensitizer. Since a photosensitizer may exhibit some dark toxicity when used at high concentrations, we had a dark control for each data point. Figures 2A and 2B show the photosensitizer dose dependent killing of the four compounds (the In-Cl compound **MH10** was by this time available) for both cell lines. The best way to plot this data is as a double-log plot as both the killing obtained and the concentrations used spanned a large range of values. As expected from the previous experiment, **MH4** was highly phototoxic to both cell lines with measurable killing being observed at concentrations as low as 100 nM and maximal at 500 nM. Next in the order of effectiveness was **MH10**, where concentrations between 250 nM and 1 μM showed a dose dependent phototoxicity in both cell lines with the HeLa cells again being more susceptible. The zinc chelate of cationic imidazolim-porphyrin (**MH2**) was effective at concentrations between 2 and 10 μM , while the zinc chelate anionic imidazolim-porphyrin (**MH3**) did show some phototoxicity when used at concentrations between 10 and 50 μM .



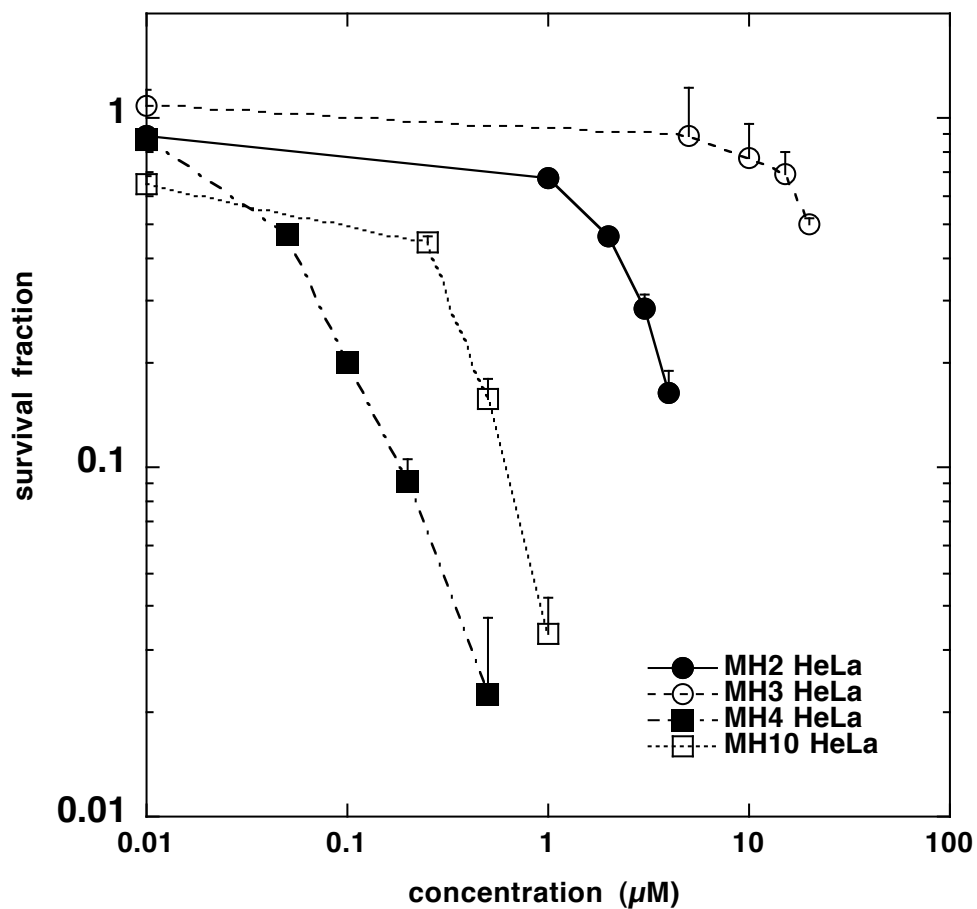


Figure 2. Graphs showing PS concentration-dependent dark toxicity (A and C) and phototoxicity (B and D) after 10 J/cm^2 white light delivered to HeLa cells (A and B) and CT26 cells (C and D). Cells were incubated with PS for 24 h, and each data point is the mean of 8 wells and bars are SD.

Although we had used an incubation time throughout these experiments of 24 h, it was not clear that this length of incubation time was necessary. Therefore, for **MH2** and **MH4** in HeLa cells we used a single concentration of 5 μM for **MH2** and 500 nM for **MH4**, together with a single fluence of 10 J/cm^2 of white light and varied the incubation time. As can be seen in Figure 3 there was increasing cell death with increasing incubation time up to 6 h, but no further increase after 24 h incubation time. Interestingly, the Pd(II) imidazolium compound **MH4** was taken up significantly faster than the equivalent Zn(II) imidazolium compound **MH2**.

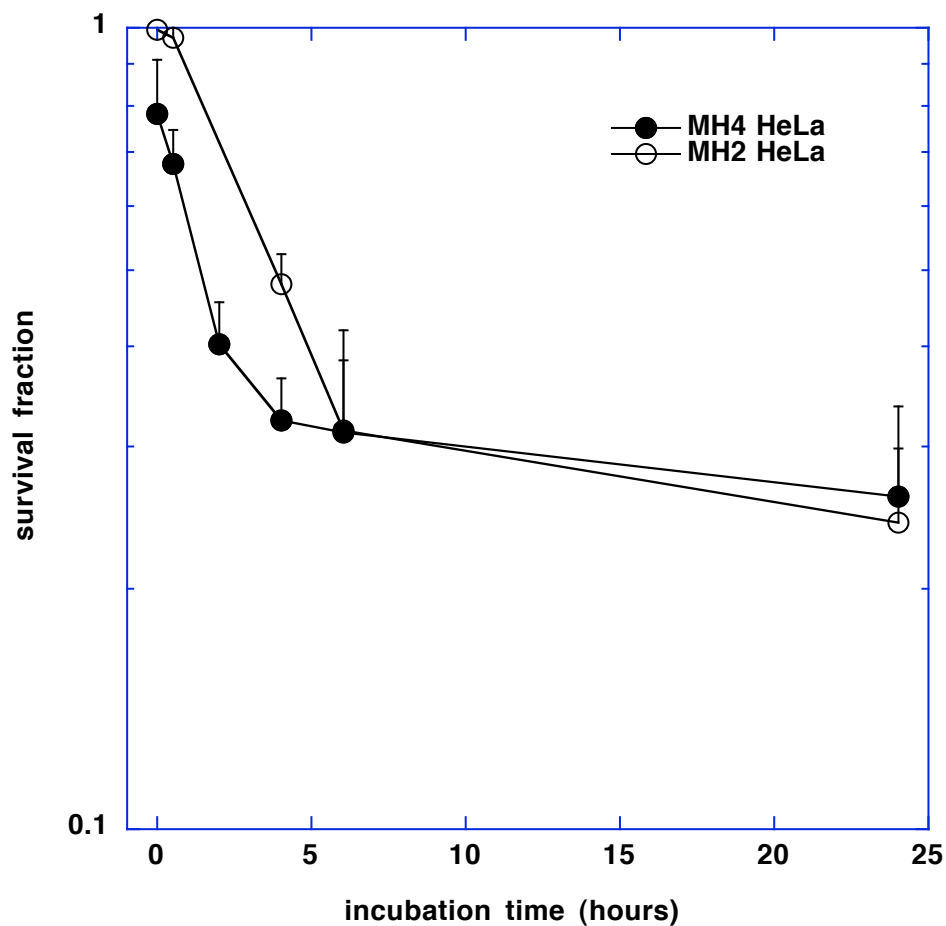


Figure 3. Effect of varying the incubation time on PDT killing of HeLa cells mediated by 5 μ M **MH2** or 500 nM **MH4** and 10 J/cm² white light. Regardless of incubation time cells were incubated for 24 h before MTT assay. Data points are means of 8 wells and bars are SD.

C. Cell Uptake Experiments.

Traditionally, the cell uptake of photosensitizers has been measured by extraction of cells after incubation with photosensitizer and quantification of the dissolved photosensitizer in the cell extract by fluorescence spectrophotometry. In the case of the four compounds studied herein, the Zn porphyrins **MH2** and **MH3** had the expected fluorescence consistent with their structure, while the In-Cl and Pd porphyrins **MH10** and **MH4** had no detectable fluorescence. This result is understood owing to the higher rate of intersystem crossing in the case of Pd(II) and In(III) chelates from the excited singlet state to the triplet state. Therefore we compared the uptake of **MH2** and **MH3** with increasing concentration in the incubation medium by fluorescence extraction in both cell lines (Figure 4). There was a dose-dependent increase in cell uptake for both photosensitizers in both cell lines. The uptake of **MH2** was higher for HeLa than for CT26 cells, consistent with the greater killing observed in HeLa cells compared to CT26 cells. The uptake of **MH3** was similar for both cell lines, and interestingly, although it was lower than that seen for **MH2**, it did not appear to be as low as might be expected from the lack of phototoxicity observed with these concentrations. This observation suggests that **MH2** is a more efficient photosensitizer on a molecule per cell basis than is **MH3**.

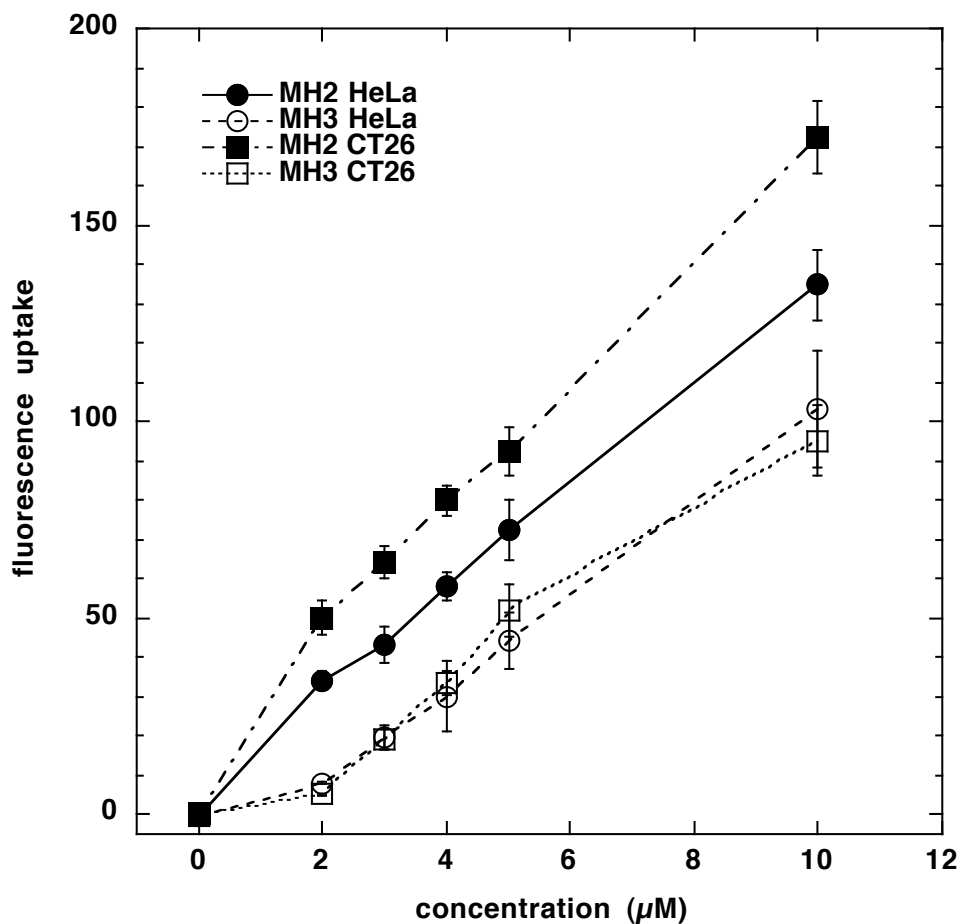


Figure 4. Cell uptake of **MH2** and **MH3** by HeLa and CT26 cells after 24 h incubation time determined by fluorescence spectrophotometry of cell extracts.

D. Fluorescence Microscopy.

Since the Zn porphyrins had sufficient fluorescence to detect, we were able to carry out confocal microscopy experiments to determine the intracellular localization of these dyes with the use of green fluorescent intracellular tracers for lysosomes and mitochondria.

E. Apoptosis.

It is known that many photosensitizers cause the death of cancer cells upon illumination by initiating the process of apoptosis via pathways involving mitochondrial damage leading to cytochrome c release, caspase activation and nuclear fragmentation.

Conclusion

Trans-AB imidazolyl-porphyrins were synthesized following recently developed rational routes to imidazolyl-porphyrins.¹⁵ Such porphyrins were alkylated at the pyrrolic and imino nitrogen of the imidazole group thereby imparting charge proximal to the porphyrin molecule. Porphyrins **MH2**, **MH3**, and **MH4** were synthesized following the procedures described in the above-mentioned literature. Indium-chelated porphyrin **MH10** was prepared as an example of a porphyrin with two positive charges. We synthesized imidazolium-porphyrins with various metal atoms [(Zn(II), Pd(II) and In(III)] so that their photophysical and photosensitizing properties could be determined in order to obtain a structure-property relationship.

A novel structure function relationship among PDT agents consisting of cationic imidazole-substituted porphyrins with different central metal atom substituents was found. There have only been a few reports of a series of porphyrinoid compounds with different central metal substituents that have been directly compared with regard to PDT effectiveness as photosensitizers *in vitro*.

As expected, the Zn(II) chelate of cationic porphyrin was a much better photosensitizer than the Zn(II) chelate of the anionic porphyrin. Cationic dyes are thought to be more easily taken up into cells by virtue of being better able to bind to the anionic plasma

membrane and therefore more likely to be internalized by endocytotic processes. Although lipophilic photosensitizers are also able to bind to cell membranes and show high uptake into cells, they are not usually water-soluble and require some delivery system such as liposomes, micelles or emulsions to deliver them into cells.

There have been several tetrapyrrole photosensitizers with central metal substituents that have been tested or proposed clinically. Such compounds include TOOKAD (a palladium bacteriopheophorbide),¹⁷ purlytin (a tin ethyl etiopurpurin),¹⁸ motexafin lutetium or Lu-tex (lutetium texaphyrin),¹⁹ MV6401 (indium chloride methyl pheophorbide),²⁰ PC4 (a silicon phthalocyanine derivative)²¹ and zinc phthalocyanine.²² Nevertheless, direct comparisons of PDT activity of any of these structures with a series of different central metal substituents have not been published. Taken together, we were able to establish different responses of metal chelates of imidazolium–porphyrins as photosensitizers towards various carcinoma cells.

Experimental Section

(A) Cell Culture. HeLa (human cervical squamous carcinoma cells),²³ and CT26 (murine colon adenocarcinoma)²⁴ were obtained from ATCC (Manassas, VA) and cultured in RPMI1600 medium (Gibco Invitrogen, Carlsbad, CA) with L-glutamine and NaHCO₃ supplemented with heat inactivated fetal bovine serum 10% (vol/vol), penicillin (100 U/mL) and streptomycin (100 µg/mL) (all from Sigma, St Louis, MO) at 37 °C in 5% CO₂ humidified atmosphere in 75 cm² flasks (BD Falcon, San Jose, CA). When the cells reached 80% confluence, they were washed with PBS (Sigma) and harvested with 2 mL of 0.25% Trypsin-EDTA solution (Sigma). Cells were centrifuged and counted in trypan blue (Sigma) and plated at 5000 cells/well in flat-bottomed 96 well plates (Fisher). Cells were allowed to attach for 24 h.

(B) PDT Experiments. The photosensitizers were dissolved in DMSO at a concentration of 5-mM and stored in the dark at room temperature. Photosensitizers were added at different concentrations to cells in fresh complete medium for 24 h incubation periods. After incubation the photosensitizer-containing medium was removed from each well, replaced with 200 µL of fresh medium, and PDT with broadband white light was performed. The light source was a non-coherent lamp fitted with a filtered light guide (LumaCare, Newport Beach, CA) delivering 400-700-nm light. For experiments where the light dose was varied we used fluences of 0 (dark toxicity), 2, 4, 8, 10, 12, 16, and 20 J/cm² delivered at an irradiance of 100 mW/cm² as measured with a power meter (model DMM 199 with 201 Standard head, Coherent, Santa Clara, CA) and 4 wells (one group) were illuminated at one time. Controls were cells with no treatment and cells with light alone at the highest fluence and both controls demonstrated no loss of viability. For experiments

where the porphyrin concentration was varied (concentrations between 100 nM and 24 μ M) we used a fixed fluence of 10 J/cm² delivered at the same irradiance. Here additional groups of cells incubated with all the concentrations of porphyrins but no illumination were used to determine the dark toxicity of the photosensitizer. At the completion of the illumination the plates were returned to the incubator for a further 24 h to allow cell death processes to occur. A MTT assay for mitochondrial activity was carried out and read at 560 nm wavelength as described previously.²⁵

(C) Synthesis of Imidazole-Porphyrins.

Noncommercial Compounds. **MH2**,¹⁵ **MH3**¹⁵ and **MH4**¹⁵ were prepared following previously reported procedures.

ClIn(III)-5-(1,3-Diethylimidazol-2-ium)-10-phenylporphyrin (MH10). Following a general procedure,¹⁶ porphyrin **Zn-1-SEM** (23 mg, 0.035 mmol) in EtOH (7 mL) was treated with conc. HCl (7 mL). The resulting mixture was refluxed for 21 h under argon. The reaction mixture was then cooled to room temperature, whereupon the volatile solvent was removed. The resulting suspension was poured into a large volume of ethyl acetate and water. Saturated aqueous NaHCO₃ solution was added slowly to the aqueous-organic mixture. The organic layer was separated, and the aqueous layer was extracted twice with ethyl acetate. The organic layers were combined and washed with saturated aqueous NH₄Cl solution and water. The organic layer was separated, dried (Na₂SO₄) and concentrated affording **1** as a dark purple solid. Data for **1**: LD-MS obsd 452.2, calcd 452.2 (C₂₉H₂₀N₆); λ_{abs} (MeOH) 402, 500, 534, 574, nm; λ_{em} (MeOH) 625, 700 nm. A solution of porphyrin **1** (~0.035 mmol) in anhydrous DMF (7 mL) was treated with InCl₃ (0.30 g, 1.4 mmol). The reaction mixture was heated to reflux for 40 h under argon. The crude reaction mixture was

concentrated. The residue was chromatographed [silica, CH₂Cl₂/MeOH (9:1) → (4:1)] affording porphyrin **ClIn-1** as a green solid. Data for **ClIn-1**: MALDI (HCCA) obsd 595.8, calcd 600.0 (C₂₉H₁₈ClInN₆); λ_{abs} (MeOH) 410, 598 nm; λ_{em} (MeOH) 620 nm. The entire sample of **ClIn-1** (~0.035 mmol) was treated with EtI (0.28 mL, 3.5 mmol) in DMF (2.0 mL), and the resulting reaction mixture was heated at 65 °C for 3 days. The reaction mixture was then concentrated and chromatographed twice [(1) silica, CH₂Cl₂/MeOH (9:1); (2) neutral alumina, CH₂Cl₂ → CH₂Cl₂/MeOH (9:1)] to afford a solid residue. The solid residue was purified by preparative size-exclusion chromatography (SEC, 3 x 30 cm) eluted with HPLC grade THF. A final chromatographic procedure [alumina, CH₂Cl₂/MeOH (9:1) → (3:1)] afforded the title compound (**MH10**) as a dark green solid (9.0 mg, 33% overall yield, assuming an iodide counterion): MALDI (HCCA) obsd 656.8, calcd 657.1 (C₃₃H₂₇ClInN₆, lacking a counterion); λ_{abs} (MeOH) 411, 601 nm; λ_{em} (MeOH) 620, 670 nm.

References

- (1) "Mechanisms in photodynamic therapy: part one--photosensitizers, photochemistry and cellular localization," Castano, A. P.; Demidova, T. N.; Hamblin, M. R. *Photodiagn. Photodyn. Ther.* **2004**, *1*, 279–293.
- (2) "Current clinical and preclinical photosensitizers for use in photodynamic therapy," Detty, M. R.; Gibson, S. L.; Wagner, S. J. *J. Med. Chem.* **2004**, *47*, 3897–3915.
- (3) "Structure and biodistribution relationships of photodynamic sensitizers," Boyle, R. W.; Dolphin, D. *Photochem. Photobiol.* **1996**, *64*, 469–485.
- (4) "What makes a good photosensitizer for photodynamic therapy?" Gomer, C. J. *J. Photochem. Photobiol. B* **1988**, *1*, 376–378.
- (5) "Mitochondrion-targeted photosensitizer enhances the photodynamic effect-induced mitochondrial dysfunction and apoptosis," Peng, T. I.; Chang, C. J.; Guo, M. J.; Wang, Y. H.; Yu, J. S.; Wu, H. Y.; Jou, M. J. *Ann. N. Y. Acad. Sci.* **2005**, *1042*, 419–428.
- (6) "Light-induced aggregation of cationic porphyrins," Mosinger, J.; Janosková, M.; Lang, K.; Kubát, P. *J. Photochem. Photobiol. A: Chem.* **2006**, *181*, 283–289.
- (7) "Binding of tetrakis(pyrazoliumyl)porphyrin and its copper(II) and zinc(II) complexes to poly(dG-dC)₂ and poly(dA-dT)₂," Tjahjono, D. H.; Kartasmita, R. E.; Nawawi, A.; Mima, S.; Akutsu, T.; Yoshioka, N.; Inoue, H. *J. Biol. Inorg. Chem.* **2006**, *11*, 527–538.
- (8) "Interaction of dicationic bis(imidazoliumyl)-porphyrinatometals with DNA," Yamamoto, T.; Tjahjono, D. H.; Yoshioka, N.; Inoue, H. *Bull. Chem. Soc. Jpn.* **2003**, *76*, 1947–1955.

- (9) "New class of potent catalysts of O₂-dismutation. Mn(III)*ortho*-methoxyethylpyridyl- and di-*ortho*-methoxyethylimidazolylporphyrins," Batinić-Haberle, I.; Spasojevic, I.; Stevens, R. D.; Hambright, P.; Neta, P.; Okado-Matsumoto, A.; Fridovich, I. *Dalton Trans.* **2004**, *11*, 1696–1702.
- (10) "Antioxidant Therapeutic Targets in COPD," Rahman, I.; Kilty, I. *Curr. Drug Targets* **2006**, *7*, 707–720.
- (11) "Inhibition of tobacco smoke-induced lung inflammation by a catalytic antioxidant," Smith, K. R.; Uyeminami, D. L.; Kodavaanti, U. P.; Capo, J. D.; Chang, L.-Y.; Pinkerton, K. E. *Free Radical Biol. Med.* **2002**, *33*, 1106–1114.
- (12) "New PEG-ylated Mn(III) porphyrins approaching catalytic activity of SOD enzyme," Batinić-Haberle, I.; Spasojevic, I.; Stevens, R. D.; Bondurant, B.; Okado-Matsumoto, A.; Fridovich, I.; Vujaskovic, Z.; Dewhirst, M. W. *Dalton Trans.* **2006**, *4*, 617–624.
- (13) "Fluorescence microscopy in the intracellular localization of non-cationic porphyrins in malignant cells," Barragan, E.; Gordillo, B.; Vargas, G.; Cortez, M. T.; Jaramillo, B. E.; Villa-Trevino, S.; Fattel-Fazanda, S.; Ortega, S.; Velazco, L. *Arcivoc* **2005**, *6*, 436–438.
- (14) "Photodynamic therapy for *Staphylococcus aureus* infected burn wounds in mice," Lambrechts, S. A. G.; Demidova, T. N.; Aalders, M. C. G.; Hasan, T.; Hamblin, M. R. *Photochem. Photobiol. Sci.* **2005**, *7*, 503–509.
- (15) "Masked imidazolyl-dipyrrromethanes in the synthesis of imidazole-substituted porphyrins," Bhaumik, J.; Yao, Z.; Borbas, K. E.; Taniguchi, M.; Lindsey, J. S. *J. Org. Chem.* **2006**, *71*, 8807–8817.

- (16) "[2-(Trimethylsilyl)ethoxy]methyl (SEM) as a novel and effective imidazole and fused aromatic imidazole protecting group," Whitten, J. P.; Matthews, D. P.; McCarthy, J. R. *J. Org. Chem.* **1986**, *51*, 1891–1894.
- (17) "Photodynamic therapy with Pd-Bacteriopheophorbide (TOOKAD): successful in vivo treatment of human prostatic small cell carcinoma xenografts," Koudinova, N. V.; Pinthus, J. H.; Brandis, A.; Brenner, O.; Bendel, P.; Ramon, J., Eshhar, Z.; Scherz, A.; Salomon, Y. *Int. J. Cancer* **2003**, *104*, 782–789.
- (18) "A phase II/III clinical study of tin ethyl etiopurpurin (Purlytin)-induced photodynamic therapy for the treatment of recurrent cutaneous metastatic breast cancer," Mang, T. S.; Allison, R.; Hewson, G.; Snider, W.; Moskowitz, R. *Cancer J. Sci. Am.* **1998**, *4*, 378–384.
- (19) "Updated results of a phase I trial of motexafin lutetium-mediated interstitial photodynamic therapy in patients with locally recurrent prostate cancer," Verigos, K.; Stripp, D. C.; Mick, R.; Zhu, T. C.; Whittington, R.; Smith, D.; Dimofte, A.; Finlay, J.; Busch, T. M.; Tochner, Z. A.; Malkowicz, S.; Glatstein, E.; Hahn, S. M. *J. Environ. Pathol. Toxicol. Oncol.* **2006**, *25*, 373–387.
- (20) "Photodynamic therapy with PhotoPoint photosensitizer MV6401, indium chloride methyl pyropheophorbide, achieves selective closure of rat corneal neovascularisation and rabbit choriocapillaris," Ciulla, T. A.; Criswell, M. H.; Snyder, W. J.; Small, W. T. *Br. J. Ophthalmol.* **2005**, *89*, 113–119.
- (21) "The synthesis, photophysical and photobiological properties and in vitro structure-activity relationships of a set of silicon phthalocyanine PDT photosensitizers," He, J.;

- Larkin, H. E.; Li, Y. S.; Rihter, D.; Zaidi, S. I.; Rodgers, M. A.; Mukhtar, H.; Kenney, M. E.; Oleinick, N. L. *Photochem. Photobiol.* **1997**, *65*, 581–586.
- (22) "Liposome-bound Zn (II)-phthalocyanine. Mechanisms for cellular uptake and photosensitization," Rodal, G. H.; Rodal, S. K.; Moan, J.; Berg, K. *J. Photochem. Photobiol. B* **1998**, *45*, 150–159.
- (23) "Cultivation of large cultures of HeLa cells in horse serum," Perry, V. P. *Science* **1955**, *121*, 805.
- (24) "Establishment of mouse colonic carcinoma cell lines with different metastatic properties," Brattain, M. G.; Strobel-Stevens, J.; Fine, D.; Webb, M.; Sarraf, A. *M.Cancer Res.* **1980**, *40*, 2142–2146.
- (25) "Scavenger-receptor targeted photodynamic therapy," Hamblin, M. R.; Miller, J. L.; Ortel, B. *Photochem. Photobiol.* **2000**, *72*, 533–540.

Chapter IV: ^{11}B NMR and ^{15}N NMR Spectroscopic Studies of Imidazolyl–Pyrrolic Compounds

Introduction

NMR spectroscopy is an invaluable tool for confirming the chemical structure of organic compounds. The most common NMR-active nuclei include ^1H , ^{13}C , ^{11}B , ^{15}N , ^{17}O , ^{19}F , ^{31}P , ^{29}Si , ^{119}Sn , ^{195}Pt and ^{199}Hg . ^1H and ^{13}C NMR studies are very useful for structural elucidation of hydrocarbons, whereas heterocyclic compounds often benefit from the corresponding heteronuclear NMR spectroscopy.

For applications in porphyrin chemistry, we have been interested in applying ^{15}N NMR spectroscopy for structural elucidation and characterization. We also have employed dialkylboron complexation as a means of manipulating various pyrrolic and imidazolyl compounds.¹ Hence, we have employed ^{11}B and ^{15}N NMR spectroscopy. With the use of modern 2D NMR spectroscopic techniques such as gHMBC (gradient heteronuclear multiple bond correlation) and gHSQC (gradient heteronuclear single quantum coherence) methods there is diminished necessity for the presence of isotopically enriched samples, rather, the isotopes in natural abundance can be detected indirectly.

^{15}N NMR spectroscopy is particularly valuable for structural elucidation of nitrogen containing compounds when the structures are not resolvable by ^1H or ^{13}C NMR spectroscopy.² A good example is provided by the free base and the zinc chelated dipyrrens (**2a** and **Zn-2a**), which show similar ^1H NMR spectra (Figure 1). ^{15}N NMR studies of the dipyrrens would be helpful to distinguish the two different compounds. Thompson and coworkers recently described the use of ^{15}N NMR spectroscopy for the identification of

dipyrromethane compounds.³ They reported that the ^{15}N NMR resonance of the nitrogen atoms of a free-base dipyrin appears at -213.1 ppm, whereas that of the corresponding zinc analogue appears at -169.5 ppm. Therefore, where ^1H and ^{13}C NMR spectroscopy are insufficient to distinguish between the two different nitrogen-containing compounds, ^{15}N NMR spectroscopy can be utilized to support the molecular structures.

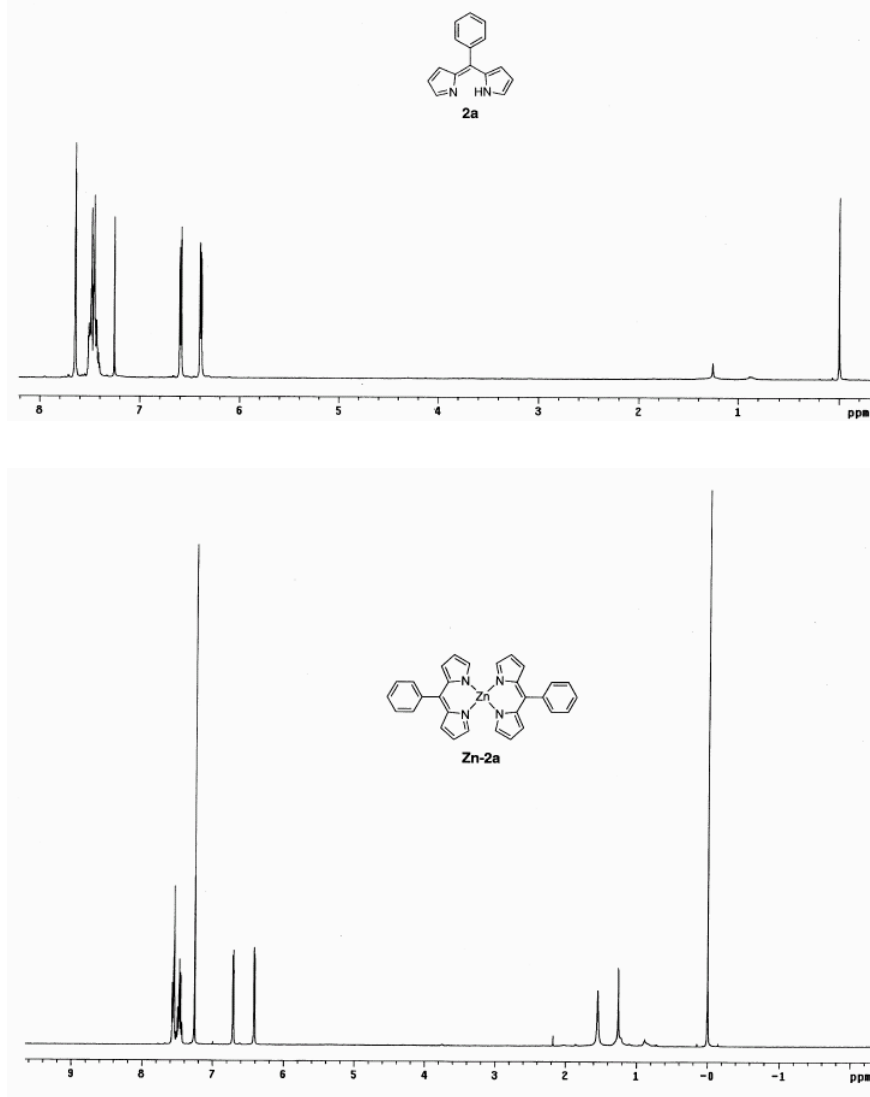


Figure 1: ^1H NMR Spectra for free-base dipyrin (**2a**) and zinc chelate of dipyrin (**Zn-2a**). The absence of the pyrrolic N-H signal in **2a** makes it difficult to distinguish **2a** and **Zn-2a** by ^1H NMR spectroscopy.

^{15}N NMR spectroscopy is widely used in the field of inorganic, organometallic and bioinorganic chemistry.⁴ ^{15}N NMR spectroscopy has been used for structural determination of pyrrolic compounds such as bile pigments,⁵ porphyrins,⁶ and the chlorin bonellin.⁷ ^{11}B NMR spectroscopy has been used in a variety of biomedical applications,⁸ particularly for compounds designed for boron neutron capture therapy (BNCT). ^{11}B NMR spectroscopy was utilized to elucidate the nature of the interaction between borate and boron-selective adsorbents such as crosslinked dextran (Sephadex).⁹ The relation between ^{11}B chemical shifts and the electronic structure of metallaboranes was examined.¹⁰ ^{11}B chemical shift values were shown to change with the nature of transition metals. Our group confirmed the presence of boron atoms in the boron complex of 1-acyldipyrromethanes through use of ^{11}B NMR spectroscopy.¹¹

There are several examples where both ^{11}B and ^{15}N NMR spectroscopy were utilized for detection purposes. For example, ^{11}B and ^{15}N NMR spectroscopy were found to be powerful tools for the estimation of hydrolytic stabilities of 8-membered boron-nitrogen-oxygen heterocycles such as *N*-alkyl-2-phenyl-1,3,6,2-perhydrodioxazaborocines.¹² The color reactions of boron with derivatives of 3-hydroxy-4-[(2-hydroxyphenyl)azo]-2,7-naphthalenedisulfonic acid and the structure of the complexes were studied by ^{11}B , ^{15}N and ^1H NMR spectroscopy. The results thus obtained provide evidence for tetrahedral coordination of boron in the complexes.¹³ Both ^{11}B and ^{15}N NMR spectroscopic techniques were also used to confirm the chain-like structure of poly(aminoboranes),¹⁴ or to monitor the interaction of absorbed MeCN with microporous [Si, Al]-ZSM-5 and (Si, B)-ZSM-5.¹⁵ Additional examples of ^{11}B and ^{15}N NMR spectroscopy include studies of trimethylamine

adducts of the mixed trihalides of boron,¹⁶ characterization of *B*-trichloroborazene ($B_3N_3H_3Cl_3$),¹⁷ investigation of structure-property relationships in boron nitrides,¹⁸ and the characterization of certain boronates.¹⁹

Here we report ^{11}B NMR data for boron complexes of dipyrromethanes, and ^{15}N NMR spectroscopic data for various imidazole-containing compounds. The presence of two boron units in 1-acyldipyrromethanes was confirmed by different chemical shift values during ^{11}B NMR spectroscopy. The presence of different types of nitrogen atoms in imidazolyl-dipyrromethanes was detected by 2D ^{15}N NMR spectroscopy. Taken together, both ^{11}B and ^{15}N NMR spectroscopic techniques are invaluable in the structural elucidation of various imidazolyl-pyrrolic compounds as well as other boron and nitrogen containing compounds.

Results and Discussion

^{15}N NMR and ^{11}B NMR Spectroscopic Studies on Imidazolyl–Pyrrolic Compounds.

Imidazolyl–porphyrins find their applications ranging from material chemistry to life sciences. Recently rational synthetic routes were developed to obtain various types of imidazolyl–porphyrins.¹ During the development of porphyrin synthetic methodology, various imidazole-containing precursors such as aldehydes, dipyrromethanes, 1-acyldipyrromethanes were synthesized. The nitrogen and boron atoms exhibit different connectivity, as shown below (Figure 2). In order to assign different types of nitrogen or boron atoms present in the imidazolyl compounds, ^{15}N and ^{11}B NMR spectroscopic studies were performed.

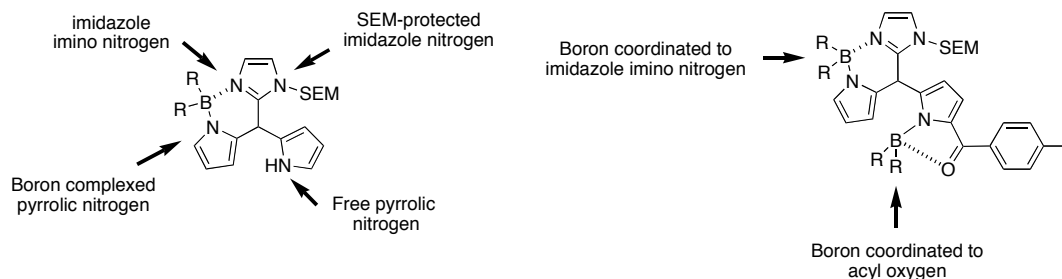


Figure 2. Demonstration of different types of nitrogen and boron atoms in the imidazolyl-pyrrolic compounds.

^{15}N NMR Spectroscopy. The assignments are revealed in Chart 1. The results of ^{15}N NMR spectroscopy are summarized in Table 1.

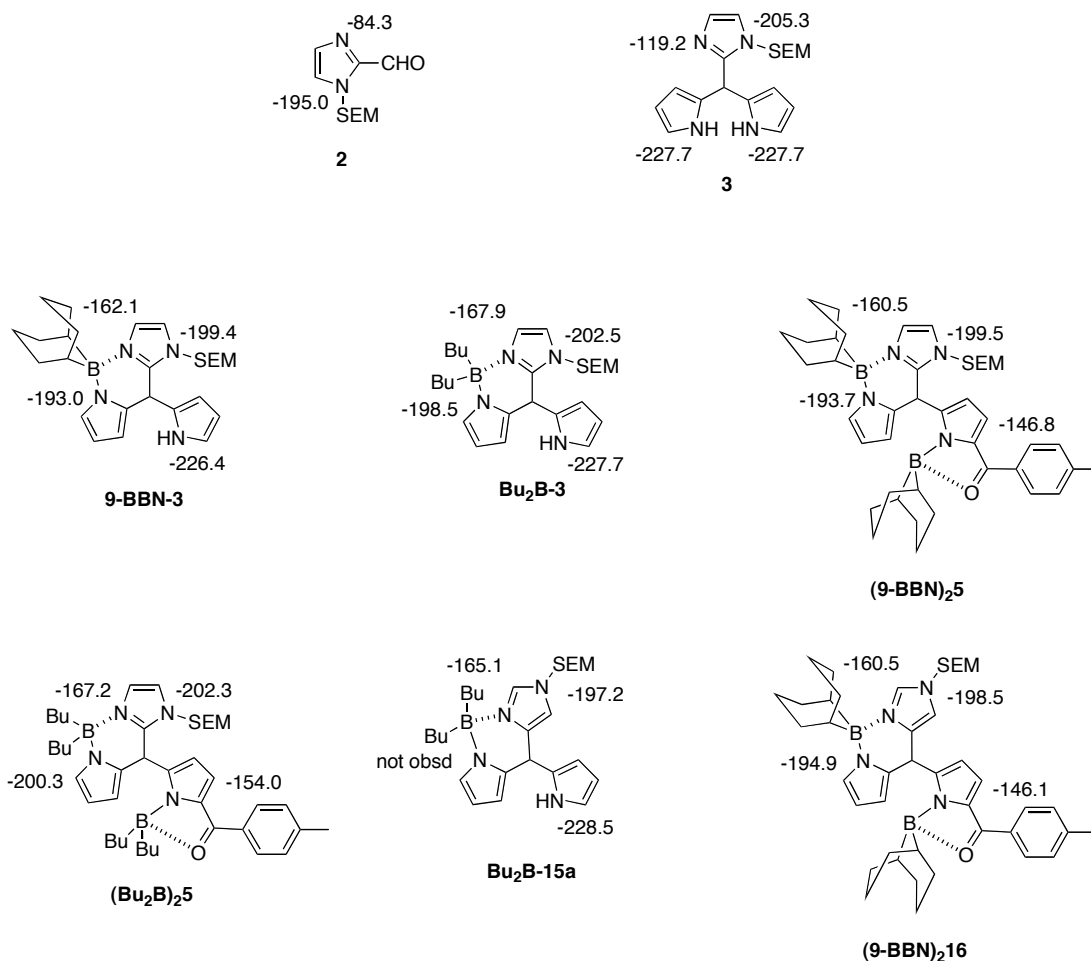


Chart 1. ^{15}N NMR chemical shift assignments

Table 1. ¹⁵N NMR Spectroscopic Data for Imidazolyl-containing Compounds.^a

Compound	δ ¹⁵ N NMR resonances (ppm) ^b	
	gHSQC	gHMBC
2	--- ^c	-84.3, -195.0
3	-227.7	-119.2, -205.3, -227.7
9-BBN-3^d	-226.4	-162.1, -193.0, -199.4, -226.4
Bu₂B-3	-227.7	-167.9, -198.5, -202.5, -227.7
(9-BBN)₂5^d	--- ^c	-146.8, -160.5, -193.7, -199.5
(Bu₂B)₂5	--- ^c	-154.0, -167.2, -200.3, -202.3
Bu₂B-15a^e	-228.4	-165.1, -197.2, -228.5
(9-BBN)₂16	--- ^c	-146.1, -160.5, -194.9, -198.5

^a ¹⁵N NMR spectroscopic data were collected with 0.2 M samples in THF-*d*₈ unless noted otherwise. ^b Chemical shifts were standardized with respect to 1.0 M MeNO₂ (δ 0.0 ppm). ^c Not applicable. ^d A 0.1-M sample was used. ^e The resonance from the boron-complexed pyrrolic nitrogen was not observed.

Proton-coupled gHMBC analysis for SEM-protected aldehyde showed two peaks (-84.3 and -195.0 ppm) corresponding to the imidazole imino nitrogen and SEM-protected imidazole pyrrolic nitrogen, respectively. Upon proton-coupled gHSQC analysis, dipyrromethane **3** showed a single peak at -227.7 ppm corresponding to the two, identical pyrrolic nitrogens. Proton-coupled gHMBC analysis for dipyrromethane **3** showed peaks at -119.2, -205.3 and -227.7 ppm, attributed to the imidazole imino nitrogen, SEM-protected imidazole pyrrolic nitrogen, and the pyrrole nitrogen, respectively.²⁰

The dialkylboron-complexed imidazole-dipyrromethane **Bu₂B-3**, **Bu₂B-15a**, or **9-BBN-3** also showed only one peak in the gHSQC experiment, owing to the single NH in each molecule. The dialkylboron-complexed dipyrromethanes **9-BBN-3** and **Bu₂B-3** each showed four peaks upon gHMBC analysis. (Compound **Bu₂B-15a** exhibited only three

peaks as the resonance from the boron-complexed pyrrole nitrogen was not observed.) For example, **9-BBN-3** revealed four resonances at distinct chemical shifts (−162.1, −193.0, −199.4, −226.4 ppm) as expected owing to the distinct environment of the imidazole imino nitrogen, the boron-complexed pyrrole nitrogen, the SEM-protected imidazole pyrrolic nitrogen, and the free pyrrole nitrogen, respectively. In general, dialkylboron complexation of the imidazole imino nitrogen caused an upfield chemical shift ($\Delta\delta = -41$ ppm for 9-BBN; -49 ppm for Bu_2B) with respect to dipyrromethane **3** (−119.2 ppm). On the other hand, dialkylborylation of the pyrrole nitrogen caused deshielding ($\Delta\delta = 35$ ppm for 9-BBN; 27 ppm for Bu_2B) compared to the free pyrrole nitrogen in **3** (−227.7 ppm).

The bis(dialkylboron) complexes of 1-acyl-5-imidazole-dipyrromethanes [(**9-BBN**)₂**5**, (**Bu**₂**B**)₂**5** and (**9-BBN**)₂**16**] typically exhibited four distinct resonances. Examination of the spectra indicate a downfield chemical shift ($\Delta\delta = 74$ – 82 ppm) for the pyrrole nitrogen complexed by an oxygen-coordinated boron moiety versus that of dipyrromethane **3** (−227.7 ppm), which can be attributed to the combined electron-withdrawing effect of the alkylboron moiety and the acyl group. The assignments of the resonances of various nitrogen atoms in the dipyrromethanes are displayed in Chart 1. Examples for 2D gHSQC and gHMBC NMR spectra of **9-BBN-3** are provided in Figure 3 and 4 respectively. In summary, ¹⁵N NMR chemical shift values were quite useful for structural comparison of compounds with multiple nitrogen atoms.

¹⁵N NMR Spectrum (gHSQC) of 9-BBN-3

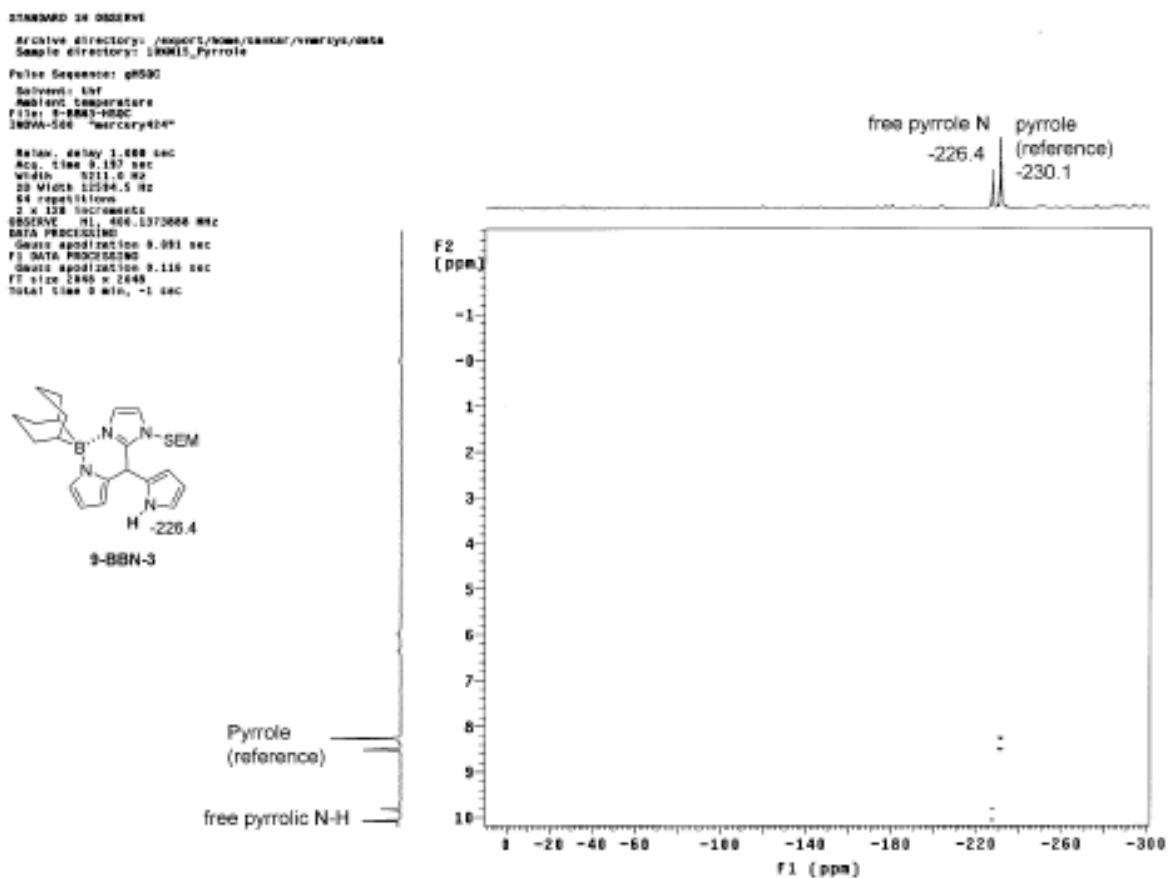


Figure 3: 2D ¹⁵N NMR (gHSQC) data for **9-BBN-3**. Due to the presence of only one free pyrrolic N-H, a single peak was observed at -226.4 ppm.

¹⁵N NMR Spectrum (gHMBC) of 9-BBN-3

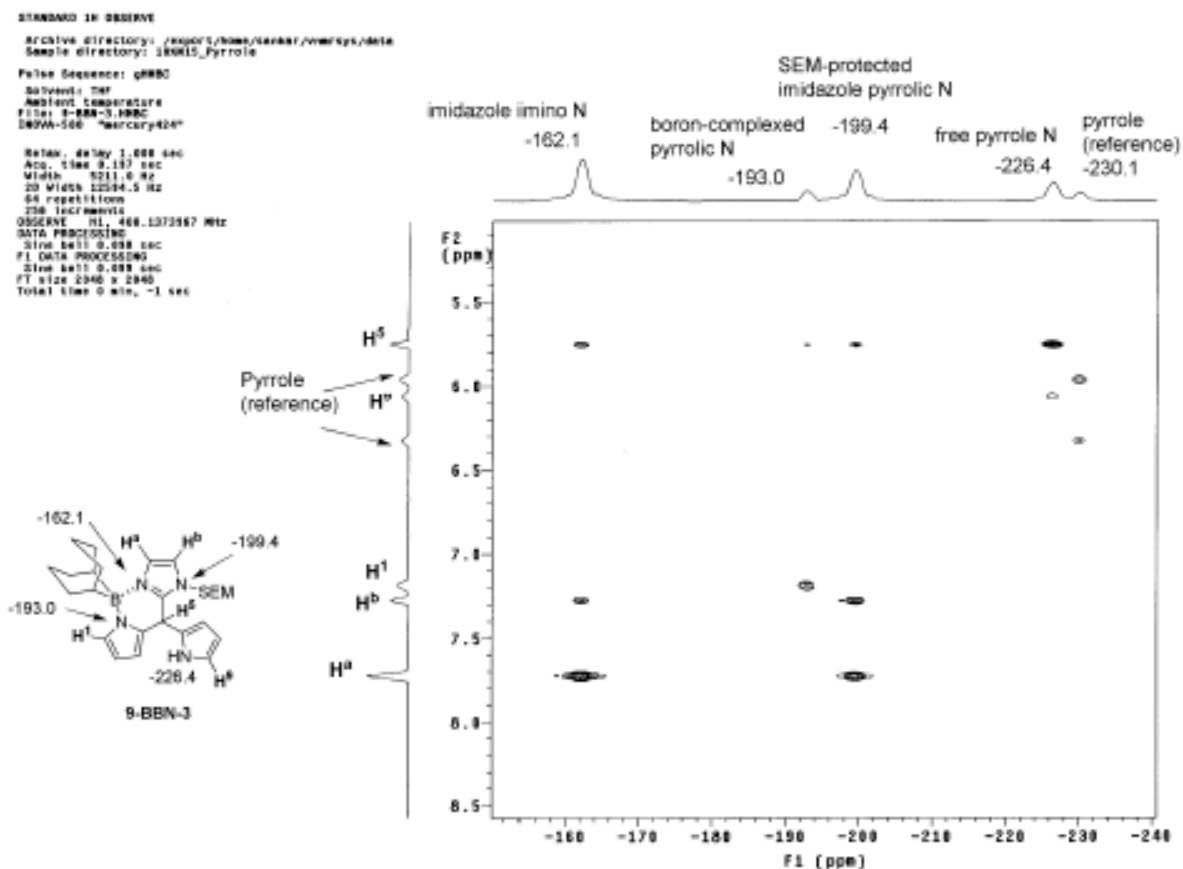


Figure 4: 2D ¹⁵N NMR (gHMBC) data for **9-BBN-3**. The presence of four distinct nitrogen atoms gives four separate signals at -162.1, -193.0, -199.4 and -226.4 ppm corresponding to the imidazole imino nitrogen, boron complexed pyrrolic nitrogen, SEM-protected imidazole pyrrolic nitrogen, and free pyrrole nitrogen respectively.

¹¹B NMR Spectroscopy. ¹¹B NMR studies were performed using 1D NMR spectroscopy with selected dialkylboron complexes of the imidazole-containing dipyrromethanes. ¹¹B NMR spectroscopy of (**9-BBN**)₂**5** showed two peaks (δ 12.65 and -0.04 ppm) for the two boron moieties relative to the ¹¹B standard (BF₃·O(Et)₂ at 0 ppm). The

two peaks are consistent with coordination of one boron atom to the carbonyl oxygen and the other boron atom to the imidazole imino nitrogen, respectively. By comparison, **Bu₂B-3** gave only one peak (1.94 ppm), to be compared with *N*-(9-borabicyclo[3.3.1]non-9-yl)pyrrole, which lacks intramolecular coordination and resonates downfield at 59.9 ppm.²¹ The results of the ¹¹B NMR studies are summarized in Table 2. In general, imidazole coordination results in an upfield resonance near that of the standard BF₃·O(Et)₂ whereas acyl oxygen coordination results in a slight downfield shift near 12-13 ppm. The ¹¹B NMR assignments are displayed in Chart 2.

Table 2. ¹¹B NMR Spectroscopic Data for Boron-Complexes of Dipyrromethanes^a

Compound	δ ¹¹ B NMR resonances (ppm)	
	N-BR ₂	O-BR ₂
Bu₂B-3	1.94	---
9-BBN-3	1.93	---
(9-BBN)₂5	-0.04	12.65
(Bu₂B)₂5	1.08	13.24
(9-BBN)₂16^b	1.44	12.06

^a¹¹B NMR spectroscopy was performed at 50 °C. ^bData were obtained at room temperature.

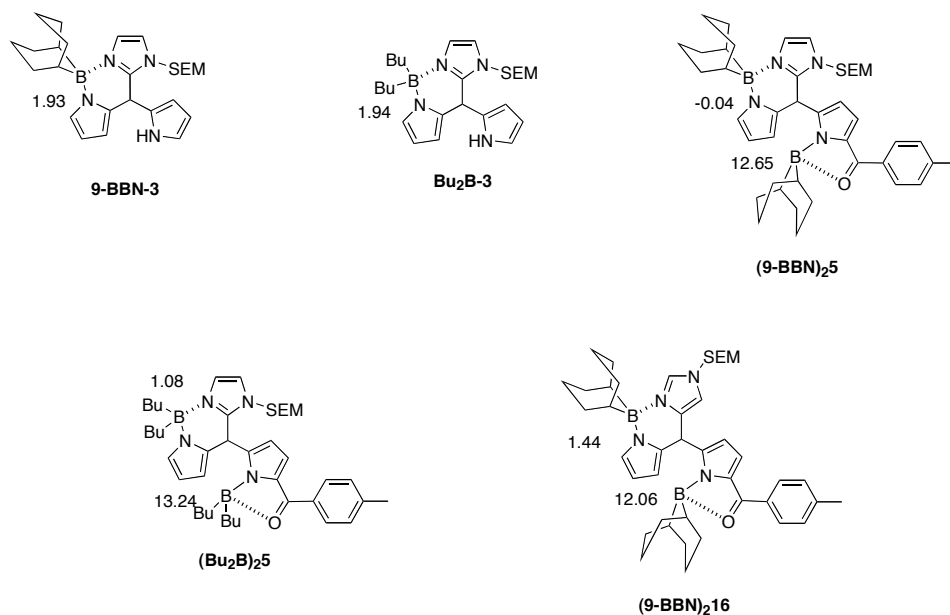


Chart 2. ^{11}B NMR Assignments

Outlook

^{11}B and ^{15}N NMR spectroscopic data for masked imidazolyl–dipyrromethanes, which contain two types of boron atoms and up to four distinct nitrogen atoms, were collected and interpreted. ^{15}N NMR data were helpful in assigning the various types of nitrogen atoms present. ^{11}B NMR chemical shifts were utilized to establish molecular identity and the different connectivity present in the boron complexes of imidazolyl–dipyrromethanes. Taken together, both spectroscopic techniques were very helpful for confirming the presence of various types of boron and nitrogen atoms in the imidazolyl–pyrrolic compounds.

Experimental Section

General. A 400 MHz Varian NMR spectrometer was used for NMR spectroscopy. Special boron and nitrogen filters were used for the purpose of maximizing the signal-noise ratio. All data were collected at room temperature unless noted otherwise.

Non-commercial Compounds. All compounds were synthesized following existing literature procedures.²¹

¹¹B NMR Spectroscopy: ¹¹B NMR spectroscopy (128 MHz) was performed using boron-free NMR tubes and THF-*d*₈ as solvent, with a sample of BF₃·OEt₂ as an external standard. The concentrations varied from 50–200 mM, and the acquisition time was 15 min to 1 h. Spectra were collected at 50 °C unless noted otherwise.

¹⁵N NMR Spectroscopy: ¹⁵N NMR spectroscopic (41 MHz) data for ¹⁵N chemical shifts are reported relative to that of nitromethane (δ 0.0) as an indirect reference using pyrrole as a direct reference. Although nitromethane is typically used as a direct reference in ¹⁵N NMR spectroscopy, nitromethane cannot be used as a reference for gHSQC spectroscopy due to the lack of an N-H bond. Furthermore, in some cases, artifacts in the region of –5 to 5 ppm (which arise from the NMR spectrometer filters) often accompany CH₃NO₂, which makes this solvent a less desirable reference. Thus, pyrrole in an NMR microtube insert was used as a reference for the gHSQC and gHMBC spectroscopy measurement. An NMR microtube containing 8.0 M pyrrole in THF-*d*₈ (70 μ L) was placed in an NMR tube containing 1.0 M CH₃NO₂ in THF-*d*₈ (500 μ L). The pseudo-concentration of each component in the entire NMR tube was ~0.9 M (CH₃NO₂) and ~1 M (pyrrole). The gHMBC (N-H) spectrum showed the resonance of the pyrrole nitrogen at –230.1 ppm relative to nitromethane (δ 0.0 ppm). Note that several different combinations of the concentrations

including (1) CH₃NO₂ (0.2 M) and pyrrole (0.2 M), (2) CH₃NO₂ (1.0 M) and pyrrole (1.0 M), and (3) CH₃NO₂ (6.2 M) and pyrrole (4.8 M), were examined to identify suitable pseudo-concentrations of the CH₃NO₂ and pyrrole for desired spectral quality.

Next, the pyrrole-containing NMR microtube was placed in an NMR tube containing the imidazolyl-dipyrromethane sample (0.2 M) in THF-*d*₈ (500 μL), whereupon gHSQC and gHMBC spectroscopy was carried out (32 scans, ~3 h each). When 0.1-M samples were measured, 64 scans (~6 h) were applied. Each gHSQC and gHMBC spectrum was referenced from the resonance of pyrrole (δ -230.1 ppm).

References

- (1) Bhaumik, J.; Yao, Z.; Borbas, K. E.; Taniguchi, M.; Lindsey, J. S. *J. Org. Chem.* **2006**, *71*, 8807–8817.
- (2) Yu, L.; Muthukumar, K.; Sazanovich, I. V.; Karmaier, C.; Hindin, E.; Diers, J. R.; Boyle, P. D.; Bocian, D. F.; Holten, D.; Lindsey, J. S. *Inorg. Chem.* **2003**, *42*, 6629–6647.
- (3) Wood, T. E.; Berno, B.; Beshara, C. S.; Thompson, A. *J. Org. Chem.* **2006**, *71*, 2964–2971.
- (4) Mason, J. *Chem. Rev.* **1981**, *81*, 205–227.
- (5) Falk, H.; Mueller, N. *Mag. Reson. Chem.* **1985**, *23*, 353–357.
- (6) Gust, D.; Roberts, J. D. *J. Am. Chem. Soc.* **1977**, *99*, 3637–3640.
- (7) Helaja, J. Monforts, F.P.; Kilpeläinen, I.; Hynninen, P. H. *J. Org. Chem.* **1999**, *64*, 432–437.
- (8) Bendel, P. *NMR Biomed.* **2005**, *18*, 74–82.
- (9) Yoshimara, K.; Shao, C.; Matsuoka, S.; Miyazaki, Y. *Kyushu Daigaku Chuo Bunseki Senta Hokoko* **2002**, *20*, 2–11.
- (10) Fehlner, T. P. *Coll. Czech. Chem. Commun.* **1999**, *64*, 767–782.
- (11) Muthukumar, K.; Ptaszek, M.; Noll, B.; Scheidt, W. R.; Lindsey, J. S. *J. Org. Chem.* **2004**, *69*, 5354–5364.
- (12) Csuk, R.; Mueller, N.; Sterk, H. *Organ. Chemie* **1985**, *40B*, 987–989.
- (13) Dedkov, Y. M.; Lozinskaya, E. F. *Khimiya I Khimicheskaya Tekhnologiya* **2002**, *45*, 118–120.

- (14) Kim, D.-P.; Moon, K.-T.; Kho, J.-G.; Economy, J.; Gervais, C.; Babonneau, F. *Polymers Adv. Technol.* **1999**, *10*, 702–712.
- (15) Feyen, F. C.; Burkert, P. K. *Z. Naturforsch. B, Chem. Sci.* **1995**, *50*, 1753–1758.
- (16) Miller, J. M. *Inorg. Chem.* **1983**, *17*, 2384–2388.
- (17) Völger, K. W.; Kroke, E.; Gervais, C.; Saito, T. Babonneau, F. Riedel, R.; Iwamoto, Y.; Hirayama, T. *Chem. Mater.* **2003**, *15*, 755–764.
- (18) Marian, C. M.; Gastreich, M. *Solid State Nucl. Magn. Reson.* **2001**, *19*, 29–44.
- (19) Beltrán, H. I.; Alas, S. J.; Santilan, R.; Farfán, N. *Can. J. Chem.* **2002**, *80*, 801–812.
- (20) Berger, S.; Braun, S.; Kalinowski, H.-O. *NMR Spectroscopy of the Non-Metallic Elements*; John Wiley & Sons Ltd: Toronto, 1997, pp 111–318.
- (21) Wrackmeyer, B.; Schwarze, B. *J. Organomet. Chem.* **1997**, *534*, 207–211.

Chapter V: Dialkylboron Complexation as a Means of Masking

Both Nitrogens Atoms in Tetrahydrodipyrins

Introduction

Hydrodipyrins are used in the synthesis of hdroporphyrins such as chlorins, bacteriochlorins and isobacteriochlorins (Chart 1).¹



Chart 1

Hydrodipyrins relevant to such syntheses are composed of one pyrrole ring and a pyrroline ring connected by a methylene or methine bridge (e.g., dihydrodipyrin, tetrahydrodipyrin) (Chart 2).

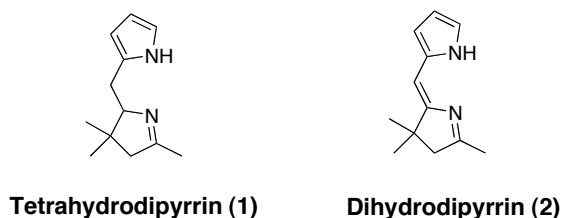
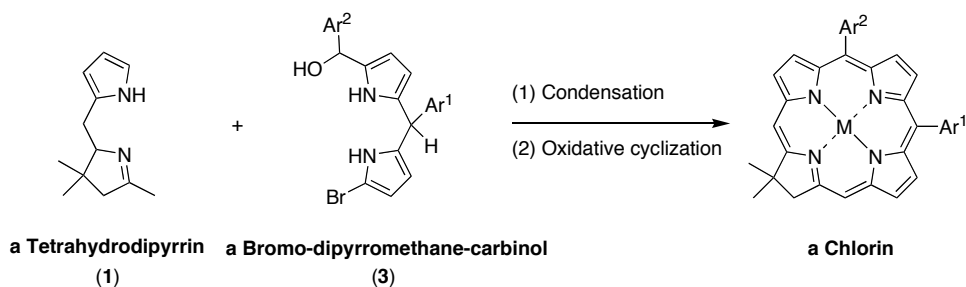


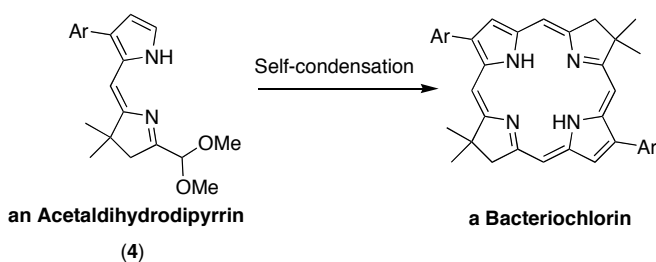
Chart 2

The stability of members of this class of compounds is highly dependent on the substitution pattern at the *meso*- and/or the β -positions.² Hdroporphyrins such as chlorins (Eqn 1) are prepared by the condensation of a tetrahydrodipyrin (**1**) with a 1-bromo-9-dipyrromethane-carbinol (**3**)³, whereas bacteriochlorins are prepared by the self-condensation of an

acetaldehydipyrin (4) (Eqn 2).¹ Hence, for better access to hydroporphyrins the availability of larger quantities of starting hydrodipyrins is required. However, the existing purification methods for isolating hydrodipyrins are laborious and have limited access to large quantities. Earlier routes to hydrodipyrins³⁻⁵ afforded very low yields and only small quantities of the final product (~500 mg) were obtained. Recently we have developed streamlined methodology to obtain large quantities of tetrahydrodipyrins such as **1** (~10 g).⁶



Equation 1. Synthesis of a chlorin.



Equation 2. Synthesis of a bacteriochlorin.

Dialkylboron complexation is a very convenient technique for the purification of various polar compounds such as 1-acyldipyrromethanes (**5**) and 1,9-diacetyldipyrromethanes (**6**) (Chart 3).^{7,8}

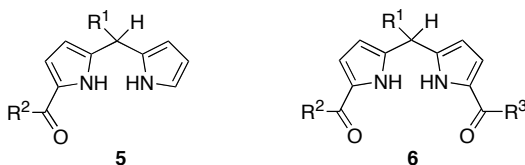


Chart 3

Prior to the development of the dialkylboron complexation technique, purification of 1-acyldipyrromethanes was very laborious due to streaking upon attempted chromatography. Large amounts of chromatographic material (e.g., silica) and solvent were necessary. But with the incorporation of dialkylboron complexation to block the pyrrolic nitrogen thereby decreasing the overall polarity, purification became much easier. Little or no column chromatography was necessary for the purification of these complexes (**5-BR₂** and **6-BR₂**) (Chart 4). In addition, dialkylboron complexes can be purified by recrystallization.

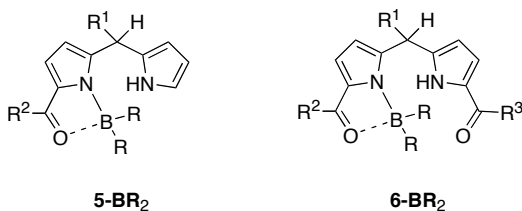


Chart 4

Dialkylboron complexes of organic molecules are well known in the literature. Boron-dipyrin (BODIPY) complexes (**7-BR₂**) (Chart 5) find versatile use as sensors and for fluorescent labeling purposes.⁹ BODIPY dyes are used as fluorescent labels for biomolecules such as proteins, lipids, and DNA. Energy transfer and electron transfer of a triad composed of boron-dipyrin, zinc porphyrin and fullerene were demonstrated as a model for a photosynthetic antenna complex.¹⁰ A family of 5-arylsubstituted boron-dipyrin dyes has been synthesized and characterized by X-ray diffraction, photophysical studies, and theory.¹¹ The excited-state dynamics and fluorescent properties of these dyes were dominated by aryl-ring rotation. BODIPY complexes can be synthesized by the reaction of a dipyrin with BF₃·OEt₂.¹² Rational color tuning and luminescent properties were determined for functionalized boron-containing pyrrolic complexes.¹³

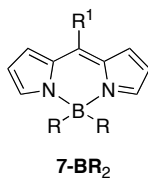


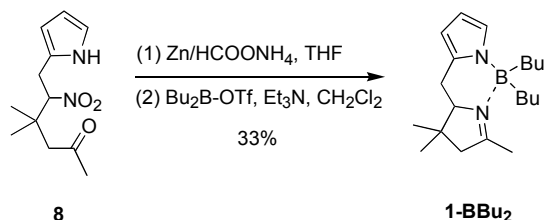
Chart 5

Recently Jacobi and coworkers have developed new methods for the synthesis of dihydrodipyrins.¹⁴ Earlier synthetic routes to hydrodipyrins resulted in a very small amount of the final product. Additionally dihydrodipyrins are not stable enough to store for a longer period of time. Tetrahydrodipyrins are comparatively more stable and can be stored for a longer period of time without any further decomposition. Therefore a modification to the synthesis of hydrodipyrins was undertaken to obtain multigram quantities of tetrahydrodipyrin **1** (Chart 2).⁶ Hence we had access to large quantities of tetrahydrodipyrin **1** as chlorin precursor. However, it turned out that the tetrahydrodipyrins are in general very polar and streak on column chromatography. Along with that, sometimes protection of the pyrrolic nitrogen of a tetrahydrodipyrin may be desirable to carry out any further reactions.

Here we report dialkylboron complexation of tetrahydrodipyrin **1** that facilitates purification of such compounds by minimizing chromatography. Two methods were employed to purify the resulting dialkylboron complex of tetrahydrodipyrin **1**: a chromatographic method and a recrystallization method. Taken together, faster purification of dialkylboron complexes of tetrahydrodipyrins provides better access to different hydrophorphyrins.

Results and Discussion

Synthesis of a Dialkylboron Complex of a Tetrahydrodipyrin. Nitrohexanone **8** was treated with 15 equivalents of each of ammonium formate and zinc dust in THF. The reaction mixture was stirred vigorously at room temperature. The progress of the reaction was monitored by GC analysis. After 2 hours nitrohexanone **8** was completely consumed, and the formation of tetrahydrodipyrin **1**⁷ was observed. The crude reaction mixture was concentrated to afford a light brown oil. The resulting oil was diluted with CH₂Cl₂ and then treated consecutively with TEA and BBU₂-OTf to facilitate purification of tetrahydrodipyrin **1**. After stirring for 1 h, the reaction mixture was filtered through a pad of silica. The dialkylboron complex of tetrahydrodipyrin **1-BBu₂** appeared as a fast-moving yellow band in silica. The fractions collected from the silica column were concentrated to afford **1-BBu₂** as a yellow solid in 33% yield (Eqn 3) (Method A). The individual yields obtained from the synthesis of **1** from nitrohexanone **8** followed by dialkylboron-complexation of **1** to obtain **1-BBu₂** were 60% and 66%, respectively. In another attempt (Method B), **1-BBu₂** was crystallized (Et₂O/MeOH) from the crude reaction mixture to give brownish crystals.



Equation 3. Synthesis of dialkylboron complex of tetrahydrodipyrin.

¹¹B NMR Spectroscopy of 1-BBu₂. A single peak at 1.89 ppm, relative to the ¹¹B standard, BF₃·O(Et)₂ (0 ppm), was observed in the ¹¹B NMR spectrum of **1-BBu₂**, which

provides evidence for incorporation of a boron atom in the tetrahydrodipyrin complex. Compared to the chemical shift of boron in similar compounds, e.g., *N*-(9-borabicyclo[3.3.1]non-9-yl)pyrrole (59.9 ppm)¹⁵ and 9-BBN complex of monoacyldipyrromethanes (~13 ppm),⁷ a distinct upfield chemical shift was observed in **1-BBu₂**. The relative upfield shift of **1-BBu₂** is characteristic for species in which boron is coordinated with a lone pair of electrons on an azomethine moiety.¹⁶

Conclusion

Dialkylboron complexation can serve as a means of protection for the pyrrolic nitrogen of the hydrodipyrin. Hydrodipyrins are highly polar and amorphous solids, whereas the dialkylboron complex of the tetrahydrodipyrin was found to be very non-polar and was obtained as a yellow crystalline solid. Hence dialkylboron complexation can be used as a quick purification technique for tetrahydrodipyrins, and the chemistry of boron-complexed tetrahydrodipyrins can be explored.

Experimental Section

General. ¹H NMR (400 MHz) and ¹³C NMR (100 MHz) spectra were collected at room temperature in CDCl₃ unless noted otherwise. Melting points are uncorrected. Column chromatography was performed with flash silica or alumina (80–200 mesh). The CHCl₃ contained 0.8% ethanol. THF was distilled from sodium benzophenone ketyl as required. CH₃CN was distilled from CaH₂ and stored over powdered molecular sieves. Other solvents were used as received.

¹¹B NMR Spectroscopy. ¹¹B NMR spectroscopy (128 MHz) was performed at room temperature using a boron-free NMR tube, and THF-*d*₈ as a solvent, with BF₃·OEt₂ as an external standard. The concentration used for NMR sample preparation was 100 mM and the acquisition time was 1 h.

Direct Conversion of 8 → 1-BBu₂. Method A. A stirred suspension of HCOONH₄ (378 mg, 6.00 mmol) and nitrohexanone **8** (95 mg, 0.40 mmol) in THF (1.6 mL) was treated with zinc dust (392 mg, 6.00 mmol). The mixture was stirred vigorously at room temperature. After 2 h, GC showed complete consumption of starting material and formation of **1**.⁶ Hence the reaction mixture was diluted with ethyl acetate (2 mL), and the mixture was filtered. The filter cake was then washed with ethyl acetate. The filtrate was washed (water and brine) and dried (Na₂SO₄). The organic layer was concentrated under reduced pressure to afford a light brown oil. The resulting oil was dissolved in CH₂Cl₂ (0.8 mL) and was treated with TEA (0.22 mL, 1.6 mmol) and dibutylboron triflate (0.8 mL of 1 M in CH₂Cl₂, 0.8 mmol). The reaction mixture was stirred at room temperature. After 1 h, the mixture was concentrated. The resulting oil was filtered (silica, CH₂Cl₂). The filtrate was concentrated to afford a yellow solid (41 mg, 33%): mp 134–136 °C; ¹H NMR δ 0.42–0.53 (m, 2H), 0.57–0.67 (m, 2H), 0.69–0.84 (m, 8H), 1.01 (s, 3H), 1.03–1.16 (m, 2H), 1.18 (m, 3H), 1.23–1.26 (m, 4H), 2.38 (m, 3H), 2.60–2.65 (m, 1H), 2.77 (m, 1H), 2.82–2.85 (m, 2H), 3.81–3.85 (m, 1H), 5.90–5.92 (m, 1H), 6.09–6.10 (m, 1H), 6.66–6.67 (m, 1H); ¹³C NMR δ 14.3, 14.4, 19.1, 23.5, 25.2, 26.2, 26.6, 26.7, 28.0, 28.4, 38.8, 56.1, 79.9, 102.8, 106.1, 121.0, 130.1, 180.1; ¹¹B NMR (THF-*d*₈) δ 1.89; FAB-MS obsd 315.2975, calcd 315.2975 [(M + H⁺), M = C₂₀H₃₅BN₂].

Method B. A stirred suspension of HCOONH₄ (378 mg, 6.00 mmol) and nitrohexanone **8** (95 mg, 0.40 mmol) in THF (1.6 mL) was treated with zinc dust (392 mg, 6.00 mmol). The mixture was stirred vigorously at room temperature. After 2 h, GC showed complete consumption of starting material and formation of **1**. Hence the reaction mixture was diluted with ethyl acetate (2 mL), and the mixture was filtered. The filter cake was then washed with ethyl acetate. The filtrate was washed with water and concentrated under reduced pressure to afford a light brown oil. The resulting oil was dissolved in CH₂Cl₂ (0.8 mL) and was treated with TEA (0.22 mL, 1.6 mmol) and dibutylboron triflate (0.8 mL of 1 M in CH₂Cl₂, 0.8 mmol). The reaction mixture was stirred at room temperature. After 1 h, the mixture was concentrated. The resulting compound was crystallized (Et₂O/MeOH) to afford brownish crystals (13 mg, 11%). Characterization data (¹H NMR, ¹³C NMR) were consistent with the values described above.

References

- (1) (a) Kim, H.-J.; Lindsey, J. S. *J. Org. Chem.* **2005**, *70*, 5475–5486. (b) Kim, H.-J.; Dogutan, D. K.; Ptaszek, M.; Lindsey, J. S. *Tetrahedron* **2007**, *63*, 37–55.
- (2) Balasubramanian, T.; Strachan, J.-P.; Boyle, P. D.; Lindsey, J. S. *J. Org. Chem.* **2000**, *65*, 7919–7929.
- (3) Taniguchi, M. Ra, D.; Mo, G.; Balasubramanian, T.; Lindsey, J. S. *J. Org. Chem.* **2001**, *66*, 7342–7356.
- (4) Taniguchi, M.; Kim, H.-J.; Ra, D.; Schwartz, J. K.; Kirmaier, C.; Hindin, E.; Diers, J. R.; Prathapan, S.; Bocian, D. F.; Holten, D.; Lindsey, J. S. *J. Org. Chem.* **2002**, *67*, 7329–7342.
- (5) Strachan, J.-P.; O’Shea, D. F.; Balasubramanian, T.; Lindsey, J. S. *J. Org. Chem.* **2000**, *65*, 3160–3172.
- (6) Ptaszek, M.; Bhaumik, J.; Kim, H.-J.; Taniguchi, M. Lindsey, J. S. *Org. Process Res. Dev.* **2005**, *9*, 651–659.
- (7) Muthukumar, K.; Ptaszek, M.; Noll, B.; Scheidt, W. R.; Lindsey, J. S. *J. Org. Chem.* **2004**, *69*, 5354–5364.
- (8) Zaidi, S. H.; Muthukumar, K.; Tamaru, S.-I.; Lindsey, J. S. *J. Org. Chem.* **2004**, *69*, 8356–8365.
- (9) Kálai, T.; Hideg, K. *Tetrahedron Lett.* **2006**, *32*, 10352–10360.
- (10) D’Souza, F.; Smith, P. M.; Zandler, M. E.; McCarthy, A. L.; Itou, M.; Araki, Y.; Ito, O. *J. Am. Chem. Soc.* **2004**, *126*, 7898–7907.

- (11) Kee, H. L.; Kirmaier, C.; Yu, L.; Thamyongkit, P.; Youngblood, J. W.; Calder, M. E.; Ramos, L.; Noll, B. C.; Bocian, D. F.; Scheidt, R. W.; Birge, R. R.; Lindsey, J. S.; Holten, D. *J. Phys. Chem. B* **2005**, *109*, 20433–30443.
- (12) Montalban, A. G.; Herrera, A. J.; Johannsen, H. J.; Beck, J.; Godet, T.; Vrettou, M.; White, A. J. P.; Williams, D. J. *Tetrahedron Lett.* **2002**, *43*, 1751–1753.
- (13) Chen, H.-Y.; Chi, Y.; Liu, C.-S.; Yu, J.-K.; Cheng, Y.-M.; Chen, K.-S.; Chou, P.-T.; Peng, S.-M.; Lee, G.-H.; Carty, A. J.; Yeh, S.-J.; Chen, C.-T. *Adv. Func. Mater.* **2005**, *15*, 567–574.
- (14) O'Neal, W. G.; Roberts, W. P.; Ghosh, I.; Jacobi, P. A. *J. Org. Chem.* **2005**, *70*, 7243–7251.
- (15) Wrackmeyer, B.; Schwarze, B. *J. Organomet. Chem.* **1997**, *534*, 207–211.
- (16) Wrackmeyer, B. *Annu. Rep. NMR Spectrosc.* **1988**, *20*, 61–203.

Chapter VI: Synthesis of *Meso*-Hydroxymethyl Porphyrins for Studies in Self-Assembly

Introduction

Nature uses chlorophyll pigments to carry out photosynthesis. The chlorophylls in green plants, chlorophyll *a* and chlorophyll *b*, are organized in pigment-protein complexes where the light-harvesting and energy transduction processes are carried out. Photosynthetic organisms in the bacterial realm employ a much broader assortment of chlorophylls, which in some cases function largely in the absence of any protein complexes. One example of such a pigment is bacteriochlorophyll *c* (Bchl *c*) as shown in Chart 1. Bchl *c* differs from chlorophyll *a* in the presence of a hydroxyalkyl group at the 3-position and the absence of an ester moiety at the 13²-position. Bacteriochlorophyll *c* undergoes self-assembly to form light-harvesting complexes (termed “chlorosomes,” i.e., green bodies); such complexes absorb light and support rapid energy transfer among the assembled pigments.

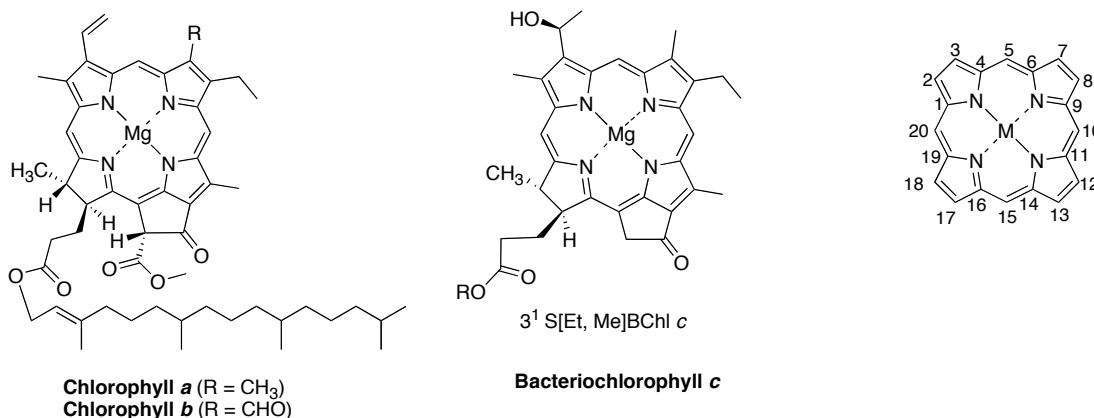


Chart 1

Recent efforts by several groups have focused on the design of synthetic analogues of bacteriochlorophyll *c* that might mimic the self-assembly and accompanying light-harvesting properties. Balaban's group has synthesized a zinc-porphyrin that contains a hydroxyl group

and a carbonyl group at distal sites in the macrocycle.¹ The same research group has also synthesized an analogous zinc-chlorin. These molecules, show broad and red shifted absorption spectra as expected upon supramolecular assembly. Hence such molecules may provide artificial mimics of the chlorosomal antennas encountered in green photosynthetic bacteria. The synthetic route employed by Balaban to obtain chlorins started from porphyrins instead of employing a de novo synthesis of chlorins.² In addition, the presence of a hydroxy group and an acyl group was achieved by statistical reduction of a diacyl-porphyrin.

Tamiaki's group has synthesized bacteriochlorophyll *d* analogues, which possess bulky substituents such as OMe, CO₂Me and CO₂^tBu at the C⁷ position of a zinc-chlorin. In 1% THF/hexane, the presence of a bathochromic shift of the absorption band indicated self-aggregation behavior of the molecules.³ Balaban's group confirmed the presence of self-assembly in hydroxymethyl-containing porphyrins by x-ray crystallographic analysis. That particular porphyrin consists of a penta-coordinating metal at the center of the macrocycle (zinc in the above-mentioned case), a keto group and hydroxymethyl moiety. The self-assembly, observed as a staircase-type stacking of porphyrins, is achieved by strong coordination of the central metal to the hydroxy group at one side, and weak coordination to the acetyl group at the other side (Chart 2) (The architecture has been reproduced with permission of the copyright holder).⁴ This architecture mimics the orientation of the natural pigment bacteriochlorophyll *c* present in photosynthetic purple bacteria.

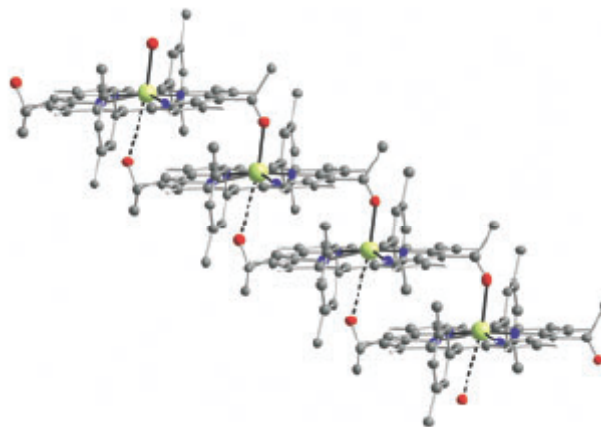
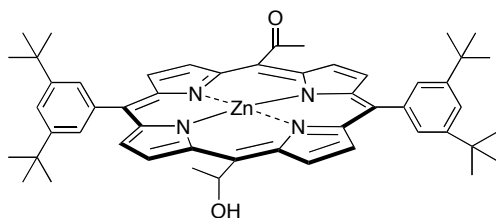


Chart 2

Our long-term goal was to develop rational de novo syntheses of hydroxymethyl chlorins that mimic natural pigments such as bacteriochlorophyll *c*. Such compounds would be versatile components for studies of self-assembling light-harvesting architectures. As an initial goal, we set out to develop routes to hydroxymethyl porphyrins owing to the more facile synthetic chemistry of porphyrins versus chlorins. We note that hydroxymethyl porphyrins and chlorins also would be useful compounds for possible applications where water solubility or bioconjugation are desired.

The hydroxymethyl group, which is quite a simple motif, would also appear to be very straightforward to introduce into porphyrins and chlorins. In principle, the introduction of an oxygen-substituted C1 synthon (e.g., carboxylic acid, ester, aldehyde, acetal) would suffice given the expected facile conversion to the hydroxymethyl motif. However, to date, most porphyrins that bear such substituents have been obtained by the modification of naturally occurring compounds. To our knowledge, few de novo routes to hydroxymethyl-porphyrins have been developed, and there are no de novo routes to hydroxymethyl-chlorins. Hence a focus of this work became the development of a rational de novo route to hydroxymethyl porphyrins.

A hydroxymethyl group can be introduced into a porphyrin by various ways: reduction of an existing acid, ester, or aldehyde; or via palladium-catalyzed Stille cross-coupling reaction of an aromatic halide with an appropriate tin reagent. We have chosen to incorporate a protected hydroxymethyl group into a porphyrin precursor (e.g. 1-acyl dipyrromethane) prior to formation of the porphyrin. This would potentially avoid extensive synthetic chemistry on the porphyrin itself. Here we report the synthesis of hydroxymethyl porphyrins (*trans*-A₂, *trans*-A₂B₂) with two hydroxymethyl groups, and a magnesium chelate of a hydroxymethyl porphyrin. The synthesis of a *trans*-A₂ and a *trans*-A₂B₂ porphyrin was achieved by the self-condensation of the corresponding dipyrromethane-1-carbinol. Hydroxymethyl-containing precursors to porphyrins such as a TBDMS-protected glycolic acid, *S*-pyridyl thioester, and 1-acyldipyrromethane were also prepared in moderate to good yield. Taken together, newly synthesized hydroxymethyl-substituted porphyrins provide access to compounds for self-assembly studies and as possible motifs for water solubility.

Results and Discussion

Retrosynthetic Approach (Chart 3). To obtain hydroxymethyl-porphyrins, we decided to protect the hydroxymethyl unit during the porphyrin-forming reaction. The *trans*-A₂B₂-porphyrin bearing two such units can be obtained by Lewis acid catalyzed self-condensation of a protected hydroxymethyl-containing 1-acyldipyrromethane. The 1-acyldipyrromethane can be obtained by acylation of a dipyrromethane with the appropriate *S*-pyridyl thioester or Mukaiyama reagent. The desired thioester can be synthesized from the protected glycolic acid. Protection of the carboxylic acid moiety of the glycolic acid can be

achieved in various ways. Hence, we settled on beginning the synthesis with a protected glycolic acid.

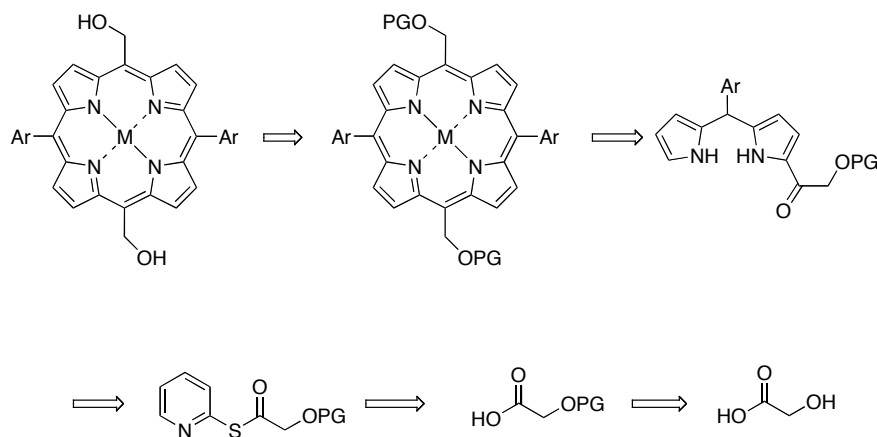
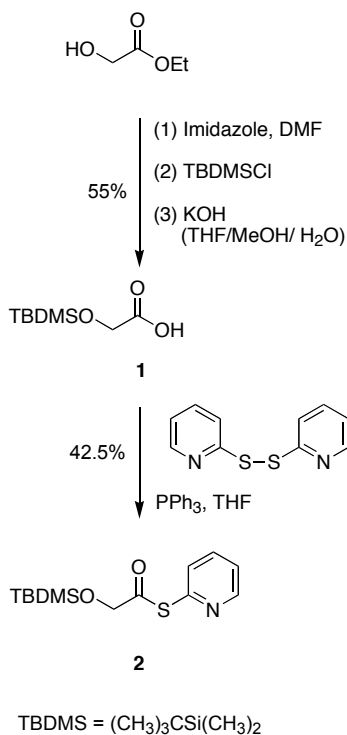


Chart 3

I. Synthetic Precursors to Hydroxymethyl Porphyrins.

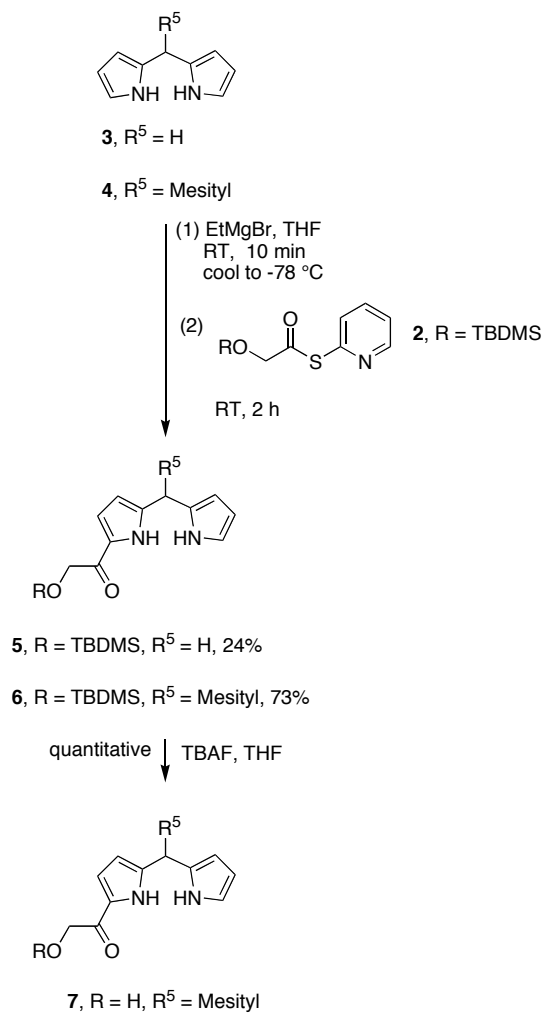
A. A Protected Glycolic Acid Acylating Agent. We chose the *tert*-butyldimethylsilyl (TBDMS) group⁵ as a protecting group, due to its ease of introduction and removal, for the hydroxyl functionality of glycolic acid. Attempts to convert glycolic acid via the bis(TBDMS)-protected glycolic ester to the mono-TBDMS-protected glycolic acid **1** following a literature procedure⁶ were not successful. In all trials, a very low yield (2-10%) of **1** was obtained whereas the literature claims a 71% yield. Hence a new route for the synthesis of TBDMS-protected glycolic acid was developed (Scheme 1). Following a known procedure for protecting butyl glycolate with a TBDMS group,⁷ ethyl glycolate was treated with TBDMSCl to afford the corresponding TBDMS-protected glycolate. The latter was then hydrolyzed in the presence of KOH to afford TBDMS-protected glycolic acid **1** in 55% yield. Another effort to synthesize compound **1** from butyl glycolate using the same procedure was unsuccessful.⁷ Following the procedures for the formation of *S*-pyridyl

thioesters,^{8,9} the TBDMS-protected glycolic acid (**1**) was treated with 2,2'-dipyridyl disulfide and triphenylphosphine to afford the desired *S*-pyridyl thioester **2** in 43% yield (Scheme 1).



Scheme 1

B. Hydroxymethyl-substituted 1-Acyl-dipyrromethane. Following a procedure for 1-acylation⁹ with slight modification, dipyrromethane **3**¹⁰ was first reacted with EtMgBr and then treated with a crude reaction mixture of the pyridyl thioester **2**. In this manner, 1-acyldipyrromethane **5** was obtained in 24% yield. Unlike the literature,⁹ 1.1 equiv of pyridyl thioester was used instead of 1.0 equiv for the reaction. Following a similar procedure for acylation,⁵ dipyrromethane **4**¹⁰ was reacted with EtMgBr and pyridyl thioester **2** to obtain TBDMS protected 1-acyldipyrromethane **6** in 73% yield (Scheme 2). The TBDMS protecting group of 1-acyldipyrromethane **6** was removed by treatment with TBAF⁵ in THF at room temperature to afford the hydroxymethyl-containing 1-acyldipyrromethane **7** in quantitative yield (Scheme 2).

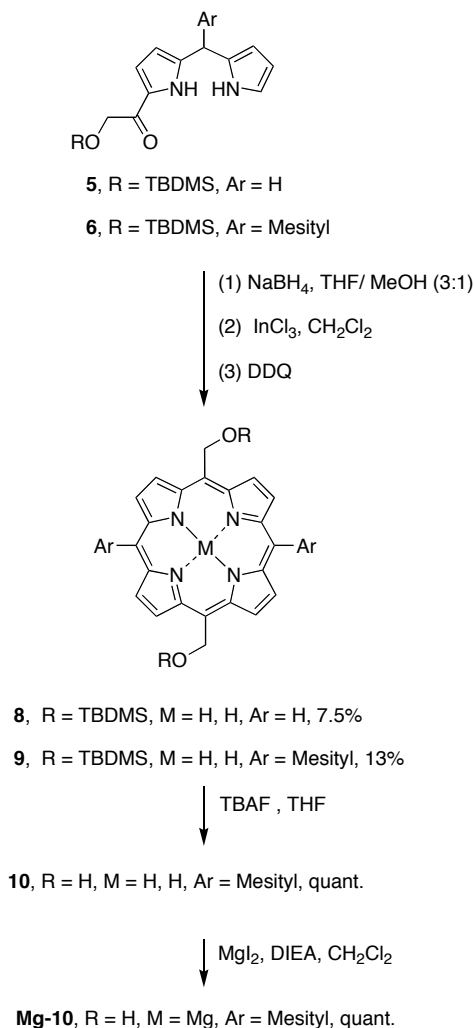


Scheme 2

II. *Trans*-A₂-Porphyrin.

Compact porphyrins bearing derivatizable functional groups are valuable for a variety of applications. We sought to synthesize a *trans*-A₂-porphyrin bearing two hydroxymethyl groups. Following a procedure for Lewis acid catalyzed condensation leading to porphyrins,¹¹ 1-acetyldipyromethane **5** was reduced with NaBH₄ to give the corresponding 1-carbinol. The resulting 1-carbinol was subjected to self-condensation by treatment with a

catalytic amount of Yb(OTf)₃ followed by DDQ-mediated oxidation, which afforded the desired *trans*-A₂-porphyrin **8** in 7.5% yield (Scheme 3).



Scheme 3

III. *Trans*-A₂B₂-Porphyrins.

A. Bis(Hydroxymethyl)Porphyrin. Following a method for porphyrin formation,¹¹ reduction of 1-acyldipyrromethane **6** afforded the corresponding 1-carbinol, which upon self-condensation in the presence of InCl₃ followed by the oxidation with DDQ afforded the protected bis(hydroxymethyl)porphyrin **9** in 13% yield (Scheme 3). LD-MS analysis of the

crude reaction mixture revealed a single porphyrin peak, with no detectable evidence for scrambled porphyrin byproducts. Deprotection⁵ of the TBDMS-protecting group from **9** using TBAF afforded **10** in quantitative yield. During exploratory work, the reduction of the 1-acyldipyrromethane **7** (which contains an unprotected hydroxymethyl moiety) followed by the self-condensation and oxidation procedures afforded an 18% yield of porphyrin (determined spectroscopically). However, LD-MS analysis of the crude reaction mixture revealed the formation of a scrambled porphyrinic byproduct (A₃B-porphyrin). This validates the importance of the presence of the TBDMS-protecting group on the hydroxymethyl group prior to the formation of the porphyrin.

B. Magnesium Chelate of Bis(Hydroxymethyl)Porphyrin. Following a general procedure for magnesium metalation,¹² free base porphyrin **10** was metalated using MgI₂ and DIEA to afford **Mg-10** in quantitative yield (Scheme 3). UV-VIS spectroscopic analysis of **Mg-10** (424 nm) in CH₂Cl₂ showed ~10 nm red shift versus that of porphyrin **10** (415 nm). Such a bathochromic shift is consistent with self-assembly, which may be due to the aggregation of the porphyrin molecules via hydrogen and coordinate bonding. Further studies are required to determine the molecular interactions that give rise to the observed spectral shift.

Conclusion

We synthesized a *trans*-A₂-porphyrin and a *trans*-A₂B₂-porphyrin, each of which bear two hydroxymethyl groups, and the magnesium chelate of a bis(hydroxymethyl)porphyrin. *Trans*-A₂- and *trans*-AB-porphyrins are good candidates for studies of self-assembly and water solubility. In addition, due to their compact size, *trans*-A₂-porphyrins are possible

precursors to bioconjugatable porphyrins. Hence, all hydroxymethyl-containing porphyrinic species prepared herein are valuable for various studies in material and biomedical sciences.

Experimental Section

General. Melting points are uncorrected. Absorption and fluorescence spectra were collected in CH₂Cl₂ at room temperature unless noted otherwise. Silica gel (40 μm average particle size) was used for column chromatography. THF was freshly distilled from sodium/benzophenone as required. CHCl₃ was stabilized with 0.8% ethanol. Anhydrous MeOH, CH₂Cl₂ and CHCl₃ (stabilized with 0.8% EtOH) were reagent grade and were used as received. All ¹H NMR spectra (400 MHz) and ¹³C NMR spectra (100 MHz) were collected in CDCl₃ unless noted otherwise.

Noncommercial Compounds. Dipyrromethanes **3**¹⁰ and **4**¹⁰ were prepared following procedures in the literature.

α-(*tert*-Butyldimethylsiloxy)acetic acid (1). Following general procedures,^{6,7} a mixture of ethyl glycolate (5.21 g, 50.0 mmol) and imidazole (4.08 g, 60.0 mmol) in DMF (50 mL) was treated with *tert*-butyldimethylchlorosilane (9.04 g, 60.0 mmol) at 0 °C. The reaction mixture was warmed to room temperature and stirred for 1 h. Water (50 mL) was added and the aqueous layer was extracted with ether. The combined organic layer was washed with water, dried (Na₂SO₄) and concentrated to afford a light yellow oil. The resulting ester (~50.0 mmol) was dissolved in THF (30 mL) and slowly treated with a solution of KOH (2.95 g, 52.5 mmol) in MeOH (6 mL) and water (12 mL) at -10 °C. The reaction mixture was then allowed to warm to 5 °C over 30 min, diluted with water (175 mL) and extracted once with ether (125 mL). The aqueous layer was separated and acidified by

the addition of a solution of conc. HCl (5.5 mL, 55 mmol) in water (11.5 mL) at 0 °C. The resulting mixture was extracted twice with ether. The organic layers were combined, washed with water, dried (Na₂SO₄) and concentrated to afford a white solid (5.2 g, 55%): mp 48–49 °C; ¹H NMR δ 0.05 (s, 6H), 0.85 (s, 9H), 4.20 (s, 2H); ¹³C NMR δ –5.3, 18.5, 25.9, 61.6, 175.3; Anal. calcd. for C₈H₁₈O₃Si: C, 50.49; H, 9.53. Found: C, 50.40; H, 9.56.

***S*-2-Pyridyl (α-*tert*-butyldimethylsiloxy)thioacetate (2).** Following a general procedure,^{8,9} a solution of protected glycolic acid **1** (3.81 g, 20.0 mmol), 2,2'-dipyridyl disulfide (8.80 g, 39.9 mmol) and triphenylphosphine (10.5 g, 40.0 mmol) in anhydrous THF (40 mL) was stirred for 24 h under argon. Removal of solvent followed by column chromatography [silica, hexanes/ethyl acetate (9:1) → hexanes/ethyl acetate (3:2)] afforded yellow crystals (2.41 g, 42.5%): mp 52 °C; ¹H NMR δ 0.18 (s, 6H), 0.99 (s, 9H), 4.38 (s, 2H), 7.28–7.34 (m, 1H), 7.58–7.62 (m, 1H), 7.72–7.78 (m, 1H), 8.64–8.68 (m, 1H); ¹³C NMR δ –5.6, 18.2, 25.7, 68.9, 123.4, 130.6, 137.1, 150.5, 151.6, 200.3; FABMS obsd 284.1126, calcd 284.1141 [(M + H)⁺, M = C₁₃H₂₁NO₂SSi].

1-(*tert*-Butyldimethylsiloxy)acetyl-dipyrromethane (5). A solution of TBDMS-protected glycolic acid **1** (1.22 g, 6.41 mmol), 2,2'-dipyridyl disulfide (2.82 g, 12.8 mmol) and triphenylphosphine (3.36 g, 12.8 mmol) in anhydrous THF (20 mL) was stirred for 24 h at room temperature under Ar to afford a crude mixture containing *S*-pyridyl thioester **2**.

EtMgBr (48 mL, 48 mmol, 1.0 M in THF) was slowly added to a stirred solution of dipyrromethane **3** (2.80 g, 19.2 mmol) in THF (20 mL) under Ar. The mixture was stirred at room temperature for 10 min and then cooled to –78 °C. The resulting solution was then treated via syringe with the crude reaction mixture containing **2**. The entire reaction mixture was stirred at –78 °C for 10 min followed by stirring at room temperature for 2 h. The

reaction was quenched by the addition of saturated aqueous NH_4Cl . The mixture was poured into CH_2Cl_2 . The organic layer was washed with water, dried (Na_2SO_4) and concentrated to furnish a dark foam. Column chromatography [silica, $\text{CH}_2\text{Cl}_2 \rightarrow \text{CH}_2\text{Cl}_2/\text{ethyl acetate}$ (20:1 to 4:1)] afforded a light brown oil (0.48 g, 24%): $^1\text{H NMR}$ δ 0.1 (s, 6H), 0.94 (s, 9H), 4.10 (s, 2H), 4.75 (s, 2H), 5.99–6.02 (m, 1H), 6.10–6.13 (m, 2H), 6.61–6.64 (m, 1H), 6.96–6.99 (m, 1H), 9.15–9.25 (br s, 1H), 10.50–10.60 (br s, 1H); $^{13}\text{C NMR}$ δ –5.0, 19.0, 26.3, 66.2, 106.2, 106.3, 108.4, 109.8, 109.9, 117.4, 119.2, 128.4, 141.6, 188.0; Anal. calcd for $\text{C}_{17}\text{H}_{26}\text{N}_2\text{O}_2\text{Si}$: C, 64.11; H, 8.23; N, 8.80. Found: C, 64.10; H, 8.18; N, 8.69.

1-[α -(*tert*-Butyldimethylsiloxy)acetyl]-5-mesityldipyrromethane (6). Following a general procedure⁹ with slight modification, a stirred solution of 5-mesityldipyrromethane (**4**) (0.630 g, 2.38 mmol) in dry THF (2.4 mL) under argon was slowly treated with a solution of EtMgBr (6.0 mL, 6.0 mmol, 1 M in THF). The resulting mixture was stirred at room temperature for 10 min and then cooled to -78°C . A solution of pyridyl thioester **2** (0.754 g, 2.66 mmol) in THF (2.4 mL) was then slowly added. The solution was maintained at -78°C for 10 min, and then the cooling bath was removed. TLC analysis [silica; $\text{CH}_2\text{Cl}_2/\text{ethyl acetate}$ (20:1)] revealed complete consumption of the pyridyl thioester after 2 h. Hence, the reaction was quenched with saturated aqueous NH_4Cl . The entire reaction mixture was poured into CH_2Cl_2 . The organic layer was separated, washed with water, dried (Na_2SO_4) and concentrated. The resulting solid residue was purified by column chromatography [silica, $\text{CH}_2\text{Cl}_2 \rightarrow \text{CH}_2\text{Cl}_2/\text{ethyl acetate}$ (9:1)], affording a light brown solid (0.77 g, 73%): mp 40°C ; $^1\text{H NMR}$ δ 0.10 (s, 6H), 0.91 (s, 9H), 2.05 (s, 6H), 2.28 (s, 3H), 4.60 (s, 2H), 5.90 (s, 1H), 6.06–6.10 (m, 2H), 6.18–6.21 (m, 1H), 6.65–6.68 (m, 1H), 6.88 (s, 2H), 7.02–7.05 (m, 1H), 7.74–7.84 (br s, 1H), 9.06–9.22 (br s, 1H); $^{13}\text{C NMR}$ δ –5.4, 18.4, 20.6, 20.8, 25.6,

25.8, 38.5, 67.3, 107.1, 108.9, 109.6, 116.8, 117.7, 128.9, 130.5, 133.0, 137.2, 137.4, 140.0, 187.8; Anal. calcd for C₂₆H₃₆N₂O₂Si: C, 71.51; H, 8.31; N, 6.42. Found: C, 71.59; H, 8.09; N, 6.25.

1-Hydroxymethyl-5-mesityldipyrromethane (7). Following a general procedure⁵ with slight modification, a solution of acyldipyrromethane **6** (0.054 g, 0.124 mmol) in anhydrous THF (2.5 mL) was treated with TBAF (0.136 mL, 0.136 mmol, 1 M in THF), and the reaction mixture was stirred under argon for 45 min. The progress of the reaction was monitored by TLC analysis [silica; hexanes/ethyl acetate (4:1)]. The reaction was quenched with water (5 mL). The mixture was extracted with CH₂Cl₂ (2 x 20 mL). The organic layers were combined, dried (Na₂SO₄) and concentrated to afford a dark red solid (0.040 g, quantitative): mp 168–170 °C; ¹H NMR δ 2.05 (s, 6H), 2.29 (s, 3H), 3.30 (t, *J* = 3.9 Hz, 1H), 4.64 (d, *J* = 3.9 Hz, 2H), 5.91 (s, 1H), 6.09–6.12 (m, 2H), 6.20–6.23 (m, 1H), 6.67–6.70 (m, 1H), 6.87–6.89 (m, 3H), 7.75–7.90 (br s, 1H), 8.95–9.25 (br s, 1H); ¹³C NMR δ 20.8, 21.0, 38.8, 64.0, 107.4, 109.1, 110.3, 117.2, 117.6, 127.0, 129.0, 130.8, 133.0, 137.5, 137.6, 141.5, 187.1; FABMS obsd 323.1741, calcd 323.1760 [(M + H)⁺, M = C₂₀H₂₂N₂O₂].

5,15-Bis(α-tert-butyl dimethylsiloxymethyl)porphyrin (8). Following a general procedure,¹¹ 1-acyldipyrromethane **5** (0.51 g, 1.6 mmol) was dissolved in THF/MeOH (3:1, 64 mL). The solution was slowly treated with NaBH₄ (1.5 g, 40 mmol). The resulting reaction mixture was stirred at room temperature under argon for 1.5 h. The reaction was quenched by dilution with CH₂Cl₂ followed by the addition of saturated aqueous NH₄Cl solution. The organic layer was separated, dried (Na₂SO₄) and concentrated to afford a pale yellow liquid. Due to limited stability, the resulting 1-carbinol was immediately used in the porphyrin-forming reaction. The 1-carbinol (~1.6 mmol) was dissolved in CH₂Cl₂ (320 mL)

and treated with Yb(OTf)₃ (0.62 g, 1.0 mmol). The reaction mixture was stirred at room temperature, and the yield of porphyrin was determined spectroscopically. After 1.5 h, DDQ (0.54 g, 2.4 mmol) was added, and the reaction mixture was stirred for 30 min. The reaction was quenched by the addition of TEA (0.28 mL, 2.0 mmol). After removal of the solvent, the resulting residue was purified by column chromatography (silica, CH₂Cl₂) affording a purple solid (36 mg, 7.5%): ¹H NMR δ -3.35 to -2.85 (br s, 2H), 0.19 (s, 12H), 0.97 (s, 18H), 7.00 (s, 4H), 9.41 (d, *J* = 4.8 Hz, 4H), 9.69 (d, *J* = 4.4 Hz, 4H), 10.21 (s, 2H); LDMS obsd 598.3; FABMS obsd 598.3158, calcd 598.3159 (C₃₄H₄₆N₄O₂Si₂); λ_{abs} (CH₂Cl₂) 402, 500, 532, 573 nm.

5,15-Bis(α-*tert*-butyldimethylsiloxymethyl)-10,20-dimesitylporphyrin (9).

Following a general procedure¹¹ with slight modification, a stirred solution of **6** (88 mg, 0.20 mmol) in THF/MeOH (3:1, 8.0 mL) was slowly treated with NaBH₄ (0.30 g, 8.0 mmol). The progress of the reduction was followed by TLC analysis [silica; hexanes/ethyl acetate (3:1)]. The reaction was complete after 1.5 h, whereupon the reaction was quenched with saturated aqueous NH₄Cl (20 mL) and then poured into ethyl acetate (20 mL). The organic layer was separated, washed (water and brine), dried (Na₂SO₄) and concentrated to afford the 1-carbinol as an orange oil. The 1-carbinol (~0.20 mmol) was dissolved immediately in CH₂Cl₂ (40 mL) and treated with InCl₃ (22 mg, 0.10 mmol). The solution slowly darkened, and the course of the reaction was monitored by absorption spectroscopy. After 1 h, the spectroscopic yield of porphyrin had essentially leveled off, and then DDQ (68 mg, 0.38 mmol) was added. The reaction mixture was stirred at room temperature for 30 min. TEA (28 μL, 0.20 mmol) was then added to quench the reaction. The entire reaction mixture was concentrated and filtered through a pad of silica (eluted with CH₂Cl₂) to afford a purple solid

(11 mg, 13%): $^1\text{H NMR}$ δ -2.90 to -2.44 (br s, 2H), 0.23 (s, 12H), 0.96 (s, 18H), 1.84 (s, 12H), 2.66 (s, 6H), 6.95 (s, 4H), 7.31 (s, 4H), 8.78 (d, $J = 5.1$ Hz, 4H), 9.52 (d, $J = 4.5$ Hz, 4H); LDMS obsd 834.6; FABMS obsd 834.4772, calcd 834.4724 ($\text{C}_{52}\text{H}_{66}\text{N}_4\text{O}_2\text{Si}_2$); λ_{abs} (toluene) 418, 514 nm; λ_{em} (toluene) 650, 725 nm.

5,15-Bis(hydroxymethyl)-10,20-dimesitylporphyrin (10). Following a general procedure⁵ with slight modification, a solution of porphyrin **9** (7.0 mg, 8.3 μmol) in THF (2.0 mL) was treated with TBAF (80 μL , 80 μmol , 1 M in THF), and the reaction mixture was stirred for 9 h under argon. The reaction was quenched with water, and extracted successively with CH_2Cl_2 and ethyl acetate. The combined organic layers were dried (Na_2SO_4) and concentrated. The solid residue was then purified by column chromatography [silica, $\text{CH}_2\text{Cl}_2 \rightarrow \text{CH}_2\text{Cl}_2/\text{ethyl acetate}$ (9:1)] to afford a purple solid (5.0 mg, quantitative): $^1\text{H NMR}$ ($\text{THF}-d_8$) δ -2.75 to -2.58 (br s, 2H), 1.83 (s, 12H), 2.64 (s, 6H), 5.26 (t, $J = 5.6$ Hz, 2H), 6.82 (d, $J = 6.0$ Hz, 4H), 7.34 (s, 4H), 8.71 (d, $J = 4.4$ Hz, 4H), 9.67 (d, $J = 4.4$ Hz, 4H); LDMS obsd 606.1; FABMS obsd 606.3017, calcd 606.2995 ($\text{C}_{40}\text{H}_{38}\text{N}_4\text{O}_2$); λ_{abs} (CH_2Cl_2) 415, 513, 544, 589 nm; λ_{em} (CH_2Cl_2) 645, 720 nm.

Mg(II)-5,15-Bis(hydroxymethyl)-10,20-dimesitylporphyrin (Mg-10). Following a general procedure for magnesium metalation,¹² a solution of porphyrin **10** (6.1 mg, 0.01 mmol) in CH_2Cl_2 (5 mL) was treated with MgI_2 (0.14 g, 0.50 mmol) and DIEA (0.17 mL, 1.0 mmol). The reaction mixture was stirred at room temperature for 18 h. The reaction mixture was diluted with CH_2Cl_2 and washed two times with 5% NaHCO_3 solution. The organic layer was dried (Na_2SO_4) and concentrated. The solid residue was purified by column chromatography [grade V alumina, $\text{CH}_2\text{Cl}_2/\text{ethyl}$ (1:1) acetate $\rightarrow \text{CH}_2\text{Cl}_2/\text{MeOH}$ (3:1)] (Note

1) to afford a purple solid (6.3 mg, quantitative): ^1H NMR (THF- d_8) δ 1.86 (s, 12H), 2.65 (s, 6H), 4.80–4.90 (m, 2H), 6.90 (d, $J = 6.9$ Hz, 4H), 7.31 (s, 4H), 8.63 (d, $J = 4.5$ Hz, 4H), 9.56 (d, $J = 4.4$ Hz, 4H); MALDI (POPOP) obsd 628.5; calcd 628.3 ($\text{C}_{40}\text{H}_{36}\text{MgN}_4\text{O}_2$); λ_{abs} (CH_2Cl_2) 424, 565, 608 nm; λ_{em} (CH_2Cl_2) 610, 660 nm.

Note 1: deactivated alumina (grade V) was prepared by the addition of 4.5 mL water to 30 g of grade I alumina in order to obtain grade V alumina.

References

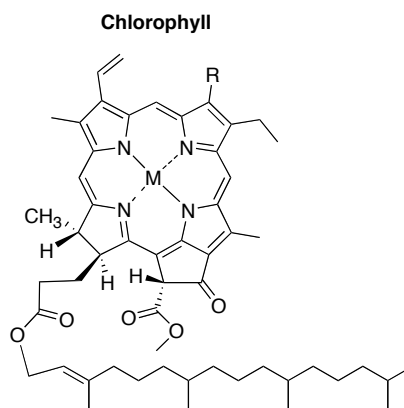
- (1) Balaban, T. S.; Eichhöfer, A.; Lehn, J.-M. *Eur. J. Chem.* **2000**, 4047–4057.
- (2) Balaban, T. S.; Linke-Schaetzel, M.; Bhise, A. D.; Vanthuynne, N.; Roussel, C. *Eur. J. Chem.* **2004**, *10*, 3919–3930.
- (3) Oba, T.; Tamiaki, H. *Supramol. Chem.* **2001**, *12*, 369–378.
- (4) Balaban, T. S.; Linke-Schaetzel, M.; Bhise, A. D.; Vanthuynne, N.; Roussel, C. Anson, C. E.; Buth, G.; Eichhöfer, A.; Foster, K.; Garab, G.; Gliemann, H.; Goddard, R.; Javorfi, T.; Powell, A. K.; Rösner, H.; Schimmel, T. *Chem. Eur. J.* **2005**, *11*, 2267–2275.
- (5) Clayden, J.; Kenworthy, M. N.; Helliwell, M. *Org. Lett.* **2003**, *5*, 831–834.
- (6) Kobayashi, S.; Horibe, M.; Saito, Y. *Tetrahedron* **1994**, *50*, 9629–9642.
- (7) Bischofberger, N.; Waldmann, H.; Saito, T.; Simon, E. S.; Lees, W.; Bednarski, M. D.; Whitesides, G. M. *J. Org. Chem.* **1988**, *53*, 3457–3465.
- (8) Nicolaou, K. C.; Claremon, D. A.; Papahatjis, D. P. *Tetrahedron Lett.* **1981**, *22*, 4647–4650.
- (9) Rao, P. D.; Littler, B. J.; Geier, G. R., III; Lindsey, J. S. *J. Org. Chem.* **2000**, *65*, 1084–1092.
- (10) Laha, J. K.; Dhanalekshmi, S.; Taniguchi, M.; Ambroise, A.; Lindsey, J. S. *Org. Process Res. Dev.* **2003**, *7*, 799–812.
- (11) Geier, G. R., III; Callinan, J. B.; Rao, P. D.; Lindsey, J. S. *J. Porphyrins Phthalocyanines* **2001**, *5*, 810–823.
- (12) O’Shea, D. F.; Miller, M. A.; Matsueda, H.; Lindsey, J. S. *Inorg. Chem.* **1996**, *35*, 7325–7338.

Chapter VII: Studies in Chlorin Chemistry

Introduction

A chlorin forms the inner core of green photosynthetic pigments such as chlorophyll *a* or chlorophyll *b* (Chart 1).¹ Chlorins also are present in non-photosynthetic pigments such as bonellin and factor I.² Chlorins are tetrapyrrolic macrocycles, which differ from porphyrins in having one pyrrolic ring reduced at the β -positions. Chlorins are superior to porphyrins in terms of light-absorption and energy-transfer processes related to photosynthesis.³ Another important difference between chlorins and porphyrins is that chlorins absorb strongly in both the blue and the red regions of the visible spectrum, whereas porphyrins absorb strongly only in the blue region. Absorption in the red region is very important for photodynamic therapy (PDT) and related applications. The photodynamic therapeutic window is 680–850 nm owing to the deeper penetration of red and near-infrared light (versus light of shorter or longer wavelengths) in soft tissue. Porphyrins do not absorb within this window, whereas chlorins and bacteriochlorins can absorb in that particular window.⁴ One clinically approved chlorin, called Foscan[®] (*meso*-tetrakis(3-hydroxyphenyl)chlorin; *m*-THPC) has been used in the European Union since 2002 to treat head and neck cancer. Halogenated chlorins were also found to be better PDT agents when compared to porphyrins or chlorins.⁵

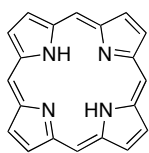
Naturally Occurring Porphyrinic Molecules



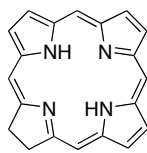
R = CH₃, M = Mg: Chlorophyll *a*

R = CHO, M = Mg: Chlorophyll *b*

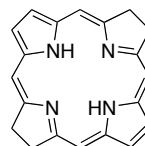
Structure of Porphyrin, Chlorin and Bacteriochlorin



Porphyrin



Chlorin



Bacteriochlorin

Chart 1

Various synthetic routes for preparing chlorins are known. Battersby,⁶ Montforts,⁷ Jacobi,⁸ Gryko⁹ and other research groups¹⁰ have worked on developing methodology for the synthesis of chlorins. In our group, we also have developed synthetic strategies for obtaining chlorins. The basic strategy is shown in Chart 2. In this approach, an Eastern half and a Western half are joined to give the corresponding chlorin. Each chlorin bears a geminal dimethyl group in the reduced, pyrroline ring to secure the reduction level of the chlorin, preventing adventitious oxidation leading to dehydrogenation and formation of the porphyrin. The Eastern half is a 1-acyl-9-bromodipyrromethane-carbinol. The Western half is 2,3,4,5-tetrahydro-1,3,3-trimethyldipyrin.

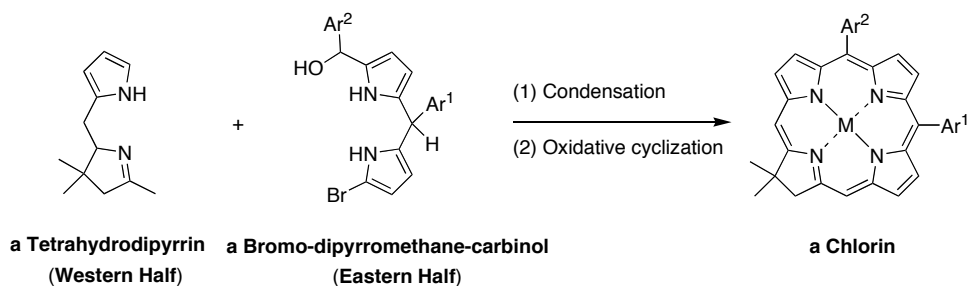


Chart 2

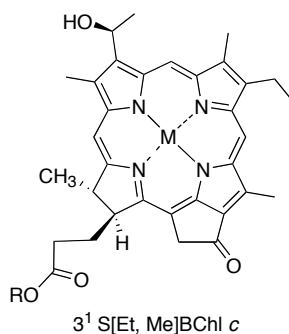
Through use of this strategy, we have been able to introduce substituents at three *meso*-positions (5, 10 and 15)^{3,11} and several β -positions (2, 3, 8, 12, 13).^{12,13} The synthetic procedures have entailed incorporation of substituents at the *meso*- or β -positions of the Eastern half prior to the synthesis of chlorins; the substituents include aryl or ethynyl groups, as well as bromo groups. The bromo group provides a convenient handle for elaboration on the intact chlorin to introduce acetyl, ethynyl, or vinyl substituents. Our group also was able to introduce an exocyclic ring into the chlorin macrocycle affording a phorbine, a simple model for chlorophyll.¹⁴

Other synthetic approaches to chlorins include (i) modification of naturally occurring chlorophyll or bacteriochlorophyll pigments, or (ii) synthesis of chlorins from porphyrin derivatives. Tamiaki's group has performed syntheses of chlorins starting from natural chlorophyll pigments.¹⁵ Much of this chemistry is quite elegant but does require extraction of the pigment from photosynthetic organisms, delicate synthetic manipulations in the presence of a variety of substituents, and in some cases, the instability of the natural pigments. Balaban and coworkers have modified porphyrin analogues to obtain chlorin derivatives, some of which undergo self-assembly.¹⁶ The latter approach sometimes gives rise to a mixture of isomers, which can be difficult to separate. Hence there exists a need for

a complementary strategy of de novo chlorin synthesis that would enable the introduction of important functional groups prior to the chlorin-forming reaction. In so doing, use of expensive natural products or laborious separation of mixtures of isomers could be avoided.

The extent of self-assembly of tetrapyrrolic macrocycles is dependent on both the functional groups and the central metal. The presence of a penta- or a hexa-coordinated metal, and one or more functional groups, able to form coordination or hydrogen-bonding interactions, is required for self-assembly (Chart 3). A chlorin with a suitably oriented hydroxymethyl moiety may mimic self-assembly in bacteriochlorophyll *c* molecules as occur in photosynthetic bacteria. Hence, we decided to synthesize chlorins bearing hydroxymethyl functionalities. Previous synthetic routes to self-assembling chlorins involve either laborious extraction of natural pigments or difficult separation procedures of chlorin isomers. Our goal was to synthesize a hydroxymethyl-chlorin via a route wherein the hydroxymethyl functionality is incorporated into the Eastern half precursor to the chlorin. Hence, we introduced a masked hydroxymethyl group to the 1-bromo-dipyrromethane-carbinol (Eastern half).

Self-assembly of Bacteriochlorophyll *c*



Bacteriochlorophyll *c*

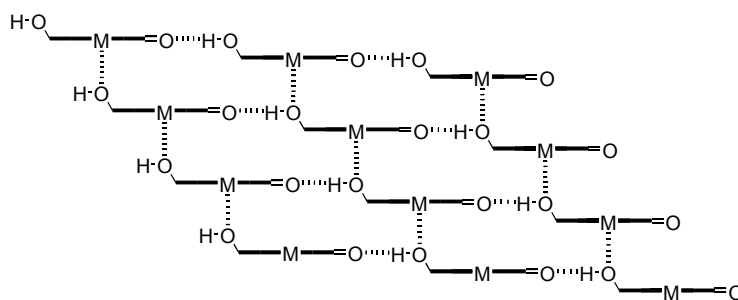


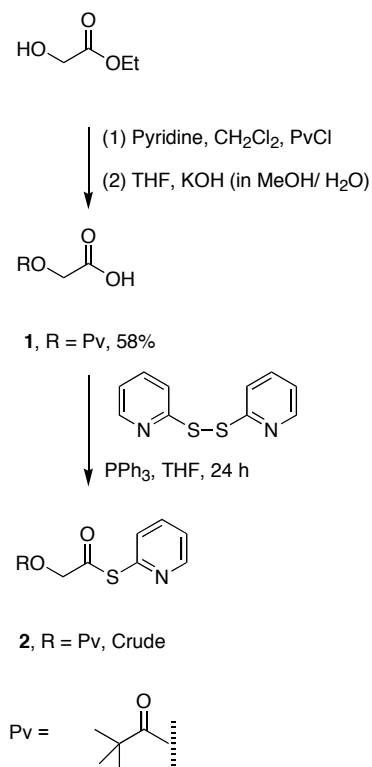
Chart 3

Here we report the synthesis of a chlorin containing a hydroxymethyl functionality at the 5-position. During the development of this synthetic route, various protecting groups (e.g., TBDMS, pivaloyl) were incorporated into the hydroxymethyl-containing precursor (e.g., *S*-pyridyl thioester, 1-acyldipyrromethane). Attempts were made wherein Pd(II) or In(III) was introduced into the chlorin core during macrocycle formation. Taken together, the new chlorins with versatile functionalities are valuable for self-assembly studies and perhaps also for biomedical applications.

Results and Discussion

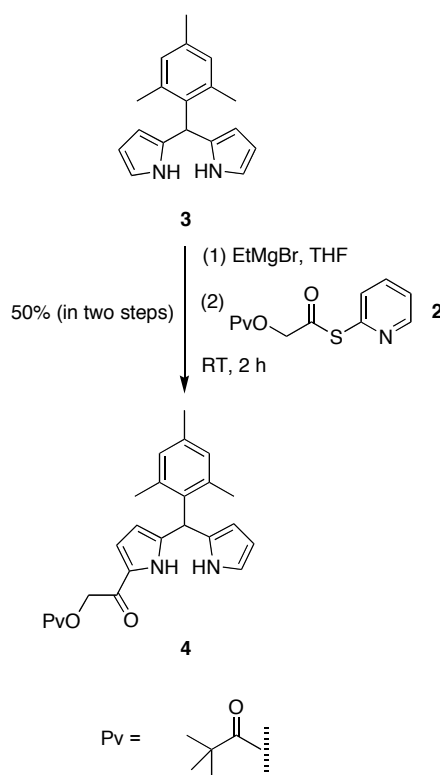
I. Synthetic Precursors for Hydroxymethyl-Chlorins.

A. Glycolic Acid Acylating Agent. Ethyl glycolate was reacted with pivaloyl chloride to afford ethyl *O*-pivaloylglycolate,¹⁷ which was then subjected to partial alkaline hydrolysis to afford *O*-pivaloylglycolic acid (**1**) in 58% yield (Scheme 1).¹⁸ The synthesis of the pyridyl thioester (a Mukaiyama reagent^{19,20} as required for acylation) directly from glycolic acid could not be achieved. Hence the pivaloyl-protected glycolic acid (**1**) was used in the synthesis of pyridyl thioester **2**. The treatment of the pivaloyl-protected glycolic acid **1** with PPh₃ and 2,2'-dipyridyl disulfide afforded pyridyl thioester **2**. The product **2** was obtained in 75% purity (by ¹H NMR spectroscopy), which could not be improved even after column chromatographic purification. However, the crude material was used as such for the 1-acylation of a dipyrromethane.



Scheme 1

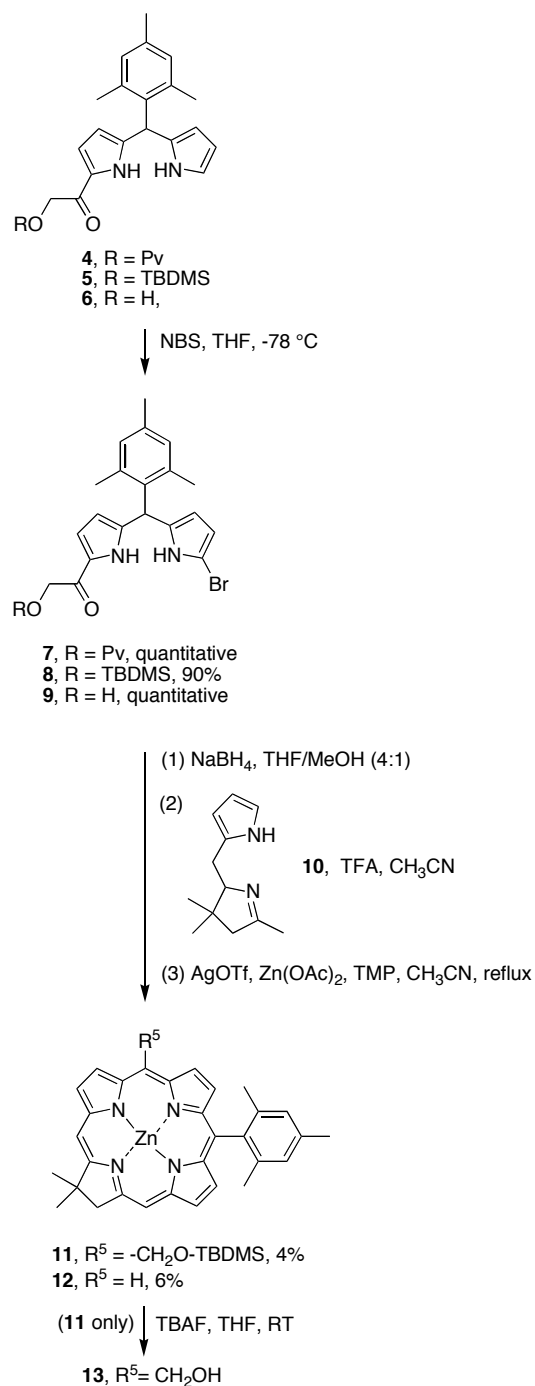
B. Hydroxymethyl-Substituted 1-Acyldipyrromethane. Following a general procedure for the synthesis of 1-acyldipyrromethanes,^{20,22} a solution of EtMgBr in THF was treated with 5-mesityldipyrromethane²¹ (**3**). After stirring the reaction mixture at room temperature for 10 min the reaction mixture was cooled to $-78\text{ }^{\circ}\text{C}$ and the pyridyl thioester (**2**, 75% pure) was added. Upon completion of the reaction (i.e., complete consumption of the Mukaiyama reagent) followed by workup and column chromatographic purification, the pivaloyl protected 1-acyldipyrromethane **4** was obtained. The yield was 50% yield in two steps starting from the synthesis of the pyridyl thioester **2** (Scheme 2).



Scheme 2

II. Synthesis of *Meso*-Hydroxymethyl-Chlorins.

A. Attempt via a Pivaloyl-Protected Eastern Half. The 1-acyldipyrromethane **4** was brominated³ using NBS at $-78\text{ }^{\circ}\text{C}$ to afford the corresponding 1-bromo-9-acyldipyrromethane (**7**) in quantitative yield (Scheme 3). The 1-bromo-9-acyldipyrromethane (**7**) was then reduced to the corresponding 1-bromo-carbinol using NaBH_4 . The latter was used immediately in the chlorin-forming reaction. Following a one-flask procedure for the synthesis of chlorins,²⁵ the 1-bromo-dipyrromethane-carbinol (Eastern half) was condensed with a tetrahydrodipyrin (**10**, Western half) which afforded an unexpected chlorin (**12**) in 6% yield. According to the characterization data (^1H NMR, LDMS and FAB-MS) the chlorin was found to be the 10-mesityl chlorin. Surprisingly, the expected product of the chlorin-formation reaction, which is a pivaloyl protected hydroxymethyl chlorin, was not formed. This can be attributed to the cleavage of the protected hydroxymethyl group during the chlorin-forming process.



Scheme 3

B. Attempt Via an Unprotected Eastern Half. Due to the failure to synthesize a pivaloyl-protected chlorin, we sought to explore the synthesis of a chlorin starting from a hydroxymethyl-containing Eastern half. Initially the bromination of the 1-

acyldipyrromethane **6**²³ was performed using NBS at $-78\text{ }^{\circ}\text{C}$, which afforded the 1-bromo-9-acyldipyrromethane **9** in quantitative yield (Scheme 3).³ The 1-bromo-9-acyldipyrromethane **9** was then reduced with NaBH_4 to the corresponding 1-bromo-dipyrromethane-9-carbinol. Owing to limited stability, the 1-bromo-dipyrromethane-carbinol was immediately used in the chlorin synthesis. Following a one-flask procedure for the synthesis of chlorins,²⁵ the 1-bromo-dipyrromethane-carbinol (Eastern half) was condensed with **10** (Western half)²⁶ once again affording the same 10-mesityl chlorin (**12**) as the only chlorin macrocycle in 4% yield. Also in this case, the formation of the desired *meso*-hydroxymethyl chlorin was not observed.

C. Synthesis Via a TBDMS-Protected Eastern Half. We decided to synthesize a TBDMS-protected hydroxymethyl-chlorin. Therefore, 1-acyldipyrromethane **5**²³ was brominated using one equiv of NBS at $-78\text{ }^{\circ}\text{C}$ for 1 h to afford 1-bromo-9-acyldipyrromethane **8** in 90% yield (Scheme 3).³ The 1-bromo-9-acyldipyrromethane (**8**) was then reduced with NaBH_4 to afford the desired 1-bromo-dipyrromethane-carbinol. Following a one-flask procedure for the synthesis of chlorins,²⁵ the 1-bromo-dipyrromethane-9-carbinol (Eastern half) was condensed with **10** (Western half) to give the TBDMS-protected hydroxymethyl-chlorin (**11**) in 4% yield. The unwanted 10-mesityl chlorin (**12**) was present as a by-product. Deprotection of the TBDMS group from **11** using TBAF afforded the desired 5-hydroxymethyl chlorin **13**.

Conclusion

We have synthesized a hydroxymethyl-chlorin and a 10-substituted chlorin. Synthesis of the chlorins involved introduction of the functional groups early in the synthetic

route to chlorins. The hydroxymethyl-chlorin may be further derivatized and utilized for a variety of studies.

Experimental Section

General. ^1H (300 MHz) and ^{13}C (75 MHz) NMR spectra were recorded in CDCl_3 unless noted otherwise. Mass spectra of porphyrins were obtained by high-resolution fast atom bombardment (FAB), by laser desorption mass spectrometry (LDMS), or by LDMS in the presence of the matrix POPOP (MALDI-MS). Absorption spectra were collected in toluene. Elemental analyses were performed by Atlantic Microlab, Inc. Melting points are uncorrected. Silica gel (Baker 40 μm average particle size) and alumina (Fisher, 80–200 mesh) were used for column chromatography. Toluene and triethylamine were freshly distilled from CaH_2 and sparged of oxygen prior to use. All reagents were purchased from Aldrich and used as received. Room temperature was determined to be 21–22 $^\circ\text{C}$ using a calibrated thermometer.

Noncommercial Compounds. Compounds **3**,²¹ **5**,²³ **6**,²³ **10**,²⁶ and **14**²⁷ were prepared following previously reported procedures.

O-Pivaloylglycolic acid (1). Following general procedures,¹⁷⁻¹⁸ a solution of ethyl glycolate (1.25 g, 12.0 mmol) in anhydrous pyridine (12 mL) and anhydrous CH_2Cl_2 (12 mL) at 0 $^\circ\text{C}$ was treated with pivaloyl chloride (1.48 mL, 12.0 mmol) under argon. The cooling bath was then removed, and the reaction mixture was stirred for 19 h at room temperature. Concentration followed by azeotropic removal of the pyridine using toluene gave an oil. The resulting oil was diluted with CH_2Cl_2 . The organic layer was washed with water. The organic layer was then separated, dried (Na_2SO_4) and concentrated *in vacuo* to afford ethyl

(*O*-pivaloyl)glycolate as a pale yellow oil. A solution of ethyl (*O*-pivaloyl)glycolate in 5 mL of THF was cooled to $-10\text{ }^{\circ}\text{C}$. The solution was slowly treated with a solution of KOH (0.486 g, 8.66 mmol) in water/MeOH (3 mL, 2:1). The reaction mixture was allowed to warm to $5\text{ }^{\circ}\text{C}$ over 30 min, diluted with 30 mL of water, and extracted with 20 mL of ether. The aqueous layer was then cooled to $0\text{ }^{\circ}\text{C}$ and acidified by the addition of a solution of 0.87 mL of conc. HCl in 2 mL of water (8.7 mmol). The reaction mixture was extracted twice with ether (20 mL). The organic layers were combined, washed with water and brine, dried (Na_2SO_4) and concentrated to afford a yellow oil, which solidified upon cooling (1.12 g, 58%): $^1\text{H NMR } \delta$ 1.18 (s, 9H), 4.58 (s, 2H), 8.25–8.35 (s, 1H).

S-2-Pyridyl pivaloxythioacetate (2). Following a general procedure,^{19,22} a solution of protected glycolic acid **1** (1.12 g, 6.99 mmol), 2,2'-dipyridyl disulfide (3.08 g, 14.0 mmol) and triphenylphosphine (3.66 g, 14.0 mmol) in anhydrous THF (19 mL) was stirred for 16 h at room temperature under argon. Removal of the solvent followed by column chromatography [silica, hexanes/ethyl acetate (9:1) \rightarrow (3:2)] afforded a yellow oil (~75% pure by $^1\text{H NMR}$ spectroscopy). This crude product was used directly for the 1-acylation of 5-mesityldipyrromethane (**3**).

1-(*O*-Pivaloxyacetyl)-5-mesityldipyrromethane (4). Following a general procedure²⁰ with slight modification, a solution of dipyrromethane **3** (53 mg, 0.2 mmol) in dry THF (0.25 mL) was slowly treated with a solution of EtMgBr (0.5 mL, 0.5 mmol, 1 M in THF). The resulting mixture was stirred at room temperature for 10 min under argon and then cooled to $-78\text{ }^{\circ}\text{C}$. The mixture was slowly treated with a solution of pyridyl thioester (**2**, 75 mg, 0.22 mmol, considering 75% purity of the thioester) in THF (0.25 mL). The resulting reaction mixture was stirred at $-78\text{ }^{\circ}\text{C}$ for 10 min, and then the cooling bath was

removed. TLC analysis [silica; CH₂Cl₂/ethyl acetate (20:1)] showed complete consumption of the pyridyl thioester after 2 h, hence the reaction was quenched with saturated aqueous NH₄Cl. The entire reaction mixture was poured into CH₂Cl₂. The organic layer was separated, washed with water, dried (Na₂SO₄) and concentrated. The resulting solid residue was purified by column chromatography [silica, CH₂Cl₂ → CH₂Cl₂/ethyl acetate (9:1)] affording a brown solid (41 mg, 50%): mp 48–50 °C; ¹H NMR δ 1.26 (s, 9H), 2.04 (s, 6H), 2.28 (s, 3H), 5.07 (s, 2H), 5.90 (s, 1H), 6.07–6.12 (m, 2H), 6.18–6.21 (m, 1H), 6.65–6.68 (m, 1H) 6.87 (s, 2H), 6.90–6.93 (m, 1H), 7.76–7.84 (br s, 1H), 8.94–9.02 (br s, 1H); ¹³C NMR δ 20.7, 20.9, 27.1, 27.3, 38.5, 38.6, 38.8, 64.8, 107.2, 108.8, 108.8, 109.9, 117.1, 117.3, 127.6, 128.9, 130.6, 133.1, 137.2, 137.5, 141.1, 178.2, 182.1; FABMS obsd 406.2253, calcd 406.2256 (C₅₂H₆₆N₄O₂Si₂).

1-Hydroxymethyl-5-mesityldipyrromethane (6). Following a general procedure²⁴ with slight modification, a solution of **3** (0.054 g, 0.124 mmol) in anhydrous THF (2.5 mL) was treated with TBAF (0.136 mL, 0.136 mmol, 1 M in THF), and the reaction mixture was stirred for 45 min under argon. The progress of the reaction was monitored by TLC analysis [(silica; hexanes/ethyl acetate (4:1)]. The reaction was quenched with water (5 mL), and extracted with CH₂Cl₂ (2 x 20 mL). The organic layers were combined, dried (Na₂SO₄) and concentrated to afford a dark red solid (0.04 g, quantitative): mp 168–170 °C; ¹H NMR δ 2.05 (s, 6H), 2.29 (s, 3H), 3.30 (t, *J* = 3.9 Hz, 1H), 4.64 (d, *J* = 3.9 Hz, 2H), 5.91 (s, 1H), 6.09–6.12 (m, 2H), 6.20–6.23 (m, 1H), 6.67–6.70 (m, 1H), 6.87–6.89 (m, 3H), 7.75–7.90 (br s, 1H), 8.95–9.25 (br s, 1H); ¹³C NMR δ 20.8, 21.0, 38.8, 64.0, 107.4, 109.1, 110.3, 117.2, 117.6, 127.0, 129.0, 130.8, 133.0, 137.5, 137.6, 141.5, 187.1; FABMS obsd 323.1741, calcd 323.1760 [(M + H)⁺, M = C₂₀H₂₂N₂O₂].

1-Bromo-9-(*O*-pivaloylacetyl)-5-mesityldipyrromethane (7). Following a general procedure,³ **4** (0.10 g, 0.25 mmol) was dissolved in 2.5 mL of dry THF and cooled to $-78\text{ }^{\circ}\text{C}$ under argon. NBS (45 mg, 0.25 mmol) was added in two portions, and the reaction mixture was stirred for 1 h at $-78\text{ }^{\circ}\text{C}$. A mixture of hexanes and water (1:1, 10 mL) was added to the reaction mixture, which was allowed to warm to room temperature. The reaction mixture was extracted with ether. The organic layer was separated, dried (Na_2SO_4) and concentrated without heating to afford a light brown viscous oil (0.12 g, quantitative): $^1\text{H NMR } \delta$ 1.20 (s, 9H), 2.05 (s, 6H), 2.29 (s, 3H), 5.07 (s, 2H), 5.82 (s, 1H), 5.96–5.99 (m, 1H), 6.09–6.13 (m, 2H), 6.88 (s, 2H), 6.90–6.94 (m, 1H), 7.59–7.71 (br s, 1H), 8.78–8.91 (br s, 1H); FABMS obsd 485.1426, calcd 485.1440 ($\text{C}_{25}\text{H}_{29}\text{N}_2\text{O}_3\text{Br}$).

1-Bromo-9-(α -*tert*-butyldimethylsiloxyacetyl)-5-mesityldipyrromethane (8). Following a general procedure,³ a solution of **5** (56 mg, 0.13 mmol) in 1.3 mL of dry THF was cooled to $-78\text{ }^{\circ}\text{C}$ under argon. NBS (23 mg, 0.13 mmol) was added, and the reaction mixture was stirred for 1 h at $-78\text{ }^{\circ}\text{C}$. A mixture of hexanes and water (1:1, 6 mL) was added to quench the reaction. The reaction mixture was allowed to warm to room temperature. The entire reaction mixture was extracted with ether. The organic layer was separated, dried (K_2CO_3), and concentrated without heating. The resulting crude solid residue was purified by column chromatography [silica, hexanes/ethyl acetate (9:1) \rightarrow hexanes/ethyl acetate (3:2)] to afford a dark brown viscous oil (60 mg, 90%): $^1\text{H NMR } \delta$ 0.11 (s, 6H), 0.93 (s, 9H), 1.95 (s, 6H), 2.23 (s, 3H), 4.58–4.68 (m, 2H), 5.51 (s, 1H), 5.74–5.76 (m, 2H), 5.90–5.92 (m, 1H), 6.81–6.83 (m, 2H), 6.87–6.89 (m, 1H), 10.35–10.46 (br s, 1H), 10.75–10.88 (br s, 1H); $^{13}\text{C NMR } \delta$ -5.8 , 18.4, 20.2, 22.8, 25.6, 39.4, 96.4, 108.8, 109.5, 109.7, 109.8, 115.8, 129.5, 130.0, 133.2, 134.6, 136.1, 137.5, 140.0, 186.4.

1-Bromo-9-hydroxymethylacetyl-5-mesityldipyrromethane (9). Following a general procedure,³ a solution of **6** (41 mg, 0.10 mmol) in 1 mL of dry THF was cooled to –78 °C under argon. NBS (18 mg, 0.10 mmol) was added in two portions, and the reaction mixture was stirred for 1 h at –78 °C. Hexanes and water were added, and the mixture was allowed to warm to room temperature. The entire reaction mixture was poured into ether. The aqueous layer was extracted with ether. The organic layer was separated, dried (Na₂SO₄), and concentrated without heating. The title compound was obtained as a light brown viscous oil (0.12 g, quantitative): ¹H NMR (THF-*d*₈) δ 2.05 (s, 6H), 2.23 (s, 3H), 3.74–3.86 (m, 1H), 4.48 (d, *J* = 3.9 Hz, 2H), 5.51 (s, 1H), 5.70–5.82 (s, 2H), 5.88–5.94 (m, 1H), 6.72–6.88 (m, 3H), 10.32–10.44 (br s, 1H), 10.92–11.08 (br s, 1H); ¹³C NMR (THF-*d*₈) δ 20.07, 20.17, 39.4, 64.2, 96.4, 108.8, 109.5, 110.0, 115.8, 130.0, 130.2, 133.1, 134.5, 136.1, 137.4, 140.5, 187.6; FABMS obsd 400.0792, calcd 400.0786 (C₂₀H₂₁N₂O₂Br).

Zn(II)-5-(α -*tert*-Butyldimethylsiloxymethyl)-17,18-dihydro-10-mesityl-18,18-dimethylporphyrin (11). Following a general procedure,³ a solution of **8** (93 mg, 0.18 mmol) in THF/MeOH [2.5 mL, (4:1)] was treated portionwise with NaBH₄ (68 mg, 1.8 mmol). The reaction was monitored by TLC analysis [silica; hexanes/ethyl acetate (3:2)] and upon completion was slowly quenched by addition of saturated aqueous NH₄Cl solution (20 mL). The reaction mixture was poured into ethyl acetate. The organic layer was separated. The aqueous layer was extracted twice with ethyl acetate. The organic layers were combined, washed with water, dried (Na₂SO₄) and concentrated. Upon initial work up, the 1-bromo-dipyrromethane-carbinol was the only product visible by TLC analysis. Owing to limited stability, the 1-bromo-dipyrromethane-carbinol was directly used in the chlorin-forming reaction. Following a one-flask procedure for the synthesis of chlorins,²⁵ the 1-

bromo-dipyrromethane-carbinol (~0.18 mmol) was dissolved in 1.8 mL of anhydrous CH₃CN. The solution was then treated with tetrahydrodipyrin **10** (34 mg, 0.18 mmol) and TFA (14 μ L, 0.18 mmol). The resulting reaction mixture was stirred at room temperature for 45 min under argon. The crude reaction mixture was diluted with CH₃CN (16.2 mL) and consecutively 2,2,6,6-tetramethylpiperidine (0.91 mL, 5.4 mmol), Zn(OAc)₂ (0.50 g, 2.7 mmol), and AgOTf (0.14 g, 0.54 mmol) were added. The resulting mixture was refluxed for 19 h exposed to air. The entire reaction mixture was concentrated. The resulting residue was chromatographed [(silica, hexanes/CH₂Cl₂ (1:1))] to afford a dark green solid (5 mg, 4%): ¹H NMR (~90% pure) δ 0.19 (s, 6H), 0.95 (s, 9H), 1.68 (s, 3H), 1.85 (s, 3H), 2.03 (s, 6H), 2.60 (s, 3H), 4.49 (s, 2H), 6.69 (s, 2H), 7.22 (s, 2H), 8.35 (d, *J* = 4.4 Hz, 1H), 8.49 (d, *J* = 4.4 Hz, 1H), 8.55–8.57 (m, 2H), 8.63 (s, 1H), 8.77 (d, *J* = 4.4 Hz, 1H), 9.13 (d, *J* = 4.4 Hz, 1H), 9.42 (d, *J* = 4.4 Hz, 1H); LDMS obsd 664.3; FABMS obsd 664.2607, calcd 664.2576 (C₃₈H₄₄N₄OSiZn); λ_{max} (toluene) 408, 608 nm, λ_{em} (CH₂Cl₂) 610, 670 nm.

Attempted Synthesis of Zn(II)-5-(Pivaloxymethyl)-17,18-dihydro-10-mesityl-18,18-dimethylporphyrin. Following a general procedure,³ a solution of **7** (49 mg, 0.10 mmol) in THF/MeOH (4:1, 1.4 mL) was treated portionwise with NaBH₄ (38 mg, 1.0 mmol). The reaction was monitored by TLC analysis [silica; hexanes/ethyl acetate (3:2)] and upon completion was slowly quenched with saturated aqueous NH₄Cl solution (5 mL). The entire reaction mixture was dissolved in ether. The organic layer was separated. The aqueous layer was extracted twice with ether. The organic extract was washed with brine, dried (Na₂SO₄) and concentrated. Upon initial work up, the 1-bromo-dipyrromethane-carbinol was the major product as observed by TLC analysis. The crude product was directly used in the chlorin-forming reaction due to limited stability. Following a general procedure,²⁵ the 1-bromo-

dipyrromethane-carbinol (~0.1 mmol) was dissolved in anhydrous CH₃CN (1 mL), and then **10** (19 mg, 0.10 mmol) and TFA (8 μL, 0.1 mmol) were added. The reaction mixture was stirred at room temperature for 1 h under argon. The reaction mixture was treated with CH₃CN (9 mL), 2,2,6,6-tetramethylpiperidine (506 μL, 3.00 mmol, 30 molar equiv), Zn(OAc)₂ (276 mg, 1.50 mmol), and AgOTf (77 mg, 0.30 mmol). The resulting mixture was heated to reflux for 15 h exposed to air. The reaction mixture was concentrated under reduced pressure. The residue was chromatographed [silica, hexanes/CH₂Cl₂ (1:1)] to afford Zn(II)-17,18-dihydro-10-mesityl-18,18-dimethylporphyrin (**12**) as a dark green solid (3.1 mg, 6.0%): ¹H NMR δ 1.84 (s, 6H), 2.04 (s, 6H), 2.59 (s, 3H), 4.53 (s, 2H), 7.22 (s, 2H), 8.37 (d, *J* = 4.0 Hz, 1H), 8.54 (d, *J* = 4.4 Hz, 1H), 8.60 (d, *J* = 4.8 Hz, 1H), 8.61 (s, 1H), 8.68 (s, 1H), 8.72 (d, *J* = 4.4 Hz, 1H), 8.82 (d, *J* = 4.0 Hz, 1H), 9.09 (d, *J* = 4.0 Hz, 1H), 9.61 (s, 1H); LDMS obsd 519.6; FABMS obsd 520.1646, calcd 520.1605, (C₃₁H₂₈N₄Zn); λ_{abs} (toluene) 406, 606 nm.

Attempted Synthesis of Zn(II)-5-(Hydroxymethyl)-17,18-dihydro-10-mesityl-18,18-dimethylporphyrin. Following a general procedure,³ a solution of **9** (36 mg, 0.09 mmol) in THF/MeOH (4:1, 1.26 mL) at 0 °C was treated portionwise with NaBH₄ (34 mg, 9.0 mmol). The progress of the reaction was monitored by TLC [silica; hexanes/ethyl acetate (3:2)] analysis. Upon completion, the reaction was quenched with saturated aqueous NH₄Cl (5 mL). The reaction mixture was then extracted with ethyl acetate. The combined organic layers were washed with brine, dried (Na₂SO₄) and concentrated. Upon initial work up, the 1-bromo-carbinol was the only product visible by TLC analysis. Due to limited stability, the 1-bromo-carbinol was directly used in the chlorin-forming reaction without further purification and characterization. Following a general procedure,²⁵ the bromo-

dipyromethane-carbinol (~0.09 mmol) was dissolved in anhydrous CH₃CN (0.9 mL), and then **10** (17 mg, 0.09 mmol) and TFA (7.0 μL, 0.09 mmol) were added. The reaction mixture was stirred at room temperature for 45 min under argon. The reaction mixture was diluted with 9 mL of CH₃CN. The resulting dilute solution was treated successively with 2,2,6,6-tetramethylpiperidine (456 μL, 2.70 mmol), Zn(OAc)₂ (248 mg, 1.35 mmol), and AgOTf (69 mg, 0.27 mmol). The resulting mixture was refluxed for 18 h exposed to air. The reaction mixture was concentrated under reduced pressure. The residue was chromatographed [silica, hexanes → hexanes/CH₂Cl₂ (1:1)] to afford Zn(II)-17,18-dihydro-10-mesityl-18,18-dimethylporphyrin (**12**) as a dark green solid (1.8 mg, 4.0%). Characterization data (¹H NMR, LDMS, UV-VIS) were consistent with the values reported above.

References

- (1) *Chlorophylls*; Scheer, H.; Ed.; CRC Press: Boca Raton, FL, 1991.
- (2) Montforts, F.-P.; Gerlach, B.; Höper, F. *Chem. Rev.* **1994**, *94*, 327–347.
- (3) Strachan, J.-P.; O’Shea, D. F.; Balasubramanian, T.; Lindsey, J. S. *J. Org. Chem.* **2000**, *65*, 3160–3172.
- (4) Laville, I.; Figueiredo, T.; Loock, B.; Pigaglio, S.; Maillard, P. H.; Grierson, D. S.; Carrez, D.; Croisy, A.; Blais, J. *Bioorg. Med. Chem.* **2003**, *11*, 1643–1652.
- (5) Pineiro, M.; Pereira, M.; Gonsalves, A. M.; Arnaut, L. G.; Formosinho, S. J. *Photochem. Photobiol.* **2001**, *138*, 147–157.
- (6) Battersby, A. R.; Fookes, C. J. R.; Snow, R. J. *J. Chem. Soc. Perkin Trans. I* **1984**, 2733–2741.
- (7) Montforts, F.-P. *Angew. Chem.* **1981**, *93*, 795–796.
- (8) Jacobi, P. A.; Lanz, S.; Ghosh, I.; Laung, S. H.; Löwer, F.; Pippin, D. *Org. Lett.* **2001**, *3*, 831–834.
- (9) Gryko, D.; Galezowski, M. *Org. Lett.* **2005**, *7*, 1749–1752.
- (10) (a) Mettah, S.; Li, G.; Srikrishnan, T.; Mehta, R.; Grossman, Z. D.; Dougherty, T. J.; Pandey, R. K. *Org. Lett.* **1999**, *12*, 1961–1964. (b) Luguya, R. Jensen, T. J.; Smith, K. M.; Vicente, M. G. H. *Bioorg. Med. Chem.* **2006**, 5890–5897. (c) Taima, H.; Okubu, A.; Yoshioka, N.; Inoue, H. *Tetrahedron Lett.* **2005**, *46*, 4161–4164.
- (11) Taniguchi, M.; Kim, M. N.; Ra, D.; Lindsey, J. S. *J. Org. Chem.* **2005**, *70*, 275–285.
- (12) Balasubramanian, T.; Strachan, J.-P.; Boyle, P. D.; Lindsey, J. S. *J. Org. Chem.* **2000**, *65*, 7919–7929.

- (13) Laha, J. K.; Muthiah, C.; Taniguchi, M.; McDowell, B. E.; Ptaszek, M.; Lindsey, J. S. *J. Org. Chem.* **2006**, *71*, 4092–4102.
- (14) Laha, J. K.; Muthiah, C.; Taniguchi, M.; Lindsey, J. S. *J. Org. Chem.* **2006**, *71*, 7049–7052.
- (15) (a) Sasaki, S.-I.; Omada, M.; Tamiaki, H. *J. Photochem. Photobiol. A: Chemistry* **2004**, *162*, 307–315. (b) Miyatake, T.; Oba, T.; Tamiyaki, H. *Chembiochem* **2001**, *2*, 325–332. (c) Oba, T.; Tamiaki, H. *Supramol. Chem.* **2001**, *12*, 369–378.
- (16) (a) Balaban T. S.; Bhise, A. D.; Fischer, M.; Linke-Schaetzel, M.; Roussel, C.; Vanthuynne, N. *Angew. Chem. Int. Ed.* **2003**, *42*, 2140–2144. (b) Balaban, T. S.; Eichhöfer, A.; Lehn, J.-M. *Eur. J. Org. Chem.* **2000**, 4047–4057. (c) Balaban, T. S.; Linke-Schaetzel, M.; Bhise, A. D.; Vanthuynne, N.; Roussel, C. *Eur. J. Org. Chem.* **2004**, 3919–3930.
- (17) Nicolaou, K. C.; Webber, S. E. *Synthesis* **1986**, 453–461.
- (18) Bischofberger, N.; Waldmann, H.; Saito, T.; Simon, E. S.; Lees, W.; Bednarski, M. D.; Whitesides, G. M. *J. Org. Chem.* **1988**, *53*, 3457–3465.
- (19) Nicolaou, K. C.; Claremon, D. A.; Papahatjis, D. P. *Tetrahedron Lett.* **1981**, *22*, 4647–4650.
- (20) Rao, P. D.; Littler, B. J.; Geier, G. R., III; Lindsey, J. S. *J. Org. Chem.* **2000**, *65*, 1084–1092.
- (21) Laha, J. K.; Dhanalekshmi, S.; Taniguchi, M.; Ambroise, A.; Lindsey, J. S. *Org. Process Res. Dev.* **2003**, *7*, 799–812.
- (22) Rao, P. D.; Dhanalekshmi, S.; Littler, B. J.; Lindsey, J. S. *J. Org. Chem.* **2000**, *65*, 7323–7344.

- (23) Chapter 4.
- (25) Taniguchi, M.; Ra, D.; Mo, G.; Balasubramanian, T.; Lindsey, J. S. *J. Org. Chem.* **2001**, *66*, 7342–7354.
- (26) Ptaszek, M.; Bhaumik, J.; Kim, H.-J.; Taniguchi, M.; Lindsey, J. S. *Org. Process Res. Dev.* **2005**, *9*, 651–659.
- (27) Kim, H.-J.; Dogutan, D. K.; Ptaszek, M. Lindsey, J. S. *Tetrahedron* **2007**, *63*, 37–55.

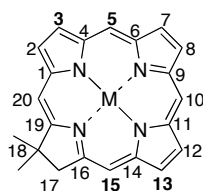
Chapter VIII: Synthesis of Formyl-Substituted Chlorins as Tools for Tuning Absorption Spectroscopic Properties

Introduction

Formyl-substituted porphyrinic macrocycles provide versatile intermediates and target molecules in bioorganic and materials chemistry.¹ As in other areas of synthetic chemistry, the porphyrinic formyl group can participate in classical reactions (e.g., Grignard, Knoevenagel, McMurry, Wittig, Schiff's base) as well as in reactions with pyrrole or a dipyrromethane leading to multi-porphyrinic architectures. Two distinct and complementary ways to introduce a formyl group into a porphyrinic molecule are as follows: (1) Vilsmeier formylation of an intact macrocycle,² and (2) construction of formyl-substituted macrocycles starting from formyl-containing acyclic precursors.¹ A typical limitation to the former route is lack of regioselectivity thereby generating a mixture of products. The latter method enables introduction of a formyl group at a designated position but requires more elaborate synthesis. At present, the latter route has been used to introduce a formyl group into a porphyrin at the 5-position or the 5,15-positions. No formyl chlorins have been prepared by de novo synthesis. An alternative approach to introduce a formyl group into a porphyrinic macrocycle relies on oxidation of an existing vinyl group with OsO₄ and sodium iodate.³ The major drawback of this method is that one must have access to a vinyl-chlorin. Chlorophyll *a* and chlorophyll *b* both bear a 3-vinyl group, but access to chlorins bearing vinyl groups at other positions is limited if existent at all.

Recently we developed a de novo synthesis of 3-, 13-, and 3-/13- functionalized chlorins.⁴ The synthetic routes proceeded via the corresponding β -bromo-substituted chlorins. The bromo-chlorins were derivatized via palladium-coupling (e.g., Stille or Sonogashira coupling) to introduce vinyl, ethynyl or acetyl substituents into the β -positions of chlorins. Additionally, we developed a route to a 15-bromo-chlorin,⁵ which was derivatized by Suzuki or Sonogashira palladium-catalyzed cross coupling reactions.

Our goal here is to develop an approach that will support the synthesis of chlorins bearing one or more formyl groups at the 3-, 5-, 13-, 3-/13-, and 15-positions. A chief motivation is to employ such formyl-chlorins in fundamental spectroscopic studies, and also prepare analogues through the homologation of the formyl-chlorins. Typical target analogues include cyanovinyl and dicyanovinyl substituted chlorins. This type of homologation may allow tuning of the absorption spectroscopic properties of the chlorin. In this regard, note that chlorophyll *a* and chlorophyll *b* have different absorption spectra owing to the difference of only one substituent, a 7-methyl versus 7-formyl group, respectively.



Here we report the synthesis of two formyl-substituted chlorins. The synthetic routes employed herein relied either on a formyl-substituted acyclic precursor (a 1-acyldipyrromethane containing a formyl moiety) or a coupling reaction of an intact bromo-chlorin with a suitable Stille coupling reagent. In the latter case, a 13-hydroxymethyl-chlorin was prepared as an intermediate which upon oxidation gave the 13-formyl chlorin. Various tin reagents such as tributyltin acetal and hydroxymethyltin were used to introduce a masked

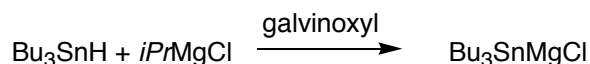
formyl functionality into the chlorin moiety. Palladium-catalyzed reductive carbonylation was found to be the most efficient way to introduce a formyl group into the chlorin. These new formyl-chlorins are useful for demonstrating absorption spectroscopic properties of chlorins, and may provide motifs for further homologation. Similar formylation procedures may be extended to bacteriochlorin chemistry. Taken together, the new synthetic routes to formyl-substituted chlorins are useful to gain access to chlorins that exhibit bathochromically shifted absorption peaks.

Results and Discussion

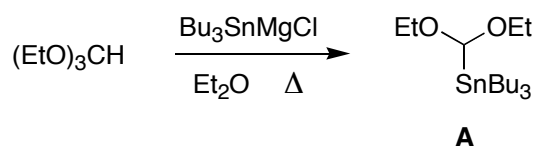
1. Synthetic Strategy. In order to introduce a formyl group at a β - or 15-position of chlorins, a bromo-chlorin can be modified via palladium-catalyzed coupling reactions affording the desired formyl chlorin. The stability, low polarity, versatility and water insolubility of organotin reagents make them promising candidates for a variety of organic reactions. Stille coupling⁶⁻⁹ is a very useful reaction for the introduction of various functionalities to an existing molecule. In order to introduce a formyl group into the porphyrinic macrocycle, a formyltributyltin reagent can be used in a Stille coupling reaction. However, the formyltributyltin reagent is known to be somewhat unstable and hence not practical for large-scale procedures.

Dialkoxymethyltributyltin reagents are masked aldehyde ionic equivalents obtained by the reaction of trialkylstannylmagnesium halide and a trialkylorthoformate.¹⁰ The most common example is diethoxymethyltributyltin.¹¹⁻¹⁶ The reaction of tributyltin magnesium chloride with triethyl orthoformate in the presence of galvinoxyl affords diethoxymethyltributyltin as a masked formyl group in 59% yield (Eqns 1 & 2).

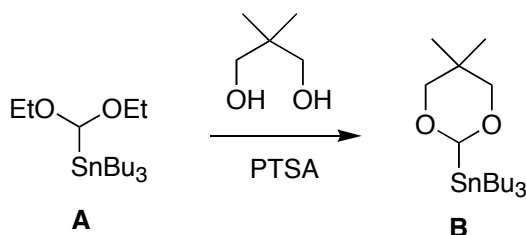
Diethoxymethyltributyltin on reaction with neopentyl glycol in the presence of PTSA can be converted in 96% yield to the masked formylating agent 2-tributylstannyl-1,3-dioxane (Eq 3). The protecting groups can be removed by treatment with TFA/H₂O to afford the desired formylated product. A hydroxymethylating agent, hydroxymethyltributyltin (C),¹⁷ can be introduced into a chlorin via palladium coupling; the resulting hydroxymethyl chlorin and can further be oxidized to the corresponding formyl derivative.



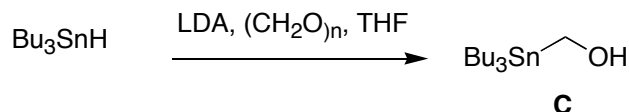
Equation 1. Tributyltin magnesium chloride synthesis.



Equation 2. Diethoxymethyltributyltin synthesis.



Equation 3. 2-Tributylstannyl-1,3-dioxane synthesis.



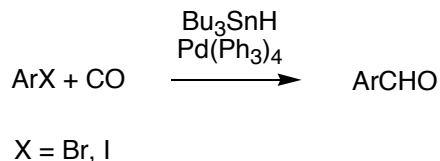
Equation 4. Hydroxymethyl tributyltin synthesis.

Palladium-coupling has been used for carbon monoxide-mediated formylation of organic molecules (Eq 5, 6).¹⁸⁻²¹ An obvious limitation to this procedure is the toxicity of

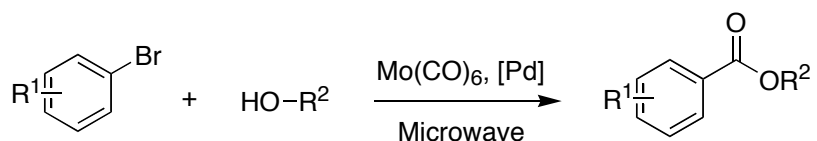
CO. A recent technique demonstrates the use of Mo(CO)₆ as a solid CO source in palladium-mediated coupling for the introduction of an ester group, thereby sidestepping the direct use of CO (Eq 7).²²



Equation 5. Carbon monoxide mediated formylation of aryl halide.



Equation 6. Formylation of aryl halide via Stille coupling.



Equation 7. Formylation of aryl halide using Mo(CO)₆.

Accordingly, we proposed four routes for the synthesis of formyl-chlorins (Chart 1). Route 1 and Route II require Stille coupling (palladium-mediated cross-coupling) of a bromo-chlorin and a dialkoxymethyltributyltin or a 2-tributylstannyl-1,3-dioxane reagent. These organotin reagents are structurally similar to the other organotin reagents such as tributyl(vinyl)tin or tributyl(1-ethoxyvinyl)tin which are known to take part in palladium-coupling reactions. The resulting acetals can further be hydrolyzed using TFA-water in order to obtain the desired formyl chlorins.

Route 3 is an indirect pathway to synthesize formyl-chlorins wherein initial introduction of hydroxymethyl group via Stille coupling is followed by oxidation of hydroxymethyl group to the formyl group.

Route 4 is a palladium catalyzed reductive carbonylation which uses carbon monoxide along with sodium formate and $\text{Pd}(\text{PPh}_3)_4$ to introduce a formyl moiety into the chlorin. Carbonylation via palladium coupling is often used for introducing formyl groups into aryl substrates.

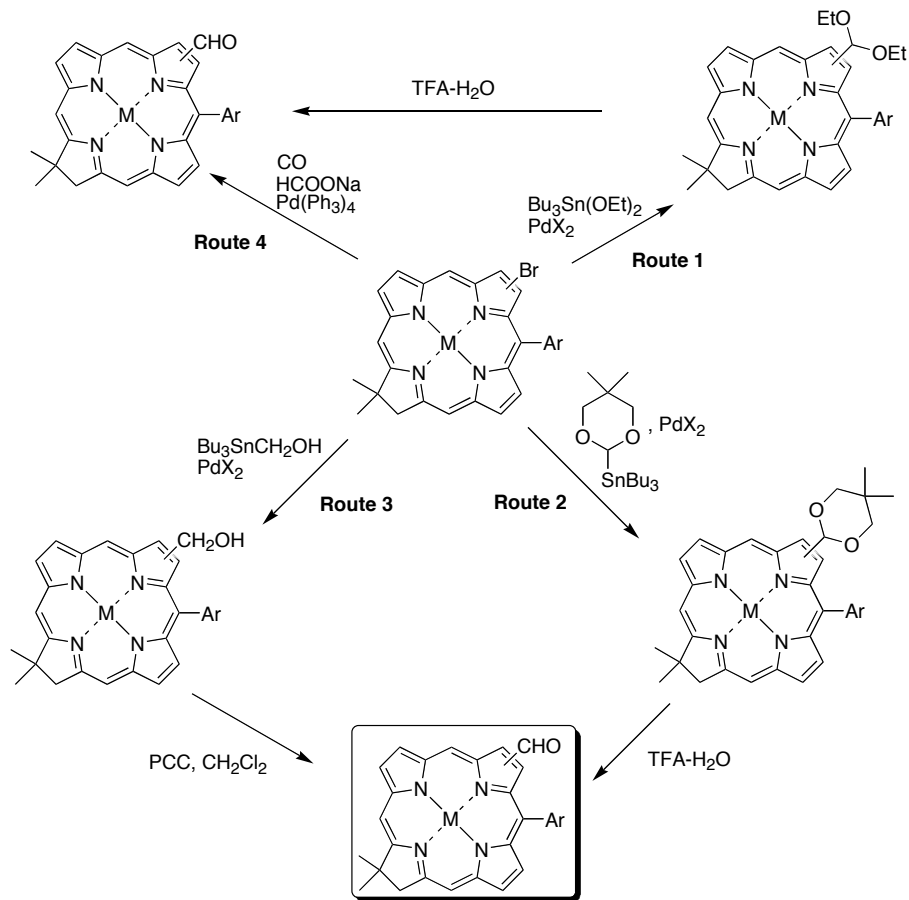
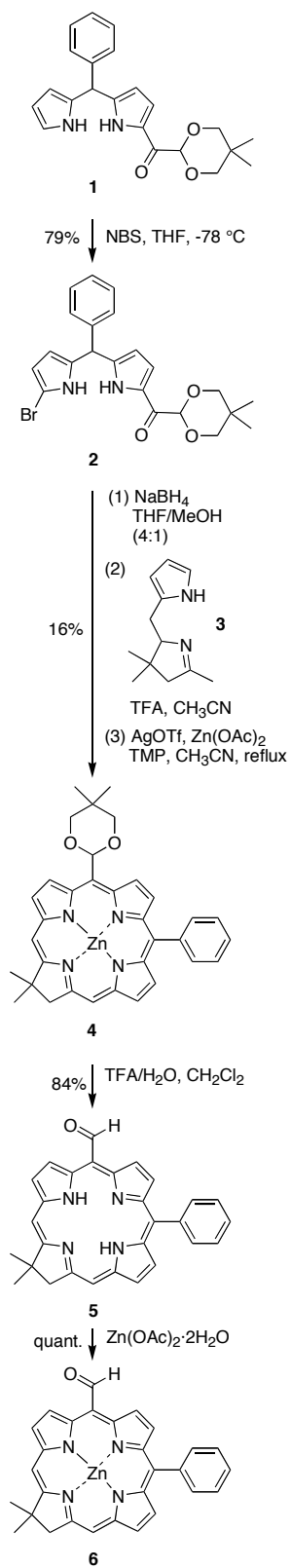


Chart 1

2. Synthesis of a Formyl Chlorin from a 1-Acyldipyrromethane.

Synthesis of 5-Formyl Chlorin. The synthesis of a 5-formyl-chlorin was approached through use of a 1-acyldipyrromethane that contains a protected formyl group (**1**).¹ Following a procedure for bromination,²³ 1-acyldipyrromethane **1** was treated with NBS at –78 °C for 1 h affording the corresponding 1-bromo-9-acyldipyrromethane (**2**) in 79% yield (Scheme 1). Reduction of **2** with NaBH₄ afforded the 1-bromo-dipyrromethane-9-carbinol (Eastern half). Due to the limited stability of the bromo-dipyrromethane-carbinol, it was not characterized and immediately utilized in the next step. Following a one-flask procedure for the synthesis of chlorins,²⁴ the bromo-dipyrromethane-carbinol was first condensed with tetrahydrodipyrin **3**²⁵ (Western Half) in the presence of TFA to obtain the tetrahydrobilene-*a* derivative. The resulting compound was then subjected to oxidative cyclization affording the 5-acetal-substituted zinc chlorin **4** in 16% yield. The acetal group was hydrolyzed (and the zinc chlorin was demetalated) by treatment of with a mixture of TFA/H₂O in CH₂Cl₂, thereby affording the free-base formyl-chlorin **5** in 84% yield. Following a procedure for zinc insertion into porphyrinic macrocycles,²⁶ treatment of chlorin **5** with Zn(OAc)₂·2H₂O afforded the zinc chelate of the formyl-chlorin (**6**) in quantitative yield. Chlorin **6** (in CH₂Cl₂) exhibited Soret and Q_y bands at 425 and 649 nm, respectively, which are significantly red-shifted versus that of acetal-chlorin **4** (407 and 613 nm). The absorption spectra both in CH₂Cl₂ and toluene were broad indicative of aggregation. When the spectrum was collected in CH₂Cl₂/MeOH (3:1), a solvent that typically disrupts any aggregated porphyrinic compounds, the broadening still remained with peaks at 430 and 653 nm. Thus, the redshift is unlikely to stem from aggregation. Such a redshift is comparable to that observed with chlorins bearing similar auxochromic groups (e.g., acetyl).

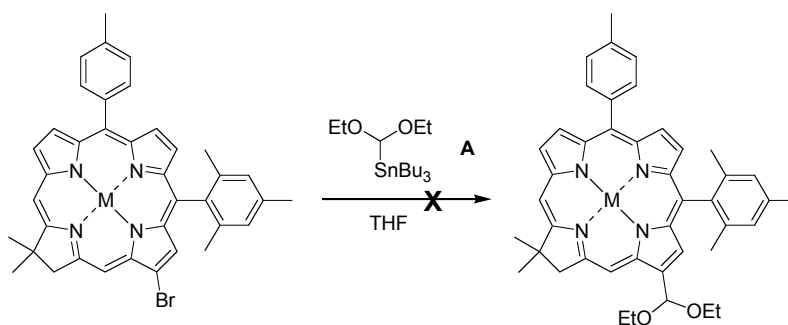


Scheme 1

2. Synthesis of Formyl Chlorins via Stille Cross-Coupling.

A. Introduction of an Acetal Group into Chlorins.

(i) **Attempts using Diethoxymethyltributyltin.** A 13-bromo free-base chlorin (**7**)²⁷ was reacted with diethoxymethyltributyltin, a masked formylating agent, in the presence of a catalytic amount (15 mol%) of Pd(PPh₃)₂Cl₂ in refluxing THF for 18 h (Scheme 2, Entry 1). After concentration and purification, a small amount of starting material and a large amount of debrominated chlorin were isolated. In addition, a trace amount of putative 13-butyl chlorin and 13-pentyl chlorin were isolated (as observed upon LDMS analysis). Surprisingly, the desired chlorin [**7-(OEt)**₂] bearing an acetal group at the 13-position was not formed.



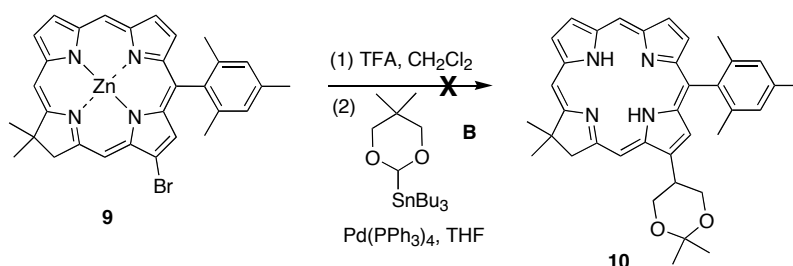
Entry	13-Bromo Chlorin	Pd Catalyst	Product
1	7 , M = H, H	Pd(PPh ₃) ₂ Cl ₂	7-(OEt) ₂ , M = H, H
2	8 , M = Zn	Pd(PPh ₃) ₄	8-(OEt) ₂ , M = Zn

Scheme 2

Failure to obtain the required acetal-chlorin prompted a reaction with the zinc chelate of the 13-bromo chlorin (**8**)²⁷ in the presence of Pd(PPh₃)₄ (Scheme 2, Entry 2). In this attempt a major quantity of the starting material, a small amount of debrominated chlorin and

again a trace amount of putative 13-butyl chlorin as well as 13-methyl chlorin were isolated. Thereafter, we changed the solvent to toluene instead of THF keeping in mind the effect of different solvents in altering the course of palladium-coupling reactions. In this case also, the desired product [**8-(OEt)₂**] was not observed.

(ii) **Attempts using 2-Tributylstannyl-1,3-dioxane.** A 13-bromo free-base chlorin (**9**)⁴ was reacted with 2-tributylstannyl-1,3-dioxane, a masked formylating agent, in the presence of 15 mol% of Pd(PPh₃)₄ in refluxing THF for 26 h (Scheme 3). Afterwards, a small amount of starting material as well as a large amount of debrominated chlorin were isolated. The desired chlorin (**10**) bearing the cyclic acetal group at the 13-position was not obtained.

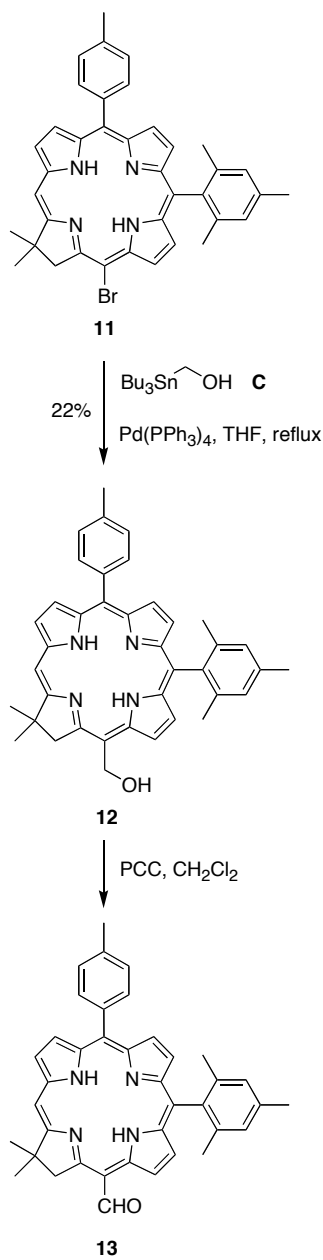


Scheme 3

B. Introduction of a Hydroxymethyl Group into Chlorins via Palladium-Coupling.

(i) **Use of Hydroxymethyltributyltin with a 15-Bromo-chlorin (Scheme 4).** Since we did not obtain satisfactory results with tributyltin acetals (masked formyl groups), we decided to change the tin reagent to one bearing a hydroxymethyl substituent. A sample of 15-bromo chlorin (**11**)⁵ was reacted with hydroxymethyltributyltin in THF for 24 h in the presence of Pd(PPh₃)₄. The required product (15-hydroxymethyl chlorin, **12**) was isolated in

22% yield with recovery of a substantial quantity of starting material (~60%) and a trace amount of debrominated chlorin species (~10%). In order to promote the reaction, a similar reaction was carried out in the presence of excess LiCl (3 equiv) as an activating agent. In this case, no product was observed. Rather, recovery of the starting material along with debrominated chlorin and putative 15-pentyl chlorin were obtained.

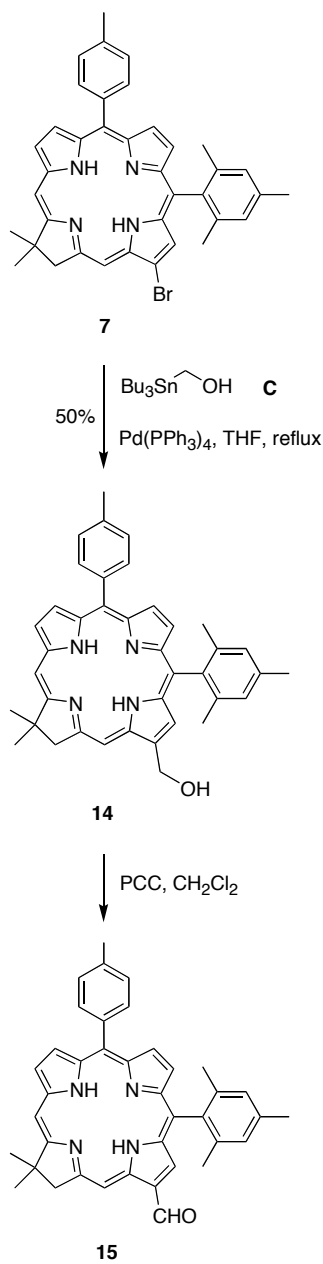


Scheme 4

(ii) **Microscale Oxidation of 15-Hydroxymethyl-chlorin.** We carried out the oxidation of the 15-hydroxymethyl chlorin (**12**) in the presence of the mild oxidant pyridinium chlorochromate (PCC), which afforded the corresponding 15-formyl chlorin (**13**)

in low yield (~25%). It must be noted that none of the corresponding oxochlorin species was observed (i.e., no 17-oxo derivative was obtained), thereby indicating the selectivity of the PCC-mediated oxidation.

(iii) Use of Hydroxymethyltributyltin with a 13-Bromo-chlorin (Scheme 5). We explored the reactivity of 13-bromo free-base chlorin (**7**) towards hydroxymethyl tributyltin in the presence of Pd(PPh₃)₄. Upon refluxing the reaction mixture in THF for 30 h followed by chromatographic purification, the desired 13-hydroxymethyl-chlorin (**14**) was obtained in 52% yield. This chlorin was characterized by absorption spectroscopy, ¹H NMR spectroscopy, LDMS, and FABMS.



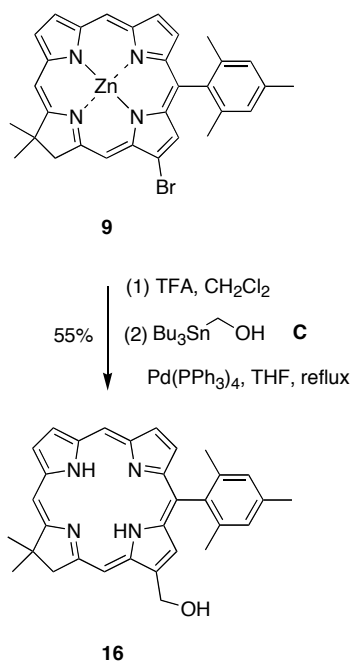
Scheme 5

(iv) **Microscale Oxidation of 13-Hydroxymethyl-chlorin.** Since our goal was to obtain a formyl-chlorin, we subjected the 13-hydroxymethyl-chlorin (**14**) to mild oxidation conditions. 13-Hydroxymethyl chlorin (**14**) was treated with pyridinium chlorochromate

(PCC) at room temperature using CH_2Cl_2 as a solvent. Even though complete consumption of the starting material (**14**) was confirmed by TLC analysis, the desired 13-formyl chlorin (**15**) was not isolated. The origin of the failure to isolate **15** remains unclear.

(v) Stille-Coupling Reaction to Obtain 13-Hydroxymethyl Chlorin (Scheme 6).

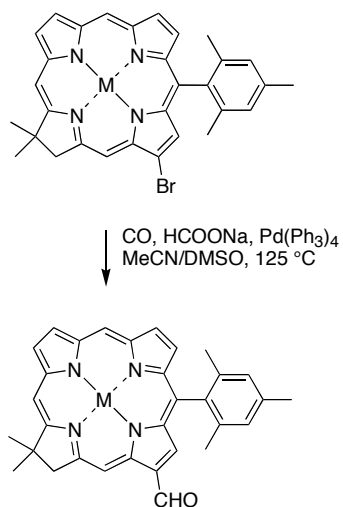
A sample of the zinc chelate of chlorin **9** was treated with TFA in CH_2Cl_2 . The reaction mixture was stirred at room temperature for 5 h affording a 13-bromo free-base chlorin. The crude reaction mixture was directly used after work up without further purification for the next step. The 13-bromo free-base chlorin was reacted with $\text{Bu}_3\text{SnCH}_2\text{OH}$ (**C**) in the presence of $\text{Pd}(\text{PPh}_3)_4$ in THF to afford the 13-hydroxymethyl chlorin (**16**) in 55% yield. No attempts were made to oxidize **16** in order to prepare the corresponding 13-formyl-chlorin.



Scheme 6

3. Formylation via Reductive Carbonylation (Scheme 7).

Several unsuccessful attempts were made to introduce an acetal group into the chlorin moiety (*vide supra*). Though we were able to insert a hydroxymethyl group at the 13-position and the 15-position of the chlorin macrocycle, PCC-mediated oxidation gave a low yield of the corresponding formyl-chlorin. Hence, we finally moved to CO-mediated formylation²¹ of chlorins via palladium coupling. Initially a 13-bromo zinc chlorin (**9**)⁴ was treated with a catalytic amount of Pd(PPh₃)₄ and sodium formate under an atmosphere of CO (maintained with a CO-containing balloon) (Scheme 7). In this case, a trace amount of 13-formyl chlorin (**18**) was observed. A second set of reactions was carried out using a crude 13-bromo free-base chlorin (**17**)⁴ under similar conditions with bubbling CO gas into the reaction mixture. Here also the desired chlorin (**19**) was not obtained. When a third set of reactions was performed with bubbling CO gas into the reaction mixture containing 13-bromo zinc chlorin **9**, the desired formyl-chlorin (**18**) was isolated in 20% yield. The relative low yield could be due to the following reasons. In addition to the desired product, a large amount of debrominated zinc chlorin and 13-hydroxymethyl chlorin (**20**) also were formed (Chart 2). We suspect that the sodium formate-mediated hydrogenation gave rise to two competitive side reactions including (i) debromination of the starting bromo-chlorin, and (ii) reduction of the 13-formyl chlorin to give 13-hydroxymethyl chlorin (Chart 2).



<u>Entry</u>	<u>13-Bromo Chlorin</u>	<u>Product</u>	<u>Yield</u>
1	17, M = H, H	19, M = H, H	0%
2	9, M = Zn	18, M = Zn	20%

Scheme 7

Palladium Catalyzed Reductive Carbonylation

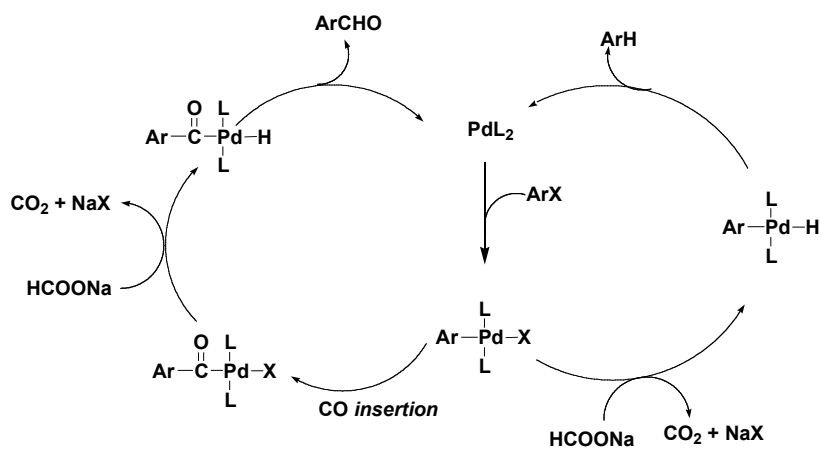


Chart 2

4. Absorption Spectroscopic Studies of Chlorins.

To establish the relationship between structure and absorption spectroscopic properties, the absorption spectra of the two hydroxymethyl-chlorins and two formyl-chlorins were collected in a non-polar solvent (e.g., toluene, CH_2Cl_2). 13-Hydroxymethyl chlorin **16** showed a broad peak at 405 nm (Soret band) and a sharp peak at 640 nm (Q_y band) (Figure 1). The zinc chelate of 13-hydroxymethyl chlorin **20** exhibited two peaks at 406 and 608 nm (Figure 2).

In the case of 5-formyl chlorin **6**, two broad peaks appeared at 425 and 649 nm (Figure 3). In 13-formyl-chlorin **18**, the peaks appeared at 418 and 634 nm (Figure 4). Here also a red shift as well as strong absorption in the red region of the visible spectrum were observed. The relative intensity of the Q_y band (relative to the B band) in the 13-formyl chlorin is greater than that of the 5-formyl chlorin, hence, depending upon the position of the formyl group in the chlorin the absorption spectra may vary.

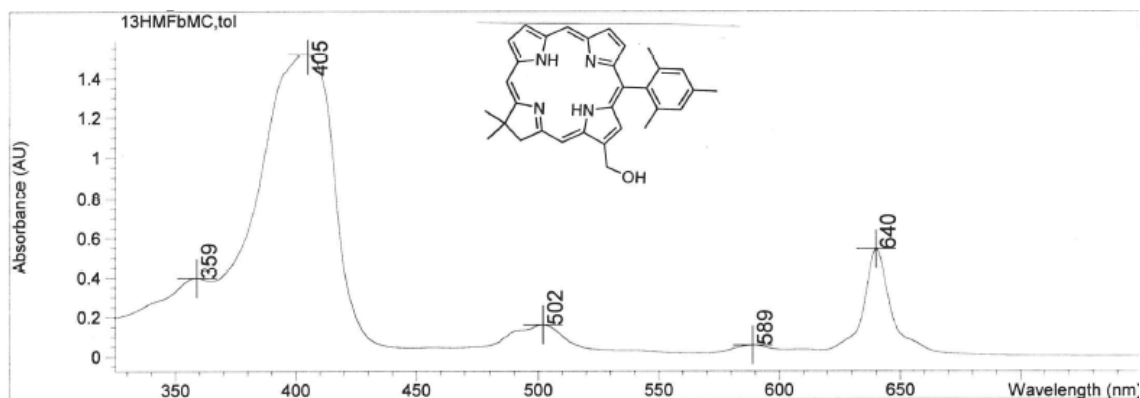


Figure 1. Absorption spectrum of 13-hydroxymethyl chlorin (**16**).

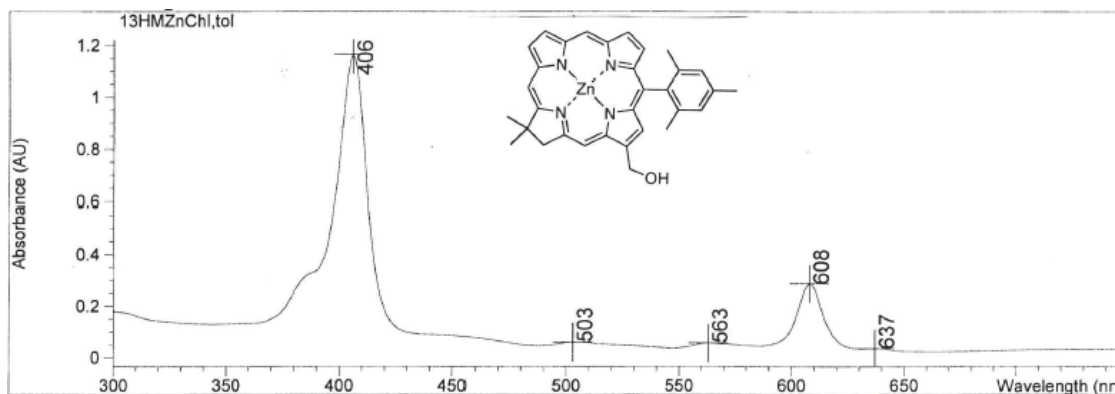


Figure 2. Absorption spectrum of 13-Hydroxymethyl chlorin (**20**).

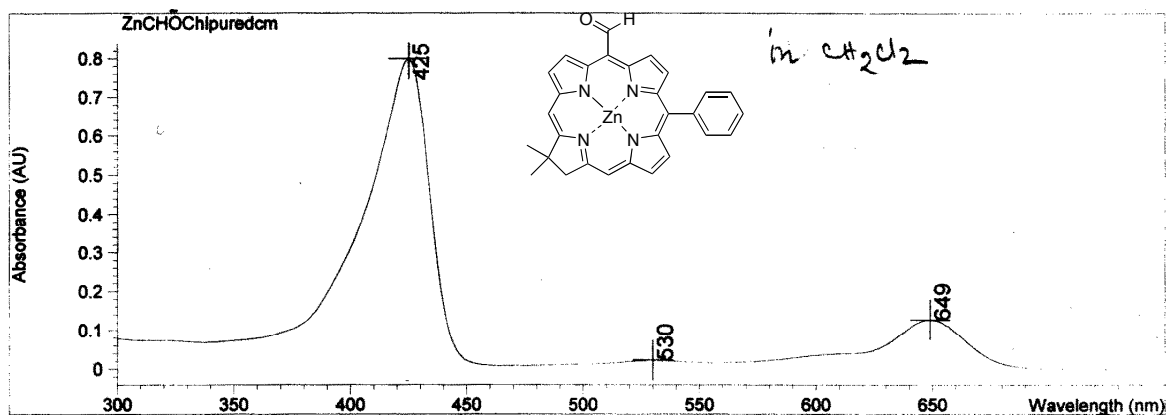


Figure 3. Absorption spectrum of 5-formyl chlorin (**6**).

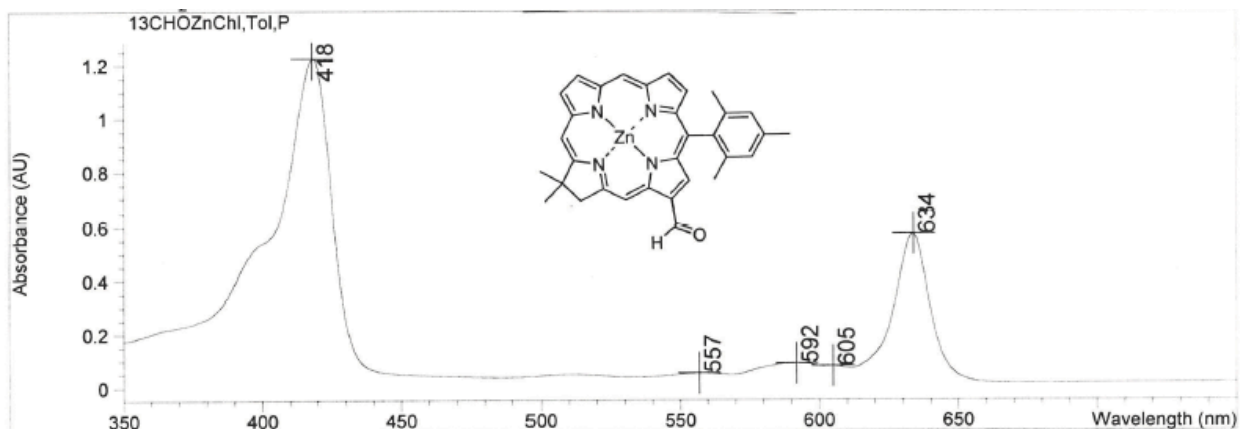


Figure 4. Absorption spectrum of 13-formyl chlorin (**18**).

Outlook

We successfully synthesized a 5-formyl-chlorin using a 1-acyldipyrromethane that contains an acetal group. However, our attempts to introduce acetals via direct Stille cross-coupling reaction of bromo-chlorins with appropriate trialkyltin reagents did not give satisfactory results. However, a hydroxymethyl group was introduced directly at the 13- and 15-positions of chlorins. It must be noted that the 13-bromo-chlorin was more reactive towards Stille coupling (for hydroxymethyl introduction) than the 15-bromo-chlorin. A 13-formyl-chlorin was prepared via reductive carbonylation of a 13-bromo-chlorin using carbon monoxide. The absorption spectra of zinc chelates of 5- and 13-formyl-chlorins were obtained, which revealed a significant effect of the position of the formyl group on the chlorin absorption spectra. Taken together, the formyl chlorins are useful for absorption spectroscopic studies and may provide a valuable motif for homologation for further tuning of absorption spectroscopic properties.

Experimental Section

General. Absorption and fluorescence spectra were collected in CH_2Cl_2 at room temperature unless noted otherwise. Silica gel (40 μm average particle size) was used for column chromatography. THF was freshly distilled from sodium/benzophenone as required. Toluene was distilled from CaH_2 . CHCl_3 was stabilized with 0.8% ethanol. Anhydrous MeOH, CH_2Cl_2 and CHCl_3 (stabilized with 0.8% EtOH) were reagent grade and were used as received.

Non-commercial compounds. Diethoxymethyltributyltin (**A**),⁷ 2-tributylstannyl-1,3-dioxane (**B**),¹² hydroxymethyl-tributyltin (**C**),¹⁷ **1**,¹ **3**,²⁵ **7**,²⁷ **8**,²⁷ **9**,⁴ **11**,⁵ and **17**⁴ were synthesized following reported procedures.

1-Bromo-9-[(5,5-dimethyl-1,3-dioxan-2-yl)carbonyl]-5-phenyldipyrromethane

(2). Following a general procedure,³ a solution of **1** (91 mg, 0.25 mmol) in 2.5 mL of anhydrous THF was cooled to -78 °C under argon. NBS (44 mg, 0.25 mmol) was added, and the reaction mixture was stirred for 1 h at -78 °C. Hexanes and water were added, and the mixture was allowed to warm to room temperature. The entire reaction mixture was poured into ether. The aqueous layer was extracted with ether. The organic layer was separated, dried (K_2CO_3), and concentrated without heating. The resulting solid residue was purified by chromatography [silica, hexanes/ethyl acetate (3:2)] to afford a light brown viscous oil (88 mg, 79%): 1H NMR (300 MHz, THF- d_8) δ 0.77 (s, 3H), 1.94 (s, 3H), 3.50–3.60 (m, 2H), 3.69 (d, $J = 11.4$ Hz, 2H), 3.98–4.08 (m, 1H), 4.99 (s, 1H), 5.43 (s, 1H), 5.60 (s, 1H), 5.82–5.85 (m, 1H), 5.90–5.93 (m, 1H), 7.12–7.29 (m, 5H), 10.48–10.54 (br s, 1H), 10.85–11.04 (br s, 1H); ^{13}C NMR (75 MHz, THF- d_8) δ 21.4, 22.9, 30.4, 44.2, 77.1, 97.1, 102.1, 109.27, 109.44, 109.9, 119.2, 126.8, 128.3, 128.6, 129.1, 134.0, 141.5, 141.8, 181.0; FABMS obsd 443.0956, calcd 443.0970 [(M + H)⁺, M = C₂₂H₂₃BrN₂O₃].

Zn(II)-17,18-Dihydro-18,18-dimethyl-5-(5,5-dimethyl-1,3-dioxan-2-yl)-10-phenylporphyrin (4). Following a general procedure for chlorin formation,²⁴ a solution of **2** (84 mg, 0.19 mmol) in THF/MeOH [20 mL, (4:1)] was treated portionwise with NaBH₄ (0.544 g, 14.4 mmol). The progress of the reaction was monitored by TLC analysis. Upon completion (~2 h), the reaction was slowly quenched by the addition of saturated aqueous NH₄Cl solution (50 mL). The reaction mixture was then poured into ethyl acetate. The

organic layer was separated. The aqueous layer was extracted twice with ethyl acetate. The organic layers were combined, washed with water, dried (Na₂SO₄) and concentrated. Upon initial work up, the 1-bromo-dipyrromethane-9-carbinol was the only product visible by TLC analysis. Due to limited stability, the 1-bromo-dipyrromethane-9-carbinol was directly used in the chlorin-forming reaction. The 1-bromo-dipyrromethane-9-carbinol (~0.19 mmol) was dissolved in anhydrous CH₃CN (1.9 mL). The solution was treated with **3** (36 mg, 0.19 mmol) and TFA (15 μL, 0.19 mmol). The reaction mixture was stirred for 45 min at room temperature under argon. The reaction mixture was then diluted with CH₃CN (17.1 mL). The diluted reaction mixture was then treated successively with 2,2,6,6-tetramethylpiperidine (0.97 mL, 5.7 mmol), Zn(OAc)₂ (0.523 g, 2.85 mmol) and AgOTf (0.15 g, 0.57 mmol). The resulting mixture was refluxed for 21 h exposed to air. The entire reaction mixture was concentrated to afford a solid residue. The resulting residue was chromatographed twice [(i) silica, CH₂Cl₂/ethyl acetate (9:1), (ii) silica, hexanes/CH₂Cl₂ (1:1)] to afford the title compound as a dark green solid (18 mg, 16%): ¹H NMR (400 MHz, THF-*d*₈) δ 1.06 (s, 3H), 1.85 (s, 3H), 2.03 (s, 6H), 4.13 (d, *J* = 12.0 Hz, 2H), 4.26 (d, *J* = 12.0 Hz, 2H), 4.53 (s, 2H), 7.64–7.68 (m, 3H), 7.73 (s, 1H), 8.01–8.06 (m, 2H), 8.35 (d, *J* = 4.4 Hz, 1H), 8.50 (d, *J* = 4.4 Hz, 1H), 8.56 (d, *J* = 4.4 Hz, 1H), 8.61 (s, 1H), 8.64 (s, 1H), 8.70 (d, *J* = 4.4 Hz, 1H), 9.49 d, *J* = 4.4 Hz, 1H), 9.84 (d, *J* = 4.4 Hz, 1H); LDMS obsd 592.3; FABMS obsd 592.1811, calcd 592.1817 (C₃₄H₃₂N₄O₂Zn); λ_{abs} (CH₂Cl₂) 407, 613 nm; λ_{em} (CH₂Cl₂) 620, 670 nm.

5-Formyl-17,18-dihydro-18,18-dimethyl-10-phenylporphyrin (5). Following a general procedure for the hydrolysis of acetals,¹ a solution of **4** (5.0 mg, 8.0 μmol) CH₂Cl₂ (1 mL) was treated with a mixture of TFA/H₂O [0.5 mL, (1:1)], and the reaction mixture was stirred under argon at room temperature for 16 h. The reaction mixture was then diluted with

CH₂Cl₂, and the organic layer was separated, washed (saturated NaHCO₃ solution and brine respectively), dried (Na₂SO₄) and concentrated. The resulting solid residue was chromatographed [silica, hexanes/CH₂Cl₂ (1:1) → CH₂Cl₂] to afford the title compound as a dark green solid (3.0 mg, 84%): ¹H NMR (300 MHz, THF-*d*₈, 50 °C) δ -2.15 to 1.85 (brs, 2H), 2.08 (s, 6H), 4.64 (s, 2H), 7.58–7.84 (m, 3H), 8.02–8.18 (m, 2H), 8.63 (d, *J* = 4.8 Hz, 1H), 8.77 (d, *J* = 4.5 Hz, 1H), 8.95 (d, *J* = 4.5 Hz, 1H), 9.15–9.25 (s, 2H), 9.24 (s, 1H), 9.72 (d, *J* = 4.8 Hz, 1H), 10.19 (d, *J* = 4.8 Hz, 1H), 12.39 (s, 1H); LDMS obsd 443.9; FABMS obsd 445.2015, calcd 445.2028 [(M + H)⁺, M = C₂₉H₂₄N₄O]; λ_{abs} (CH₂Cl₂) 416, 517, 559, 617, 672 nm; λ_{em} (CH₂Cl₂) 690 nm.

Zn(II)-5-Formyl-17,18-dihydro-18,18-dimethyl-10-phenylporphyrin (6).

Following a procedure for zinc insertion into porphyrins,²⁶ a solution of **5** (3.0 mg, 7.0 μmol) in CH₂Cl₂/MeOH [2 mL, (3:1)] was treated with Zn(OAc)₂·2H₂O (46 mg, 0.21 mmol), and the reaction mixture was stirred at room temperature for 8 h. The reaction mixture was then diluted with CH₂Cl₂. The organic layer was separated, washed (saturated NaHCO₃ solution and H₂O), dried (Na₂SO₄) and concentrated. The resulting solid residue was washed twice with hexanes and washed once with hexanes/MeOH (2:1) affording a green solid (3.5 mg, quantitative): ¹H NMR (300 MHz, THF-*d*₈) δ 2.07 (s, 6H), 5.59 (s, 2H), 7.62–7.78 (m, 3H), 7.98–8.12 (m, 2H), 8.51 (d, *J* = 4.5 Hz, 1H), 8.54 (d, *J* = 4.2 Hz, 1H), 8.63 (d, *J* = 4.2 Hz, 1H), 8.84 (s, 1H), 8.87 (s, 1H), 8.95 (d, *J* = 4.5 Hz, 1H), 9.75 (d, *J* = 4.8 Hz, 1H), 9.99 (d, *J* = 4.8 Hz, 1H), 12.38 (s, 1H); LDMS obsd 505.9; FABMS obsd 506.1082, calcd 506.1085 (C₂₉H₂₂N₄OZn); λ_{abs} (CH₂Cl₂) 425, 649 nm; λ_{em} (CH₂Cl₂) 670 nm.

13-Hydroxymethyl-17,18-dihydro-10-mesityl-18,18-dimethyl-5-*p*-tolylporphyrin

(14). Following a procedure for Stille coupling with chlorins,⁴ a mixture of **7** (6.0 mg, 10 μ mol) and Pd(PPh₃)₄, (2.3 mg, 2.0 μ mol) was dried in a Schlenk flask for 30 min. Hydroxymethyltributyltin¹⁷ (9.6 mg, 30 μ mol) and THF (1.0 mL) were added and the entire reaction mixture was refluxed for 31 h. The reaction mixture was concentrated and the residue was chromatographed [silica, packed with GC grade hexanes, eluted with hexanes/CH₂Cl₂ (1:1) \rightarrow CH₂Cl₂ \rightarrow CH₂Cl₂/ethyl acetate (4:1)] affording a dark green solid (3.0 mg, 52%): ¹H NMR (300 MHz) δ -1.85 to 1.55 (brs, 2H), 1.84 (s, 6H), 2.05 (s, 6H), 2.60 (s, 3H), 2.67 (s, 3H), 3.61–3.68 (m, 1H), 4.61 (s, 2H), 5.91 (s, 2H), 7.23 (s, 2H), 7.52–7.58 (m, 2H), 8.06 (d, *J* = 7.8 Hz, 2H), 8.28 (d, *J* = 3.9 Hz, 1H), 8.43 (d, *J* = 4.2 Hz, 1H), 8.52 (s, 1H), 8.72–8.80 (m, 2H), 8.82 (s, 1H), 9.01 (s, 1H); LDMS obsd 578.7; FABMS obsd 578.3055, calcd 578.3046 (C₃₉H₃₈N₄O); λ_{abs} (toluene) 415, 510, 559, 592, 643 nm.

13-hydroxymethyl-17,18-dihydro-10-mesityl-18,18-dimethyl-porphyrin (16).

Following a procedure for demetalation of chlorins,⁴ a sample of chlorin **9** (15 mg, 25 μ mol) was treated with TFA (58 μ l, 0.75 mmol) in CH₂Cl₂ (1.25 mL). The reaction mixture was stirred at room temperature for 5 h. The reaction was quenched by the addition of a mixture of saturated aqueous NaHCO₃ solution and CH₂Cl₂. The organic layer was separated, washed (water and brine), dried (Na₂SO₄) and concentrated to afford the free base chlorin. Following a procedure for Stille coupling with chlorins,⁴ a mixture of free base chlorin (~25 μ mol), Pd(PPh₃)₄, (5.8 mg, 5.0 μ mol) was dried in a Schlenk flask for 30 min. Hydroxymethyltributyltin (C) (24 mg, 75 μ mol) and THF (2.0 mL) were added, and the entire reaction mixture was refluxed for 27 h. The reaction mixture was concentrated, and the residue was chromatographed [silica, packed with GC grade hexanes, eluted with

hexanes/CH₂Cl₂ (1:1) → CH₂Cl₂ → CH₂Cl₂/ethyl acetate (4:1)] affording a dark green solid (7 mg, 55%): ¹H NMR (300 MHz, THF-*d*₈) δ -2.08 to -2.02 (brs, 1H), -1.98 to -1.88 (s, 1H), 1.83 (s, 6H), 2.06 (s, 6H), 2.49 (s, 3H), 2.59 (s, 3H), 4.66 (s, 2H), 5.78–5.86 (m, 2H), 7.26 (s, 2H), 8.31 (d, *J* = 4.2 Hz, 1H), 8.85 (d, *J* = 3.9 Hz, 1H), 8.98 (m, 1H), 9.16 (s, 1H), 9.21–9.58 (m, 1H), 9.80 (s, 1H); LDMS obsd 488.0; FABMS obsd 489.2641, calcd 489.2654 [(M + H)⁺, M = C₃₂H₃₂N₄O]; λ_{abs} (toluene) 405, 502, 640 nm.

Zn(II)-13-Formyl-17,18-dihydro-10-mesityl-18,18-dimethyl-porphyrin (18).

Following a procedure for CO-mediated formylation,²¹ a mixture of **9** (12 mg, 20 μmol), Pd(PPh₃)₄, (4.6 mg, 4.0 μmol, 20 mol%) and sodium formate (14 mg, 0.20 mmol) was dried in a Schlenk flask for 1 h. A mixture of MeCN/DMSO [2 mL, (1:1)] was added to the flask and CO gas was bubbled through the reaction mixture. The entire reaction mixture was heated at 125 °C for 26 h. The reaction mixture was treated with CH₂Cl₂ and water. The organic layer was separated and washed (water, brine), dried (Na₂SO₄) and concentrated. The resulting solid residue was chromatographed [silica, packed with GC grade hexanes, eluted with hexanes/CH₂Cl₂ (1:1) → CH₂Cl₂ → CH₂Cl₂/ethyl acetate (4:1)] affording a green solid (2.2 mg, 20%): ¹H NMR (300 MHz) δ 1.83 (s, 6H), 1.99 (s, 6H), 2.59 (s, 3H) 4.47 (s, 2H), 7.22 (s, 2H), 8.35 (d, *J* = 4.2 Hz, 1H), 8.48 (s, 1H), 8.64–8.74 (m, 2H), 8.94 (s, 1H), 8.98 (d, *J* = 4.2 Hz, 1H), 9.38 (s, 1H), 9.54 (s, 1H), 10.90 (s, 1H); LDMS obsd 547.8; FABMS obsd 548.1553, calcd 548.1555 (C₃₂H₂₈N₄OZn); λ_{abs} (toluene) 418, 634 nm. Zn(II)-17,18-dihydro-13-hydroxymethyl-10-mesityl-18,18-dimethylporphyrin (**20**): LDMS 550.5; FABMS obsd 550.1693, calcd 550.1711 (C₃₂H₃₀N₄OZn); λ_{abs} (toluene) 406, 608 nm.

References

- (1) "A new route to *meso*-formyl porphyrins," Balakumar, A.; Muthukumaran, K.; Lindsey, J. S. *J. Org. Chem.* **2004**, *69*, 5112–5115.
- (2) "Formylation reaction in series of *meso*-tetraaryl substituted porphyrins and chlorins," Mironov, A. F.; Moskalchuk, T. V.; Shashkov, A. S. *Russ. J. Bioorg. Chem.* **2004**, *30*, 261–267.
- (3) "Self-assembly of synthetic bacteriochlorophyll-*f* analogues having C8-formyl substituent," Sasaki, S.-I.; Tomiaki, H. *Bull. Chem. Soc. Jpn.* **2004**, *77*, 797–800.
- (4) "Synthetic chlorins bearing auxochromes at the 3- and 13-positions," Laha, J. K. Muthiah, C.; Taniguchi, M.; McDowell, B. E.; Ptaszek, M.; Lindsey, J. S. *J. Org. Chem.* **2006**, *71*, 4092–4102.
- (5) "Introduction of a third substituent into 5,10-diaryl chlorins and oxochlorins," Taniguchi, M.; Kim, M. N.; Ra, D. Lindsey, J. S. *J. Org. Chem.* **2005**, *70*, 275–285.
- (6) "The palladium-catalyzed cross-coupling reactions of organotin reagents with organic electrophiles," Stille, J. K. *Angew. Chem. Intl. Ed. Engl.* **1986**, *25*, 508–524.
- (7) "The intramolecular Stille reaction in some target natural product syntheses," Pattenden, G.; Sinclair, D. J. *J. Organomet. Chem.* **2002**, *653*, 261–268.
- (8) "The mechanisms of Stille reaction," Espinet, P.; Echavarren, A. M. *Angew. Chem. Intl. Ed. Engl.* **2004**, *43*, 508–524.
- (9) Mitchell, T. *Metal-Catalyzed Cross-Coupling reactions* (2nd Edition); Wiley-VCH Verlag GmbH & Co. KGaA; Weinheim, Germany, **2004**, *1*, 125–161.
- (10) "New organotin synthons providing α -alkoxyorganolithium reagents," Quintard, J.-P.; Elissondo, B.; Pereyre, M. *J. Organomet. Chem.* **1981**, *212*, C31–C34.

- (11) “(Dialkoxymethyl)lithiums: generation, stability, and synthetic transformations,” Shiner, C. S.; Tsunoda, T.; Goodman, B. A.; Ingham, S.; Lee, S.; Vorndam, P. E. *J. Am. Chem. Soc.* **1989**, *111*, 1381–1392.
- (12) “Diethoxymethyl lithium: generation via transmetalation of diethoxymethyltributyltin, stability, nucleophilic reactivity in addition reactions, and use as a precursor of group 14 formylmetals,” Parrain, J.-L.; Beaudet, I.; Cintrat, J.-C.; Duchêne, A.; Quintard, J.-P. *Bull. Chim. Soc. Fr.* **1994**, *131*, 304–312.
- (13) “Substitution of the acetoxy groups of dialkoxymethylacetates by organometallic reagents: a route to allyl-, propargyl-, homoallyl-, homopropargyl-, α -stannylacetals,” Beaudet, I.; Duchêne, A.; Parrain, J.-L.; Quintard, J.-P. *J. Organomet. Chem.* **1992**, *427*, 201–212.
- (14) “Homologation of boronic acids esters with (dialkoxymethyl)lithiums. Asymmetric synthesis of α -alkoxy boronate esters,” Carmès, L.; Carreaux, F.; Carboni, B. *J. Org. Chem.* **2000**, *65*, 5403–5408.
- (15) “Preparation of chiral 2-stannyloxazolidines and first considerations on the transacetalisation reaction mechanism,” Cintrat, J.-C.; Léat-Crest, V.; Parrain, J.-L.; Le Grogneac, E.; Beaudet, I.; Quintard, J.-P. *Eur. J. Org. Chem.* **2004**, 4251–4267.
- (16) “ α -Tributylstannylacetals: preparation via transacetalisation of diethoxymethyltributyltin, and use for the synthesis of new α -stannylated ethers,” Duchêne, A. Boissière, S.; Parrain, J.-L. Quintard, J.-P. *J. Organomet. Chem.* **1990**, *387*, 153–162.
- (17) (a) “Efficient synthesis of bromo- and iodomethyltributyltin,” Åhman, J.; Somfai, P. *Synth. Commun.* **1994**, *8*, 1117–1120. (b) “A hydroxymethyl anion equivalent:

- tributyl[(methoxymethoxy)methyl]stannane,” Danheiser, R. L.; Romines, K. R.; Koyama, H.; Gee, S. K. Johnson, C. R.; Medich, J. R. *Org. Syn.* **1993**, *71*, 133–139.
- (18) “Palladium-catalyzed formylation of organic halides with carbon monoxide and tin hydride,” Baillargeon, V. P.; Stille, J. K. *J. Am. Chem. Soc.* **1986**, *108*, 452–461.
- (19) “Studies directed toward the synthesis of terreulactone A: rapid construction of the A, B, C rings,” Liu, H.; Siegel, D. R.; Danishefsky, S. F. *Org. Lett.* **2006**, *8*, 423–425.
- (20) “Facile synthesis of 17-formyl steroids via palladium-catalyzed homogeneous carbonylation reaction,” Petz, A.; Horváth, J.; Tuba, Z.; Pintér, Z.; Kollár, L. *Steroids* **2002**, 777–781.
- (21) “Reductive formylation of aromatic halides under low carbon monoxide pressure catalyzed by transition-metal compounds,” Pri-Bar, I.; Buchman, O. *J. Org. Chem.* **1984**, *49*, 4009–4011.
- (22) “Rapid palladium-catalyzed synthesis of esters from aryl halides utilizing Mo(CO)₆ as a Solid carbon monoxide source,” Georgson, J.; Hallberg, A.; Larhed, M. *J. Comb. Chem.* **2003**, *5*, 350–352.
- (23) “Synthesis of meso-substituted chlorins via tetrahydrobilene-*a* intermediates,” Taniguchi, M.; Ra, D.; Mo, G.; Balasubramanian, T.; Lindsey, J. S. *J. Org. Chem.*, **2001**, *66*, 7342–7354.
- (24) “Synthesis and electronic properties of regioisomerically pure oxochlorins,” Taniguchi, M.; Kim, H.-J.; Ra, D.; Schwartz, J. K.; Kirmaier, C.; Hindin, E.; Diers, J. R.; Prathapan, S.; Bocian, D. F.; Holten, D.; Lindsey, J. S. *J. Org. Chem.* **2002**, *67*, 7329–7342.

- (25) “Refined synthesis of 2,3,4,5-tetrahydro-1,3,3-trimethyldipyrin, a deceptively simple precursor to hydroporphyrins,” Ptaszek, M.; Bhaumik, J.; Kim, H.-J.; Taniguchi, M.; Lindsey, J. S. *Org. Proc. Res. Dev.* **2005**, *9*, 651–659.
- (26) “Porphyrin architectures tailored for studies of molecular information storage,” Carcel, C. M.; Laha, J. K.; Loewe, R. S.; Thamyongkit, P.; Schweikart, K.-H.; Misra, V.; Bocian, D. F.; Lindsey, J. S. *J. Org. Chem.* **2004**, *69*, 6739–6750.
- (27) “A new route for installing the isocyclic ring on chlorins yielding 13¹-oxophorbines,” Laha, J. K.; Muthiah, C.; Taniguchi, M.; Lindsey, J. S. *J. Org. Chem.* **2006**, *71*, 7049–7052.